2012

Mass Spectrometry Applied to Problems in Lipid Biochemistry: Microchip Based Approach for Lipidomics Profiling and Analysis of Lipid Metabolites by LC-MS/MS

Tao Sun

MASS SPECTROMETRY APPLIED TO PROBLEMS IN LIPID BIOCHEMISTRY: MICROCHIP BASED APPROACH FOR LIPIDOMICS PROFILING AND ANALYSIS OF LIPID METABOLITES BY LC-MS/MS

A Dissertation

Submitted to the Bayer School of Natural and Environmental Sciences

Duquesne University

In partial fulfillment of the requirements for

the degree of Doctor of Philosophy

By

Tao Sun

May 2012

MASS SPECTROMETRY APPLIED TO PROBLEMS IN LIPID BIOCHEMISTRY: MICROCHIP BASED APPROACH FOR LIPIDOMICS PROFILING AND ANALYSIS OF LIPID METABOLITES BY LC-MS/MS

By

Tao Sun

Approved February 28, 2012

Jana Patton-Vogt, Ph.D. Associate Professor of Biological Science (Committee Chair)	Partha Basu, Ph.D. Professor of Chemistry (Committee Member)
Rita Mihaela Mihailescu, Ph.D. Associate Professor of Chemistry (Committee Member)	Stephanie J. Wetzel, Ph.D. Assistant Professor of Chemistry (Committee Member)
David W. Seybert, Ph.D. Dean, Bayer School of Natural and Environmental Sciences Professor of Chemistry and Biochemistry	Ralph A. Wheeler, Ph.D. Chair, Department of Chemistry and Biochemistry Professor of Chemistry and Biochemistry

ABSTRACT

MASS SPECTROMETRY APPLIED TO PROBLEMS IN LIPID BIOCHEMISTRY: MICROCHIP BASED APPROACH FOR LIPIDOMICS PROFILING AND ANALYSIS OF LIPID METABOLITES BY LC-MS/MS

By

Tao Sun

May 2012

Dissertation supervised by Jana Patton-Vogt, Ph.D.

Lipidomics and metabolomics are powerful tools for the examination of cellular metabolism and physiology. Methods for lipid analysis need to be developed that begin with small samples and do not overly dilute or disperse the sample in the separation process. Microchips provide a platform for interfacing lysis of small cell populations with on-chip solid phase extraction for isolating lipid samples to generate high quality mass spectra from very small samples. Chapter 1 of this dissertation presents a novel method for small scale lipidomics of bacterial cells by microchip based extraction coupled with untargeted profiling of glycerophospholipids using nanoelectrospray ionization mass spectrometry. Chapter 2 and 3 focus on the development of LC-MS/MS methods to study biological pathways. In Chapter 2, I describe a method for analysis of the phospholipids metabolite, GroPIns, in the medium of the pathogenic yeast *Candida*

albicans. This method was applied to aid in the characterization of the GroPIns transport protein, Git1, in *C. albicans*. Chapter 3 extends the studies of part two and describes an efficient method based on HILIC-MS/MS for the separation and quantification of five lipid-related extracellular metabolites in yeast *Saccharomyces cerevisiae*. This newly developed methodology was successfully applied to determine the extracellualr levels of glycerophosphoinositol, glycerophosphocholine, glycerol 3-phosphate, inositol and choline in wild type and mutant strains.

ACKNOWLEDGEMENT

My first and foremost thanks go to Dr. Jana Patton-Vogt who, during our time together, is a mentor in every sense of the word and paves the way and fills it with immense support, unceasing patience, many deep insights and simulating ideas during my graduate studies. Thank you Jana, you taught me molecular biology, and an appreciation for seeing life in another way.

My very special thanks go to my committee members, Drs. Partha Basu, Rita Mihaela Mihailescu and Stephanie J. Wetzel. You were always available for guidance and were willing to help me in any way that you could. I have learned so much from each of you and I send to you a well-deserved "thank you". I must thank Dr. Wetzel for reading my papers and contributing her opinions and expertise.

I greatly appreciate the generous financial support of the Department of Chemistry and Biochemistry at Duquesne University over the last five years. So much more than simple "thanks" to all my friends: Mourad Frites, Carl Brunetta, Ben Mogesa, Lihua Yao, Becky Wagner, Chelsee Donelan, Dienesh Nath and Sai Zhao. To Timothy Fahrenholz, I thank you for sharing the experiences about using the instruments. I honestly could not have done this without your help and support.

To my research fellow group members and other colleagues in the Chemistry and Biology Department: Andrew Davic, Andrew Bishop, Sean Pawlowski, Erin Devito, Beth Surlow, Dr. Kristin Kroniser, Dr. David Gallaher, and Dr. Michael Cascio, many thanks for their great help and friendship.

I would like to thank my parents, sisters, and in-laws for their unconditional support and encouragement from day one of this journey. To my wife Lu, I thank you for your countless sacrifices, and my little one Eric for the joy he brought to our family. They were all there for the triumphs and setbacks throughout the entire process. I love you all very much.

Very special thanks are reserved for my former advisor, Dr. Mitchell E. Johnson. Thank you Mitch, you taught me so much more than chemistry and were always there for me through the ups and downs of my graduate career. I am honored to have served as your student.

Tao Sun

January 29, 2012

TABLE OF CONTENTS

Page

LIST OF TABLES

Page

Chapter 1

Chapter 2

Chapter 3

Appendix 1

Appendix 2

LIST OF FIGURES

Page

Chapter 1

Chapter 2

LIST OF ABBREVIATIONS

APCI	atmospheric pressure chemical ionization
CE	capillary electrophoresis
CEC	capillary electrochromatography
Ch	cholesterol
CV	coefficient of variation
DAG	diacylglycerol (1,2-dipalmitoyl-rac-glycerol)
ESI	electrospray ionization
FA	fatty acyls
FDA	food and drug administration
FFA	free fatty acid
FITC	5-fluorescein isothiocyanate
GC/MS	gas chromatography mass spectrometry
GPXs	glycerophosphodiesters
GroP	glycero 3-phosphate
GroPIns	glycerophosphoinositol
GroPCho	glycerophosphocholine
HILIC	hydrophilic interaction liquid chromatography
HPLC	high performance liquid chromatography
HQC	high quality control
IEX	ion exchange chromatography
LC	liquid chromatography
LC-MS	liquid chromatography mass spectrometry
LIF	laser induced fluorescence
LLOQ	lower limit of quantification
LQC	low quality control
MRM	multiple reaction monitoring
MS	mass spectrometry
MS/MS	tandem mass spectrometry
μTAS	micro total analysis system
MQC	middle quality control
NP	normal phase
PA	phosphatidic acid
PC	phosphatidylcholine
PE	phosphatidylethanolamine
PG	phosphatidylglycerol
PI	phosphatidylinositol
PIp	phosphatidylinositol monophosphate
PLB	phospholipases of B type
PIS	product ion scan
PS	phosphatidylserine
QC	quality control
RE	relative error

RP	reverse phase
SP	sphingolipid
SPE	solid phase extraction
ST	sterol lipid
TAG	triacylglycerol
THF	Tetrahydrofuran
TLC	thin layer chromatography
QTOF-MS	quadruple time-of-flight mass spectrometry
UV	ultraviolet

Chapter 1

Novel Analytical Technique to Study

Glycerophospholipids on a Microchip[1]

[1]The work described in this Chapter is reprinted with permission from:

Sun, T.; Pawlowski, S.; Johnson, M. E. Highly efficient microscale purification of glycerophospholipids by microfluidic cell lysis and lipid extraction for lipidomics profiling, *Analytical Chemistry*, 2011, 83 (17), 6628-6634. Copyright (2011) American Chemical Society.

1.1 Abstract

In this chapter, a microfluidic chip-mass spectrometry based method for non-targeted profiling of lipids from cell extracts is described. The technique can in principle be used for lipid analysis in micro scale when working with small populations of cells (1 to about 1000). This is very often the case in biological applications in sample cleanup and separation for lipid identification. The developed system packed with fresh silica beads allows for on-chip cell lysis and lipid extraction without any loss during the process, which is capable of being reused for the first four runs. The acceptable extraction efficiency is obtained by integrating silica beads as the packing material with methanol as the eluent. This work demonstrates the potential of incorporating microchip-based lipid extraction into cellular lipidomics research. The application of the methodology was extended to the discovery profiling of lipid from *Sulfurospirillum barnesii* strain SES-3 cells, which revealed the presence of 173 identified phospholipid species based on the high-resolution tandem mass spectrometry data. The work has been published in the *Analytical Chemistry* journal (Sun *et al.*, 2011). The novelty of the microfluidic approach can be generally applied to any systems of interest and is the platform employed in microscale lipid studies in future research of our lab, it is thus imperative to describe its development in detail.

1.2 Introduction

Lipids are a diverse group of biomolecules that are known to exist as thousands of distinct covalent entities, each with its unique structural and physical characteristics. They are essential cellular constituents that have multiple distinct roles in cellular functions. It is commonly accepted that lipids are bioorganic hydrocarbon based molecules that are soluble in nonpolar solvents but are almost insoluble in water due to their makeup consisting mostly of carbon. Lipids have various biochemical duties including energy storage (fats and sterols such as cholesterol), cell makeup such as lipid bilayers and micelles (phospholipids), and some are essential hormones (steroids and eicosanoids). They play an important role as constituents of cellular membranes for separating cells from the external environment, compartmentalizing cells, and proving a special milieu for various biochemical processes. The contribution of lipids to the composition of membrane in different organisms and cells varies depending upon the type and function of the structures [1-3].

Phospholipids are present in all organisms, from archaebacteria, to plants, to humans [4]. These hydrophobic molecules are the building blocks for cellular membranes (lipid bilayer), yet perform a diverse number of other functions, from compartmentalization of cytoplasm to the housing of proteins involved in cell signaling, intercellular adhesion, and cytoskeletal support [5], as well as serving as a precursor pool for biologically active lipid mediators [6]. The two common structural classes of phospholipids found in eukaryotic cells are sphingomyelins and glycerophospholipids. Abundant glycophospholipids also are constituents of prokaryotic cells [7]. The general

structure of glycerophospholipid (Figure 1-1) is that of a three-carbon sugar molecule with a fatty acyl or alkyl group at the *sn*-1, fatty-acyl groups at the *sn*-2 positions, and a characteristic phosphate ester group at the sn-3 position of glycerol. The major distinct classes of glycerophospholipids are subdivided based on the nature of the polar "head group" at the *sn*-3 position of the glycerol backbone in eukaryotes and eubacteria or the *sn*-1 position in the case of archaebacteria [8].

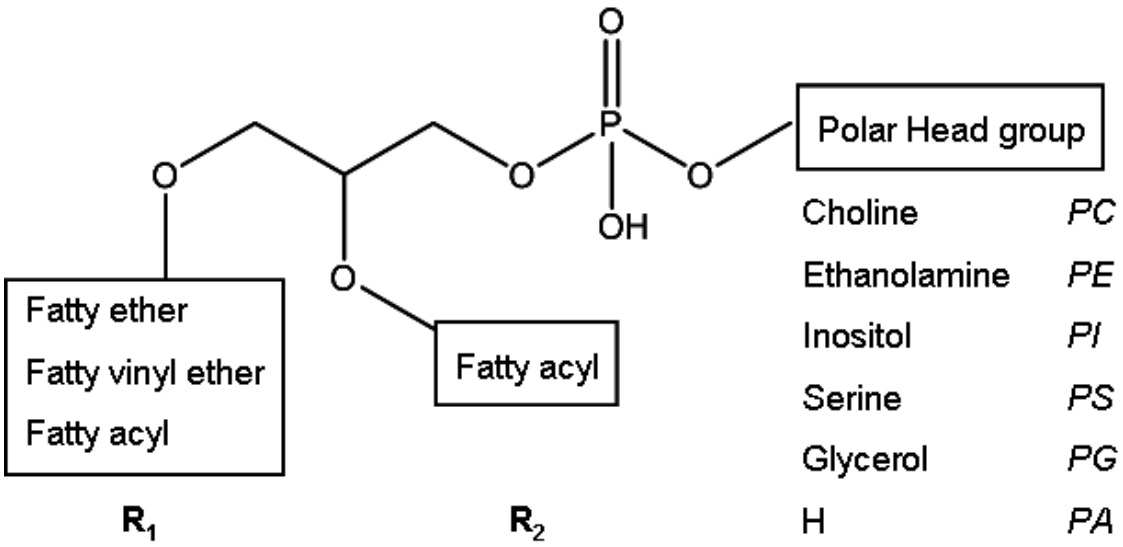

Figure 1-1 Structural relationships of glycerophospholipid classes. Different classes have either ester (acyl), alkyl ether (alkyl) or vinyl ether (alk-10-enyl) substituents at *sn*-1, fatty-acyl substituents at *sn*-2, and a polar head group at the *sn*-3 position of glycerol. The abbreviations used throughout this review are indicated for each polar head group.

Approximately 60% of the lipid mass of eukaryotic cell membrane are composed of phospholipids [9]. Minute changes in phospholipids can lead to major consequences on cell membrane function and viability. Fatty acids that are esterified at the *sn*-1 and *sn*-2 positions of the glycerol backbone can very in length from 14 to 22 carbons and can

have from 0 to 6 double bonds [10]. The nomenclature of phospholipid is due to the polar head group: phosphatidylcholine (PC), phosphatidylethanolamine (PE), phosphatidylinositol (PI), phosphatidylglycerol (PG), phosphatidylserine (PS) and phosphotidic acid (PA) as shown in Table 1-1. The cell membrane has an asymmetrical distribution of phospholipids. PE and PS are the major phospholipids found in the inner cytosolic membrane while the outer leaflet is primarily composed of PC [11]. Most cell membranes are composed of phosphatidyl linkages [9]. The *sn*-2 bond for the fatty acid is always an ester bond and unsaturated fatty acids are more possible. The format *x*:*y* represents the number of carbons is *x* and the number of double bonds is *y* for the common notation of a molecular species. Over 1000 individual molecular species of phospholipids can be devised in theory.

Name	**Head group**	**Structure**
Phosphatidylcholine	Choline	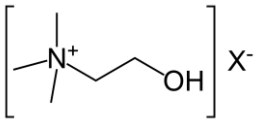
Phosphatidylinositol	Inositol	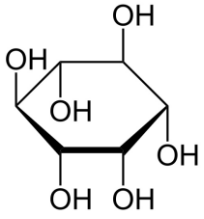
Phosphatidylglycerol	Glycerol	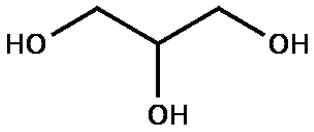

phosphatidylserine	Serine	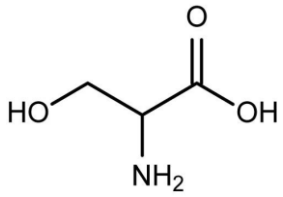
Phosphatidylethanolamine	Ethanolamine	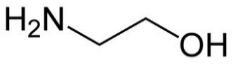

Table 1-1 Various polar head groups link to the phosphate group at the *sn*-3 poition.

The quantitative study of lipids, or "lipidomics", is a burgeoning field in bioanalytical chemistry [12-14]. Low detection limits are important to lipid studies because some lipids occur in trace (picomolar (10^{-12}) to nanomolar (10^{-9})) and even ultratrace (femtomolar (10^{-15}) and below) concentrations in samples [15-17]. Two branches of chemical analysis play an important role in "omics": separation science and mass spectrometry. In lipidomics, distinct subclasses of lipids, obtained by liquid extraction from a cell or tissue mass, are isolated by solid phase extraction, liquid chromatography, or thin-layer chromatography and then analyzed by a further dimension (or two) of liquid chromatography and two or more dimensions of mass spectrometry [9, 18]. One difficulty in profiling the chemical population of a small sample is that the lipidome exists over a wide range of concentrations. The most critical issue in analyzing such samples is that the less abundant species can easily get lost if the sample is wasted during inefficient sample processing steps. In addition, a relatively large amount of sample is required in some commonly used techniques such as thin layer chromatography (TLC) [19, 20]. One way to overcome these issues is to reduce sample transfer steps and

dead volume by applying a microchip platform for all or part of the sample preparation scheme.

Micro total analysis system (μTAS) also called "lab-on-a-chip" is a novel technique of which the applications are addressing fundamental biological questions, creating new biomedical reagents, and developing innovative cell and biochemical assays that shrink an entire experimental device to the scale of a microscope slide [21, 22]. The system is able to offer improved performance, smaller amounts of sample consumption, lower cost, and higher throughput. Additionally, it is essential for understanding physiologic and pathologic processes at the cellular level by investigating the intracellular contents of single cells. Chemical analysis and chemical synthesis are the two main fields of μTAS, which are of significant interest to biological, medical, and pharmaceutical societies. Many of these concepts were brought to fruition by the application of basic photolithography to creation of channels in glass microchips [23-27]. During the past 2 decades, the field of microfluidics has grown to include not only chips that separate compounds by capillary electrophoresis (CE) [28] but also chips that create gradients, chips that integrate cell lysis with DNA capture, and even chips that allow for nanoscale reactions. Highly assembled microchips have been developed to capture multiple single cells, lyse them, perform chemical reactions and detect chemical species in individual cells. Cell lysis is generally performed by either chemical or physical methods to rupture the cell phospholipd membrane with the goal of extracting intracellular contents. Different cell lysis methods have been developed on microfluidic platforms including chemical lysis, mechanical lysis, electrical lysis, thermal lysis, and other lysis methods.

When on a chip, the use of reduced volumes of solvent and electrophoretic separation can eliminate the need for the centrifugation and resuspension. This multidisciplinary field is comprised of physicists, chemists, engineers, and biologists all working to get the most out of these devices. The ability of microfluidic devices to efficiently handle complex samples and subsequently perform the required analytical operations on the same chip will be essential to the final successful applications of microfluidic systems. The integration of sample pretreatment within microfluidic devices has recently become an important area of emphasis in the field of μTAS. However, there are very few reports in the area of microfluidic chips associated with lipid extraction for lipidomics analysis.

The standard approach to lipid class isolation is based on either thin-layer chromatography (TLC) or solid-phase extraction (SPE), both of which are applied after a modified Bligh-Dyer extraction [29]. The biggest problem with TLC or SPE is that sample sizes are generally large (grams of tissue, $>10^7$ cells). In this chapter, a novel method for a microchip-based solid phase extraction for purification and enrichment of microscale glycerophospholipids is described. Specifically, intact bacterial cells loaded onto a chip were immediately lysed to release their lipid content. The released lipids were captured on a stationary phase and eluted with a suitable elution solvent. The nonpolar tails of the membrane lipids were captured by the nonpolar C18 beads of the column, while the polar head groups of the lipids were captured by the polar silica beads. On-chip lipid extraction efficiency and reproducibility were evaluated by comparison to the modified Bligh-Dyer method [29]. The purified lipids were reconstituted and injected directly into a quadrupole-time-of-flight mass spectrometer (Q-TOF MS) for analyzing

lipids content in the membrane. The characterization of phospholipids from lipid extracts by electrospray ionization (ESI) MS is based on the ability of each lipid class to acquire positive or negative charges when in solution under the ionization source high energy. Lipids that do not possess inherently ionizable moieties can also be ionized under the conditions of ESI. As long as there is sufficient dipole potential for interaction with counter ions, these species can be analyzed. As a result under suitable conditions of sample preparation, all molecular species that exist among cellular lipid classes can be detected in a single run of an on-chip lipid extraction. A single molecular ion with a mass-to-charge ratio (m/z) characteristic for the monoisotopic molecular weight is present for each molecular species. The MS data were analyzed using both the METLIN Personal Metabolite database [30] and the LIPID MAPS (www.lipidmaps.org) database by integrating with MassHunter Qualitative Analysis software for lipidomics discovery profiling. Several specific lipid databases and software packages have been developed (Table 1-2) over last ten years. The approach of the LIPID MAPS has attempted to establish a standard platform for lipid nomenclature [14, 31]. METLIN Personal Metabolite database is designed specifically for metabolomics, which may also be employed for lipid identification and quantification. With this method, we were able to identify over 170 phospholipid species from bacterial cell extracts.

Name	Comments	Web site
LIPID MAPS	Open-access, Web search engine	http://www.lipidmaps.org
Lipid Bank	Open-access, Web search engine	http://lipidbank.jp
METLIN	Open-access, Web search engine	http://metlin.scripps.edu

	for metabolomics studies	
AMDMS-SL	A freeware package designed for shotgun lipidomics	http://www.shotgunlipidomics.com
MZmine 2	A freeware package designed for metabolomics studies	http://mamine.sourceforge.net
LipidView	Commercial software that performs complete data analysis	http://www.mdssciex.com
LIMSA	A freeware package that can be downloaded from the Web	http://www.helsinki.fi
LipidX	A subset of the systems biology freeware Systems X	http://www.systemsm.ch
LipidQA	A freeware package that can be downloaded from the Web	http://msr.dom.wustl.edu

Table 1-2 Databases and software packages for lipid analysis.

1.3 Experimental

1.3.1 Reagents

34:2 phosphatidylcholine (PC) and 34:1 phosphatidylinositol (PI) were purchased from Sigma-Aldrich (St. Louis, MO). All solvents were HPLC grade from Fisher Scientific (Pittsburgh, PA) and were filtered through a 0.22 μm nylon membrane filter (Whatman). Tri(hydroxymethyl) aminomethane (Tris) was from Fisher Scientific.

Omnipur egg white lysozyme was purchased from EMD Chemicals (Gibbstown, NJ). A buffer solution for system washing was adjusted to 7.5 with 20 mM Tris

1.3.2 Microchip Fabrication

Microchips were fabricated roughly according to standard photolithographic technique [32]. Schott Borofloat glass plates (1.5mm thick, Telic Company, Santa Monica, CA) precoated with chrome and AZ 1518 negative photoresist (5300 Å thick) were used to fabricate microchips by standard photolithographic techniques [33]. The primary design for the microchips used in this study is a T-shape channel (Figure 1-2A). The image for the desired chip features were designed in Adobe Illustrator (CS2, Adobe, Inc.) and were printed on a high-resolution inkjet printer (Canon Pixma Pro900, 4800 × 2400 dpi). The chip features were clear on the photomask. Clear glass covered by photomask was placed in a laminar flow hood, Arilean 600 PCR Workstation (Raleigh, NC) with a red light to prevent damaging the mask, and they were exposed under UV radiation , Spectroline SB-100PC of 60 MHz, 1.05 Amp, and long wavelength of 365nm (Westbury, NY), for transferring the pattern to the photoresist for 30 second.

The exposed photomask blank was then placed in 15 mL of AZ 300 MIF developer (AZ electronics materials USA Corp., Somerville, NJ). The solution was swirled over the top of the photomask blank for 30 seconds to solubilize the exposed region of the photoresist. The developed blank was then rinsed with deionized water for 40 seconds to remove the developer, after which it was placed in 25 mL of CR-9

Chromium Photomask Etchant (Cyantek Corp, Freemont, CA) and was swirled over the top of the photomask blank for 1-2 min until the chrome was removed. The mask was then rinsed again for 40 seconds with deionized water to remove any remaining chrome in the channels. Before the photomask blank was etched, the initial width of the channel was measured using a microscope with an optical scale, and determined to be 100 μm. In order to produce a channel with a width of 300 μm and a depth of 200 μm, both top and bottom masks had line features that were 100 μm wide. A channel with a total depth of 200 μm was made by etching both the top and bottom of glass pieces 100 μm deep, and each channel was etched laterally by 100 μm, giving a channel that was 300 μm wide at its axis (Figure 1-2B). The glass was etched using a 14:20:66 (v/v/v) HNO3/HF/H2O solution with the total etching time of 28 min. The etching of the weirs in Figure 1-2C was observed under a light microscope and a zoom stereomicroscope (Leica Wild, Wetzlar, Germany), and the plate was rinsed with deionized water. The remaining chrome and photoresist were removed and the glasses were washed thoroughly.

Using an Accu Press drill (DynaArt Design, Lancaster, CA), and a diamond tipped drill bit (0.75mm), fluidic access holes were drilled in the wells at the end of each channel for capillary connections. Water was poured onto the access holes while drilling to keep the glass from cracking. More importantly, the drill bits would vaporize from heat if not cooled with water. The chip glass was vigorously washed with deionized water. Three pieces of the microchip were cut from the photomask blank using a glasscutter, and then rinsed with deionized water using a water spigot. The drilled chips were placed in 15 mL of RS-120 Resist Stripper (Cyantek Corp., Fremont, CA) at 50 ^{o}C for 5 minutes to remove the remaining photoresist. The solution was swirled until all of

the remaining resist had dissolved and then rinsed with deionized water for 2 minutes. The glass chips were then placed into CR-9 chrome etchant and swirled until the remaining chrome was dissolved. After that, they were rinsed with deionized water and then placed in 15 mL of nanostrip (Cyantek Corp., Fremont, CA) to remove any remaining organic solvents on the chips. The chips were then swirled in nanostrip for 3 minutes and then rinsed again for 40 seconds in deionized water. The water spigot was used to trace the channels to remove any excess debris. The plates were subsequently placed in RCA solution, made up of 75.0 mL deionized water, 15.0 mL NH_4OH mixed on a hot plate at 60°C. 15.0 mL of H_2O_2 was added to the RCA solution, after which the chips were put into this solution, and swirled for 30 minutes. The chips were removed from the solution and each piece was rinsed and cleaned thoroughly for 5 minutes with deionized water using the water spigot to ensure proper bonding.

The top and bottom chip were subsequently brought into contact while still wet and were held together by capillary action. Finally, the assembly was placed in a furnace (Lindberg/Blue Moldatherm, Thermo Fisher Scientific Inc., Asheville, NC). The furnace temperature was raised at a rate of 10 °C/min to 80 °C and was held for 30 min, after which it was ramped at the same rate to 610 °C and held for 8 h. The temperature was then decreased to room temperature at a rate of 10 °C /min. The chips were examined with the stereoscope to ensure that they were properly aligned and no shift occurred during the bonding process [34, 35]. The weir structures were fabricated by leaving a gap in the channels in the photomask that was etched only part way through. The isotropic etching process created a very small open portion at the top with a sloping bottom in the channel. When bonded to a top channel, the net result was a channel with a

double trapezoidal structure, 120 μm wide at top and bottom, 300 μm wide in the middle, with an elliptical weir that was about 10-15 μm wide at the widest (top to bottom) (Figure 1-2).

The microchip was firstly conditioned by sequentially pumping about 100 μL each of 1 M sodium hydroxide, deionized water, and methanol before packing. The packing material used as the stationary phase was either spherical silica gel (100 Å, 20 μm, Sorbent Technologies, Inc., Norcross, GA) or C18 silica gel (100 Å, Luna 15 μm, Phenomenex, Torrance, CA). A slurry of packing material made with methanol was introduced to the reservoir on the side arm of the chip by applying a mild vacuum through the other two reservoirs using pipet tips attached to a vacuum pump (Figure 1-2D). The packing was done under a zoom stereomicroscope. Once the chips were packed, the lower bead-hole of the T-shape was sealed with epoxy and left to dry overnight before use (Figure 1-2E). Adhesives were placed around the other two wells, to which the nanoports were attached. The nanoport of one well was connected with PEEK tubing of the injection pump, by which water was passed through the channel to test the flow of each chip.

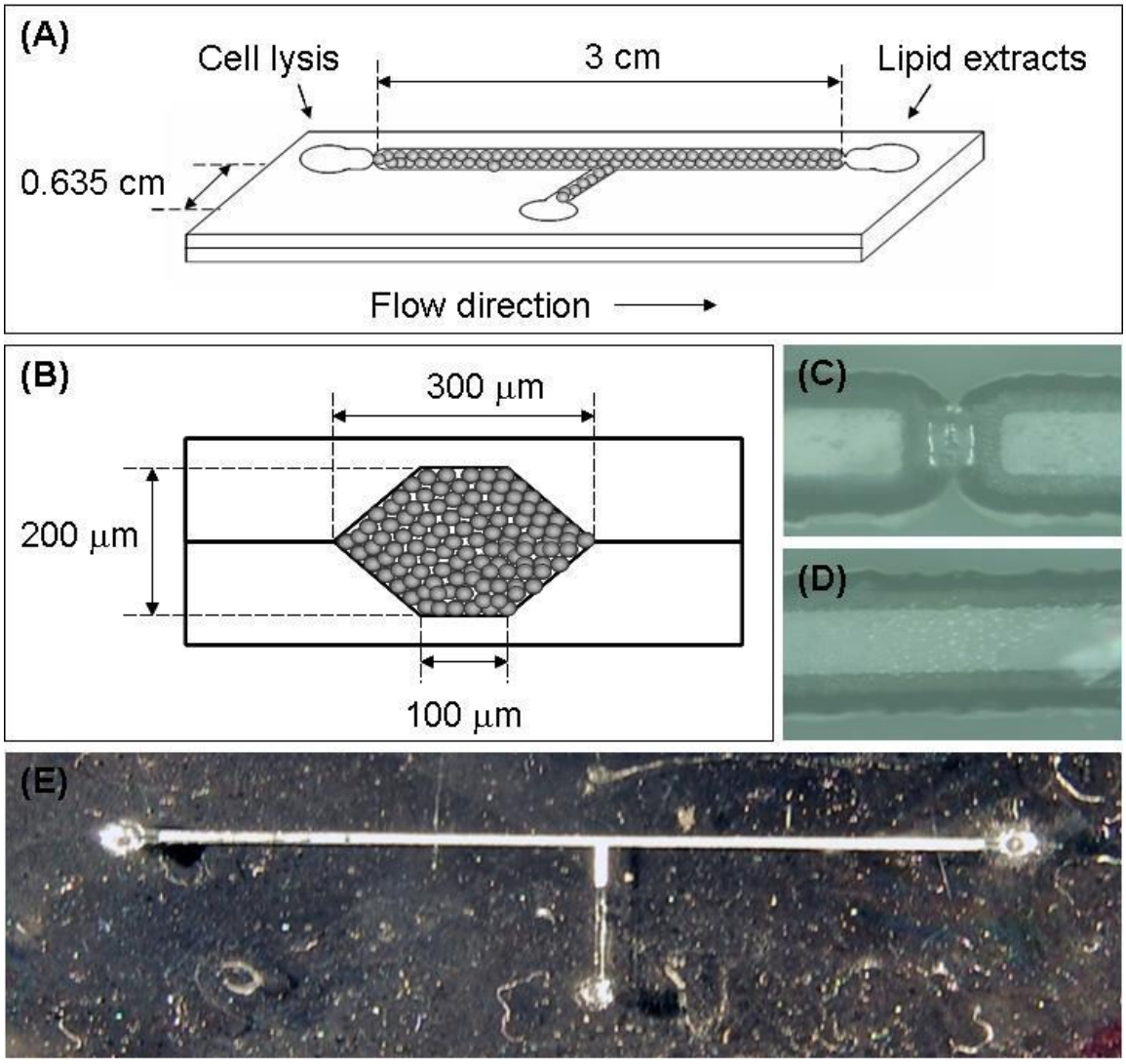

Figure 1-2 Design of the microfluidic device. (A) The schematics of the microchip for cell lysis and lipid extraction. (B) Cross-sectional diagram of the SPE channel. (C, D) Images of the weir structure and the packed column. (E) Silica beads are packed in the microchannel through the bead-hole on the side-arm of the chip using a mild vacuum until the channel is fully packed.

1.3.3 Online Extraction System

The home-built microfluidic chip apparatus for solid phase extraction consisted of a Harvard Apparatus model 11 syringe pump (Harvard Apparatus, Holliston, MA) and a 250 μL Hamilton gastight syringe (Hamilton, Las Vegas, NV). Reagents were injected using an HPLC type injection valve (Rheodyne 7725, Rohnert Park, MA) with a 40 μL injection loop. The injection port was connected to the chip with polyether ether ketone (PEEK) tubing (1/16 in. o.d. × 0.010 in. i.d., Upchurch, Oak Harbor, WA) and custom pressure holders or Upchurch Nanoports (Figure 1-3). To flush out any unreacted species and prepare the solid phase for extraction, freshly filled microchips were conditioned with 20 mM Tris buffer (pH 7.5) for 30 min at 10 μL/min. The solid phase was reconditioned under the same conditions for 10 min before each extraction step. The primary extraction protocol consisted of three pressure driven wash steps, each performed at a flow rate of 10 μL/min. First, the injection valve was switched to "load" and 20 μL of the lysing agent was loaded onto the chip. A sample of 10 μL of cells was injected immediately thereafter, followed by loading of another 20 μL of lysing agent onto the bed. The valve was then switched back to "inject", and 100 μL of the wash solution (20 mM Tris buffer) was flowed through the chip to eliminate proteins and other potential nonlipid materials. Finally, the purified lipids were eluted in selected eluent (methanol, isopropanol, or acetonitrile on a silica bed; chloroform/methanol, 2:1 (v/v) or tetrahydrofuran/methanol, 1:1 (v/v) on a C18 bed) and were collected in sample vials for subsequent mass spectrometry analysis. To eliminate carry-over, the solid phase was flushed with methanol for 30 min at a rate of 10 μL/min between each run.

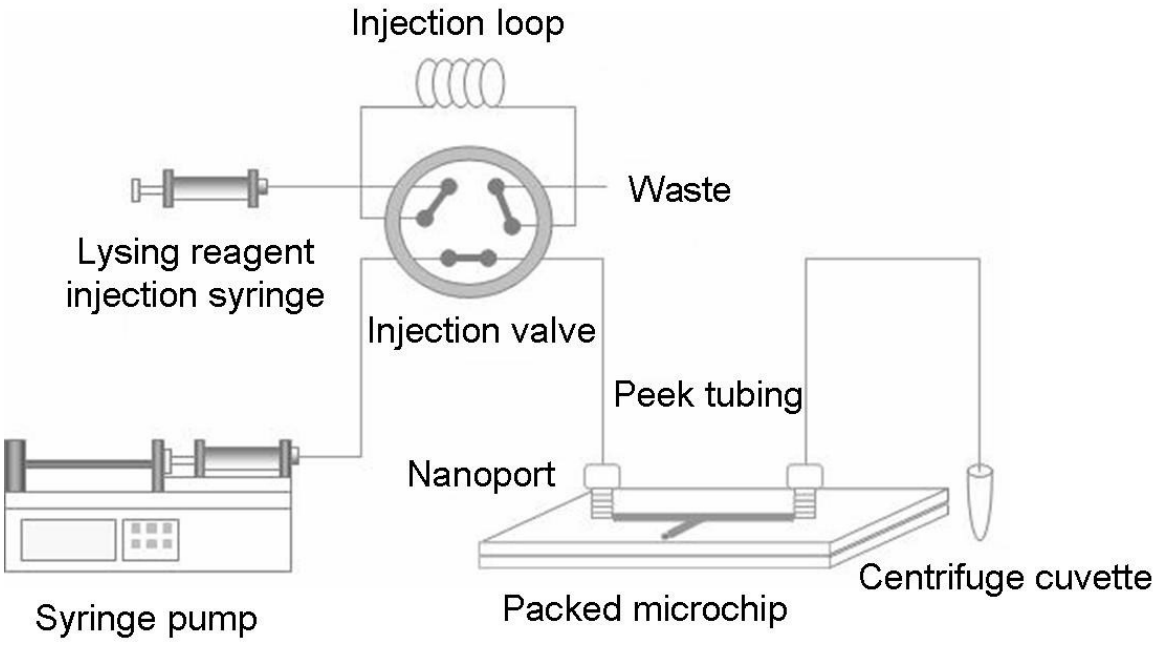

Figure 1-3 The microdevice setup used for extraction of lipid from bacterial cells. The flow system consists of a syringe pump, which is connected to an HPLC type injection valve for loading the lysing agent and Tris buffer to the microchip.

1.3.4 Cell Staining and Lysis

Sulfurospirillum barnesii strain SES-3 cells were kindly provided by Dr. P. Basu, Duquesne University. *S. barnesii* is a readily available arsenate respiring bacterium with a simple lipidome [36, 37]. The cells were treated with a cell-labeling dye that stains intact cells but displays a large decrease in fluorescence when cells are completely lysed [38]. The dye DiO (Invitrogen Molecular Probes, Inc., Carlsbad, CA) was prepared according to the manufacturer's instructions, and the prepared stock solution was stored at -20 °C. To stain the cells, a 0.5 mL portion of live cells was placed in a microcentrifuge tube. A volume of 1 μL of 1:100 diluted DiO stock solution was added

to the live cells, and the contents were vortexed for 1 min. The final concentration of the dye was 0.6 M.

A solution of washed *S. barnesii* strain SES-3 cells was prepared as follows. First, 0.5 mL of cells was placed in a 37 °C water bath for 8 min. After heating, the tube was centrifuged for 5 min at 6 900g, during which a pellet was formed and the supernatant was subsequently removed. The cells were then washed in 0.5 mL of 20 mM Tris buffer, and a pipet was used to break up the cell pellet. The tube was vortexed for 1 min, then centrifuged for another 5 min at 6 900g. The supernatant was removed and discarded after centrifugation. The pellet was finally resuspended in 0.5 mL of 0.15 M Tris buffer.

Lysing agent was prepared by adding 20 mg of Omnipur egg white lysozyme (EMD Chemicals, Gibbstown, NJ) to 6 mL of 20 mM Tris HCl buffer with a pH of 7.5. To lyse the cells, the lysing agent was loaded onto the microchip by syringe flow using a Harvard PHD 2000 syringe pump at a flow rate of 10 μL/min for 24 s followed by loading of the stained cells for 12 s. The lysing agent was then flowed over the bed at the same flow rate for another 24 s. The loading time was calculated to take into account any dead volume of the column and tubing.

In the loading and lysis steps, cells were imaged fluorescently at the inlet reservoir of the microchip using a Nikon Eclipse E-600 microscope with a 100 W mercury lamp. A FITC-HYQ filter set (excitation bandpass filter 480 (20 nm, dichroic reflector 505 nm cut-on, and emission bandpass filter 535 (25 nm) was applied for the imaging. The images were recorded using a RT-slider camera and a QED camera standalone program. The contrast of the images was enhanced using Adobe Photoshop

CS4.

1.3.5 Modified Bligh-Dyer Method and Thin Layer Chromatography

In our protocol, 0.2 mL of cultured cells were mixed with 0.75 mL of chloroform/methanol, 1:2 (v/v) and vortexed for 1 min. A volume of 0.25 mL of chloroform and 0.25 mL of deionized water containing 1% acetic acid were added into the mixture and vortexed for another 1min. The solution was subsequently centrifuged at 1300 rpm for 5 min. The lower phase was collected with a Pasteur pipet and then evaporated followed by reconstitution in 0.5 mL of methanol with 10 mM NH4OH. Samples were introduced into the electrospray ionization-quadrupole (ESI-Q) mass spectrometer for lipid profiling, and the profile was compared to that obtained using the microchip method.

A TLC method was used to facilitate developing a separation of the main phospholipids classes present in the cell membranes. TLC was performed on silica gel plates, which were pretreated (full length) in a Camag horizontal developing chamber to remove impurities by methanol: ethyl acetate (6:4). The plates were activated for 10 minutes at 130^{o}C. Phospholipids, extracted according to Bligh and Dyer, were loaded to TLC plate at 10 mm from the edge using 10 µl capillary pipette 5 times. 500 ng/µl of each standard phospholipid, phosphatidylethanolamine (PE), phosphatidylinositol (PI), sphingomyelin (SM), and their mixture, were also applied on TLC plate.

The plate was developed in a developing chamber containing dichloromethane: ethyl acetate: acetone (80:16:4) for 70 mm to separate cholesterol, free fatty acid, and triglycerides from phospholipids to prevent overloading of the silica particles at the start position. The plate was dried under an air stream (40^{o}C) for 10 minutes. The phospholipids were subsequently separated by chloroform: ethyl acetate: acetone: isopropanol: ethanol: water: acetic acid (30:6:6:6:16:28:6:2) elution for 55 mm. The plate was dried for 5 minutes at 130^{o}C and placed into the iodine staining chamber face down at a 45^{o} angle, with the top of the plate on the bottom of the chamber. After 5 minutes, the plate was removed and immediately placed face down on the bed of the scanner to ensure minimal evaporation of iodine. The images were cropped and saved in compressed TIFF format for further analysis [39-42].

1.3.6 Mass Spectrometry Conditions

The characterization of phospholipids from lipid extract by ESI-MS is based on the ability of each lipid class to acquire positive or negative charges when in solution under the ionization source high energy. Lipids that do not possess inherently ionizable moieties can also be ionized under the conditions of ESI-MS, and as long as there is sufficient dipole potential for interaction with counter ions, these species can be analyzed. Thus under suitable conditions of sample preparation, all molecular species that exist among cellular lipid classes can be detected in a single run of an on-chip lipid extraction.

A single molecular ion with a mass-to-charge ratio (m/z) characteristic for the monoisotopic molecular weight is present for each molecular species.

In order to obtain higher resolution in spectrum, an Agilent 6520 nano electrospray ionization quadrupole time-of-flight (nanoESI-Q-TOF) mass spectrometer was used for lipid extracts profiling. Aliquots (20 μL) from loading, washing, and elution steps were collected during the extraction. The lipid extracts were dried by N_2 and resuspended in HPLC-grade methanol with 10 mM NH4OH. Samples were introduced by direct infusion using a Harvard PHD 2000 syringe pump at a flow rate of 70 μL/h. MS only data was acquired in both positive and negative ion modes. The following settings were maintained throughout the analysis: drying gas flow of 10 L/min, drying gas temperature of 350 °C, nebulizer pressure of 45 psi, data range of m/z 200-1000, acquisition rate of 1000 ms/spectrum, fragmentor voltage of 150 V, skimmer voltage of 60 V, octopole rf voltage of 250 V, and capillary voltage of 3.5 kV. Typically, a 1 min period of signal averaging in the profile mode was employed for each spectrum.

1.3.7 Data Analysis

METLIN Personal Metabolite database and LIPID MAPS database were applied for the identification of phospholipids species present in cell extracts. This application enabled us to enter the m/z value of an unknown lipid ion or a batch of lipids and predict the most likely molecular species, based on internally generated lists of side-chains and headgroups of phospholipids. LIPID MAPS database was set as: intensity threshold:

100; mass tolerance: +/- 0.01 amu; ion mode: $[M+H]^+$; sort by: molecular formula. Six major phospholipid classes were detected in positive and negative ion mode: phosphatidylinositols (PI), phosphatidylserines (PS), phosphatidylglycerols (PG), phosphatidylcholines (PC), phosphatidylethanolamine (PE), and phosphatidic acid (PA). Additionally, the lyso variants for all of the above mentioned phospholipids (LPI, LPS, LPG, LPC, LPE, and LPA) and phosphatidylinositol monophosphate (PIp) were also detected during the process.

1.4 Results and Discussion

1.4.1 Overview

The goal of this work was to create a simple microdevice for effective cell lysis followed by lipid capture, cleanup, and recovery. A few preconditions must be met in order to ensure a seamless coupling of solid phase extraction and a microfluidic platform. First, the lysing agent must effectively lyse intact cells in the volume present in the microchannel. Second, the released lipids must bind to the extraction bed successfully. Finally, the retained lipids must be eluted from the solid phase with high extraction efficiency and consistent reproducibility (recovery rate). A typical MS-based lipidomic workflow is illustrated in Figure 1-4, which shows that the initial step in data analysis is lipid identification.

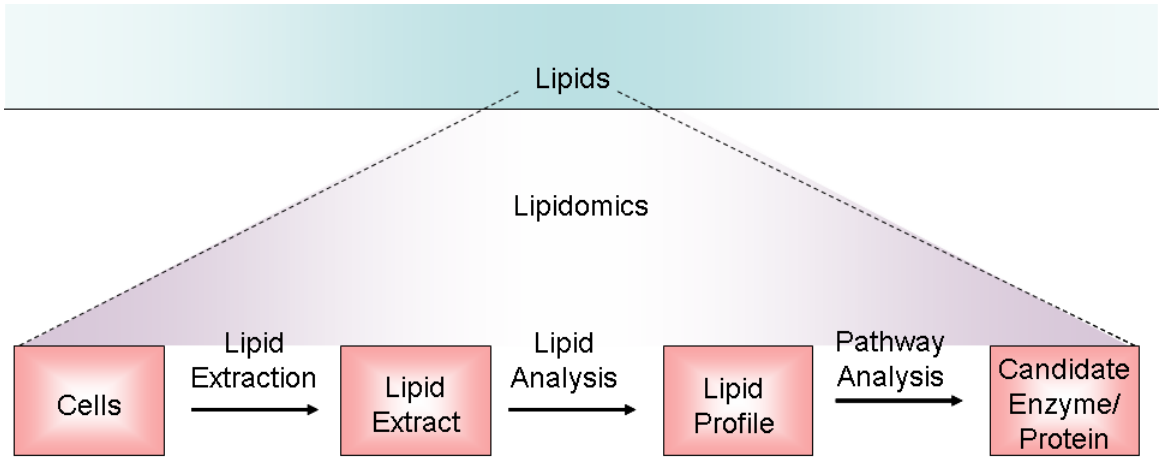

Figure 1-4 Workflow of lipidomics analysis in systems-level scale.

1.4.2 Evaluation of Lysing Agent

In order to consistently extract lipids from bacteria cells with high efficiency, it is necessary to lyse the cells completely. Figure 1-5A depicts the bacteria cells after the initiation of flow of the lysing agent into the inlet port of a complete microfluidic device. The fluorescence signal decreased after 1 min of flow and was undetectable after 3 min (Figure 1-5B), which confirms the sufficient lysis of the cells. Thus, these lysing conditions were applied in the subsequent experiments.

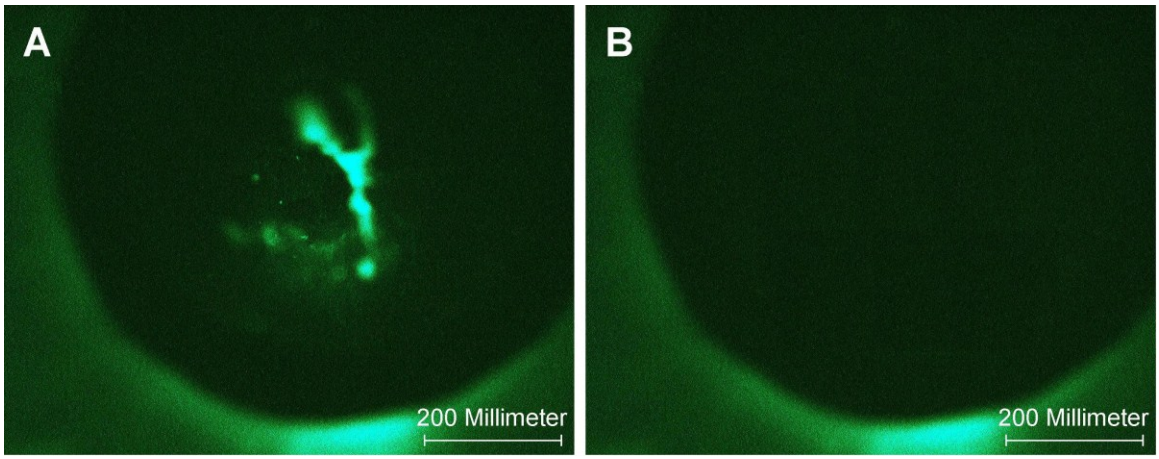

Figure 1-5 Fluorescence images of on-chip cell lysis under microscopy at 20× magnification. (A) Image taken when DIO labeled cells were flowed into the inlet irradiated with 480-560 nm light. (B) Image taken after flow of the lysing agent over 3 minutes.

1.4.3 Effect of Lipid Extraction

As the lysing agent for cell lysis had been chosen, it was necessary to make sure that released lipids successfully adsorbed to silica surfaces. Several purification goals must be achieved to recover phospholipids from cells and adsorb them to the silica phase in a single step. To make the purification protocol as simple and effective as possible, cell lysis and lipid binding to silica surfaces were accomplished using one single loading buffer. Several factors are taken into account when choosing the loading buffer. Solutions of high ionic strength facilitate the adsorption of phospholipids on the stationary phase as a result of a variety of interactions. At higher ionic strength, the negative potential of silica surfaces is reduced, thereby decreasing the electrostatic repulsion between the negatively charged phospholipid molecules and the bead surface.

However, high concentrations of salt reduce the water activity due to the formation of hydrated ions, which facilitates the dehydration of phospholipids and silica surfaces and drives the lipid to the extraction bed [43]. The electrostatic repulsion can be further reduced if the phospholipid is dissolved in a loading buffer below the pKa of the silica (pKa ≈ 8), due to the fact that increasing protonation of the surface silanol groups reduces the surface charge [44-46]. In addition, extremely acidic loading buffer conditions could affect the solubility of lipids and may induce precipitation, which could ultimately lead to a failure of the microfluidic device. Consequently, a buffer of 20 mM Tris HCl with pH of 7.5 was chosen for phospholipid adsorption to silica surfaces.

According to previous research on the physicochemical properties of silica materials for lipid extraction, surface properties play a critical role in the extraction of hundreds or even fewer cells [47, 48]. Size and shape of the particles, diameter and volume of the pores, and the packing and resin porosity are of major concerns to the overall effectiveness of phospholipid binding. In this work, two types of silica resins, silica beads (100 Å, 20 μm) and C18 beads (100 Å, Luna 15 μm), were selected as the packing material to adsorb the phospholipids. The microporous structure prevents the macromolecular proteins from going through the beads while keeping small analytes including polar lipids from entering and being retained.

The performance of lipid extraction on the microchip was evaluated by extraction efficiency and reproducibility during the purification process. The recovery of phospholipids from the device was accomplished using various elution solvents with high ionic strength. Methanol, chloroform and acetonitrile were used on silica phase while 2:1 chloroform/methanol and 1:1 tetrahydrofuran/ methanol were used on C18 phase. An

electrospray ionization-quadrupole (ESI-Q) mass spectrometer (Waters ZMD MS) was utilized in the study of lipid species profiling. The lipid extracts were eluted by methanol (Figure 1-6), acetonitrile (Figure 1-7) and isopropanol (Figure 1-8) on microchip packed with silica beads.

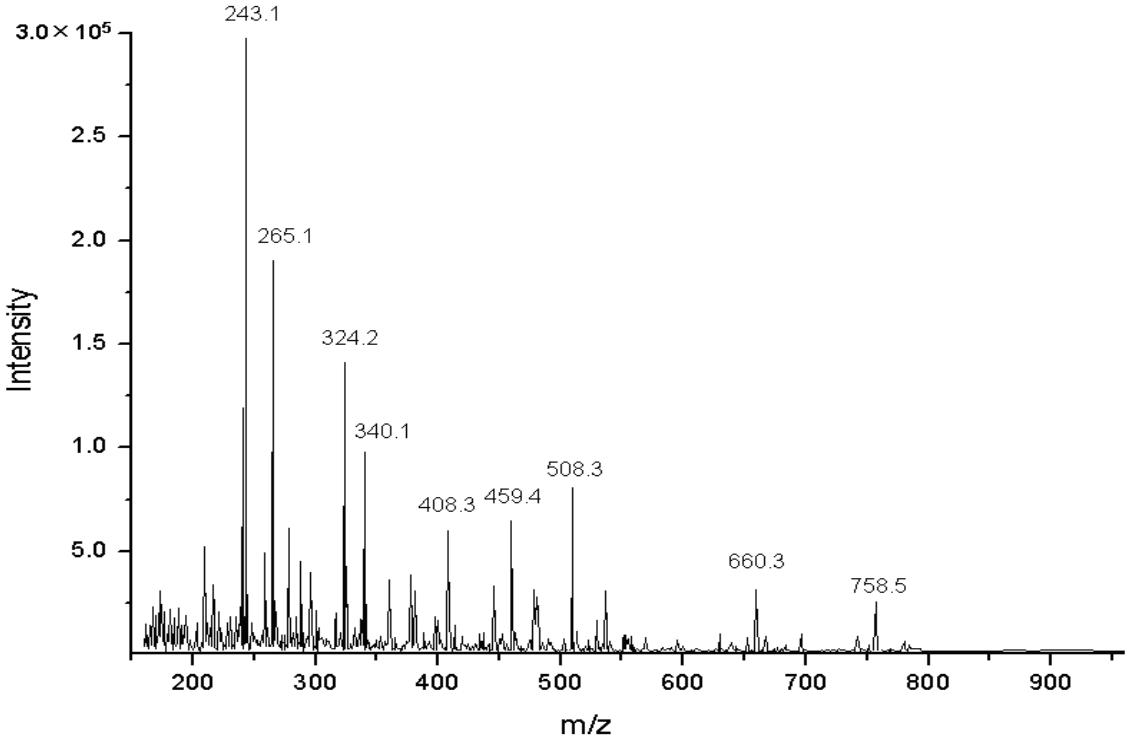

Figure 1-6 ESI-Q MS profile of lipid extracts eluted by methanol from silica packing microchip.

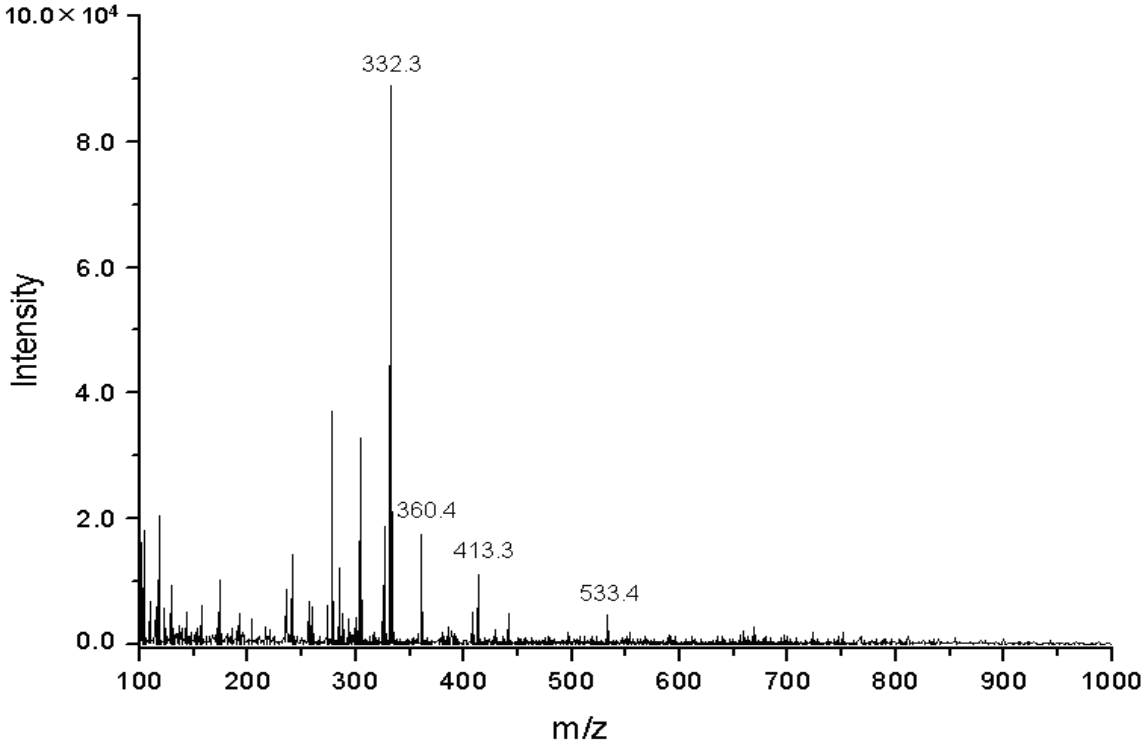

Figure 1-7 ESI-Q MS profile of lipid extracts eluted by acetonitrile from silica packing microchip.

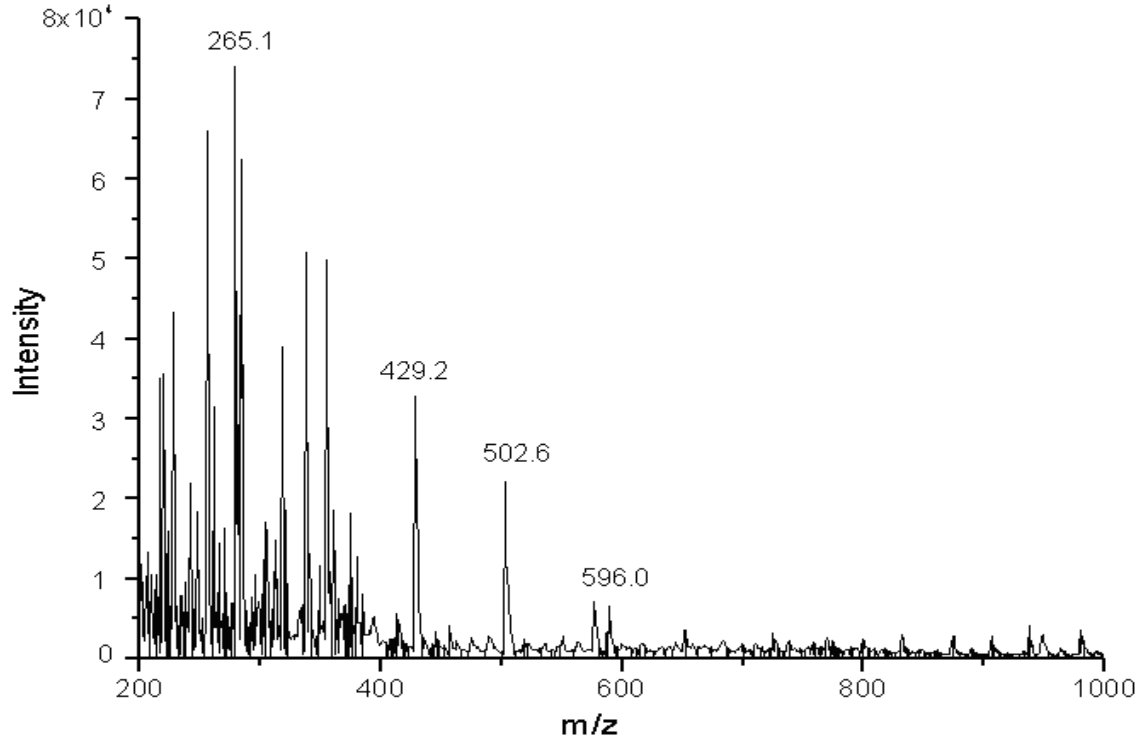

Figure 1-8 ESI-Q MS profile of lipid extracts eluted by isopropanol from silica packing microchip.

Lipids were also extracted by 2:1 chloroform/methanol (Figure 1-9) or 1:1 tetrahydrofuran/ methanol (Figure 1-10) on the microchip packed with C18 beeds. A shift in overall mass in going from C18 to silica was observed, which indicates different extraction efficiency and tendency by using different eluents.

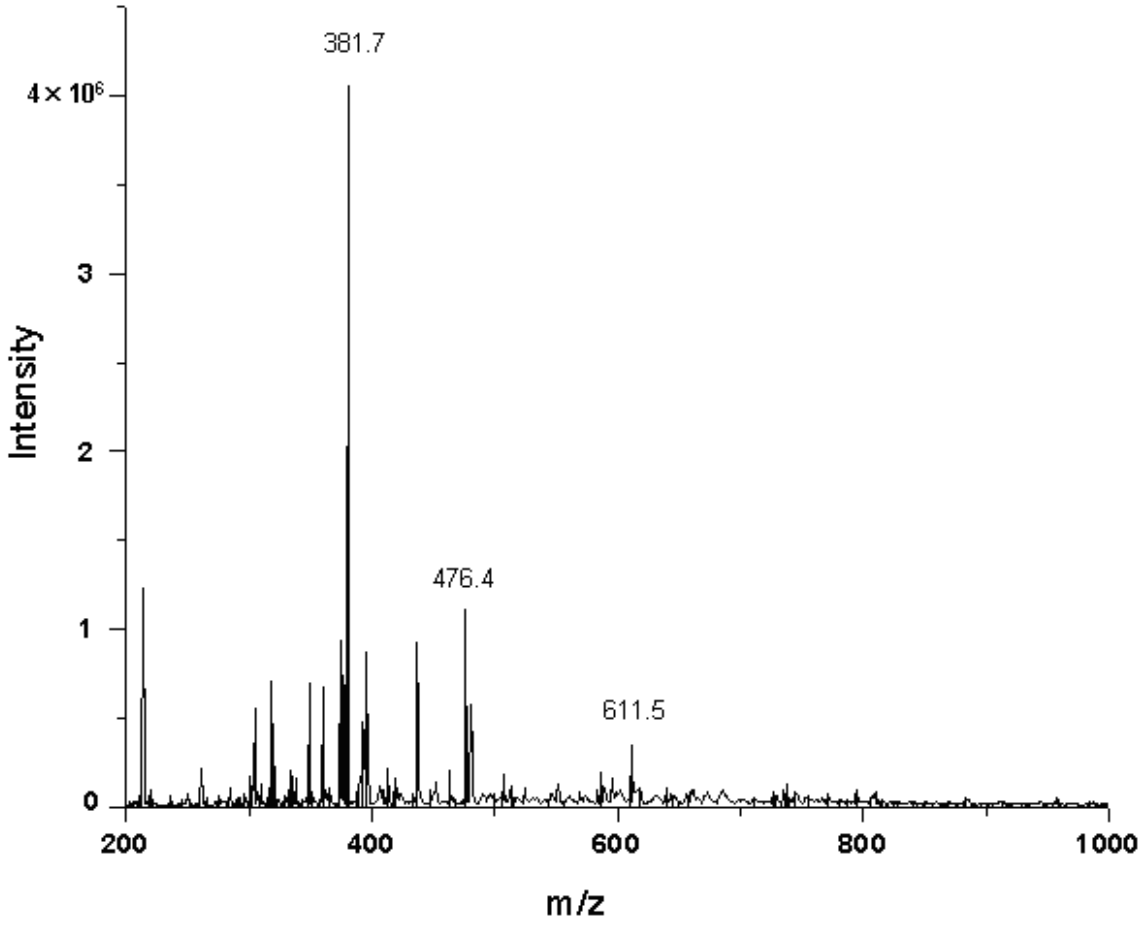

Figure 1-9 ESI-Q MS profile of lipid extracts eluted by 2:1 chloroform/methanol from C18 packing microchip.

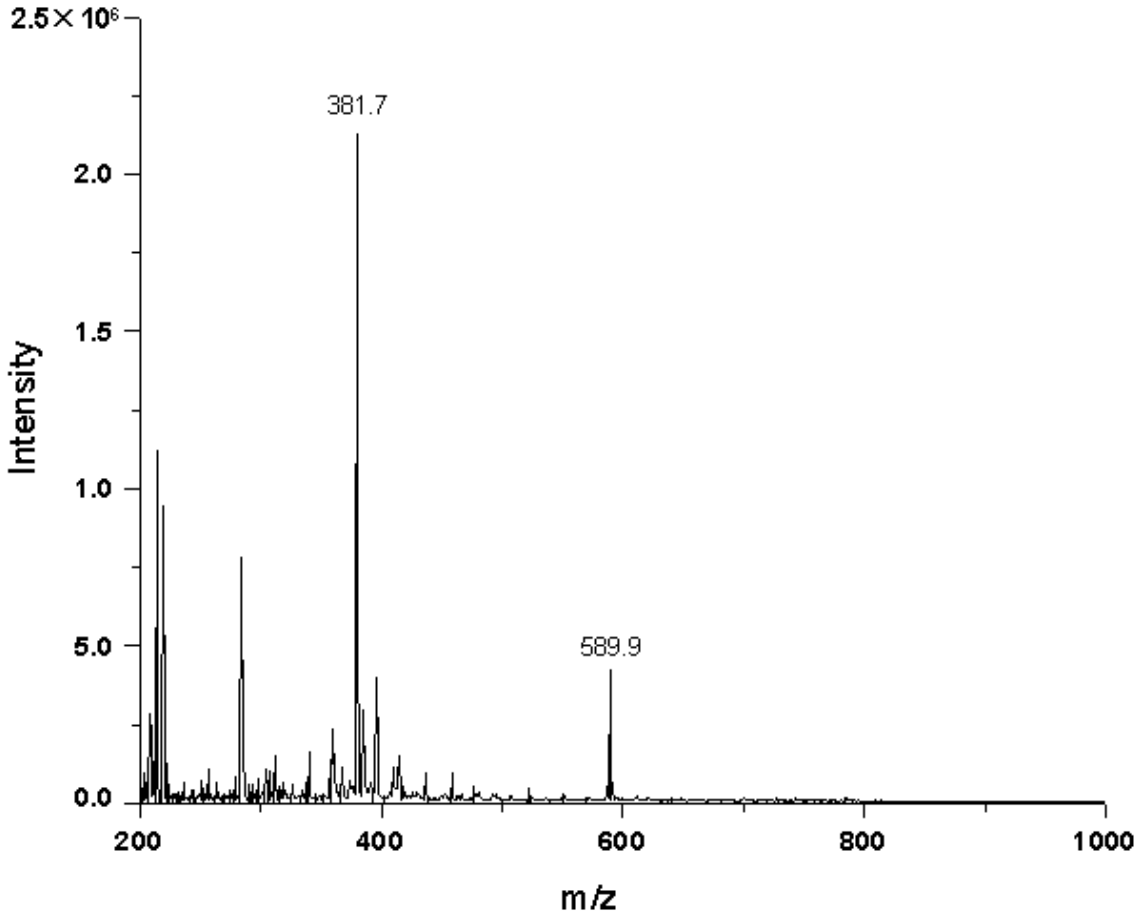

Figure 1-10 ESI-Q MS profile of lipid extracts eluted by 1:1 tetrahydrofuran/methanol from C18 packing microchip.

In contrast to loading buffer, the eluent exhibited a slightly higher back-pressure due to its high viscosity, which caused a drop in flow rate to 8 μL/min. In order to evaluate the lipid extraction efficiency, the numbers of identified phospholipid species extracted from the microchip by different eluents were compared with that obtained by the modified Bligh-Dyer method (Figure 1-11)

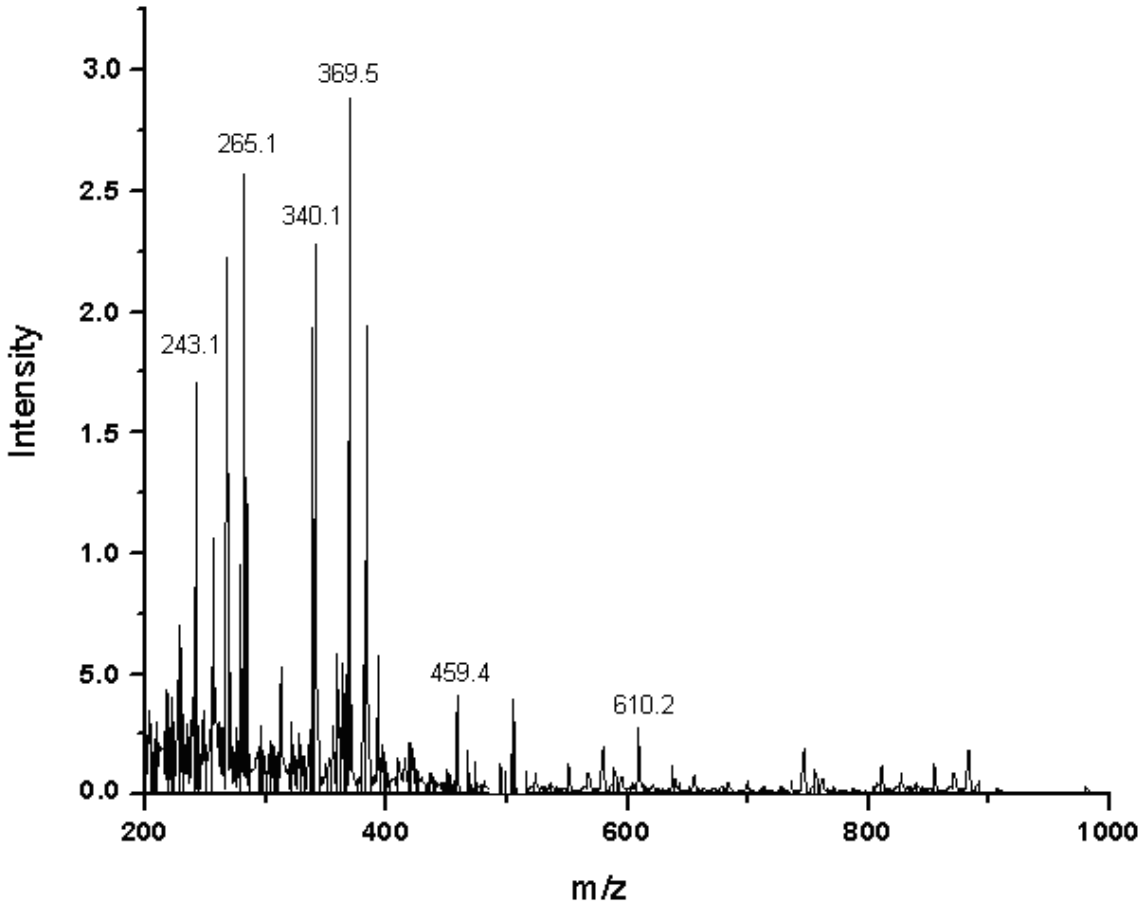

Figure 1-11 ESI-Q MS profile of total lipid extracts by Bligh and Dyer extraction methed.

The overall extraction efficiencies of the silica chip with different eluents were 83.3% (methanol), 49.3% (isopropanol), and 29% (acetonitrile), respectively (Figure 1-12). When the phospholipids were eluted from the C18 chip by chloroform/methanol (2:1, v/v) or tetrahydrofuran/methanol (1:1, v/v), the on-chip extraction efficiencies were 71.7% and 61.8% compared to that obtained using the modified Bligh-Dyer method (Table A-1 in Appendix I). Thus, silica beads were selected as the packing material with methanol as the eluent for lipid extraction in subsequent experiments. Lipid extracts from Bligh and Dyer were run through thin layer chromatography to identify the

component of lipid classes. Non-phospholipids (CE, TG, FFA) were separated from target lipids to upper plates. PI and PE were identified comparing to standards selected (data not shown). TLC was used to prove that total lipid extraction from the cell by Bligh and Dyer method did extract the expected phospholipids.

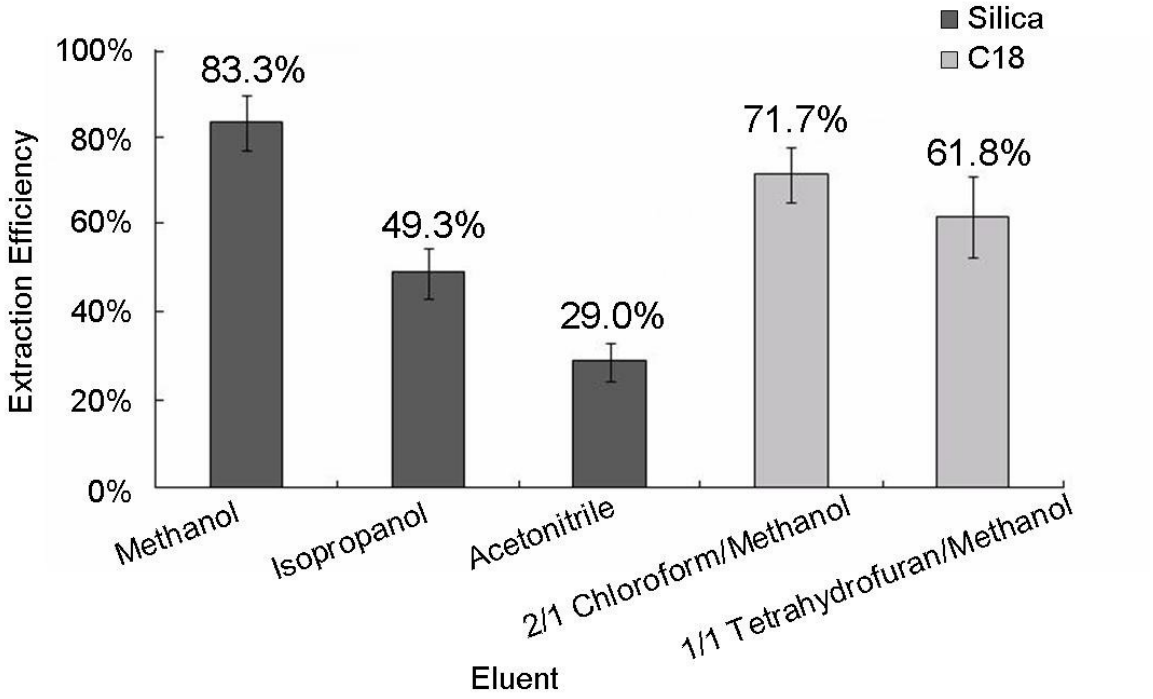

Figure 1-12 Comparison of on-chip extraction efficiencies of phospholipid using different eluents. Silica (black) and C18 (gray) resins were applied as packing materials. The error bars represent the variation of four individual experiments. Values represent mean ± S.E. of triplicate determinations.

1.4.4 Reproducibility

Before each extraction, the silica beads were reconditioned by flushing methanol for 30 min, followed by another flush with 20mMTris buffer for 10min. In a measurement where 10 μL of 34:2 phosphatidylcholine (PC) and 34:1 phosphatidylinositol (PI) (Sigma-Aldrich Chemical Co., St. Louis, MO) standard mixture were loaded at a final concentration of 5 μM for 10 successive extractions, the average phospholipid recovery rate for the microchip was 55.34% and 46.12%, respectively (Figure 1-13). It is shown that the reproducibility of lipid extraction from the silica bed decreases after the fourth run. In order to overcome this issue, new silica beads were packed to the chip, and the lipid recovery rate went back to around 65% for 34:2 PC. In summary, the microchip packed with fresh silica beads is capable of being reused four times without any loss in the lipid extraction process.

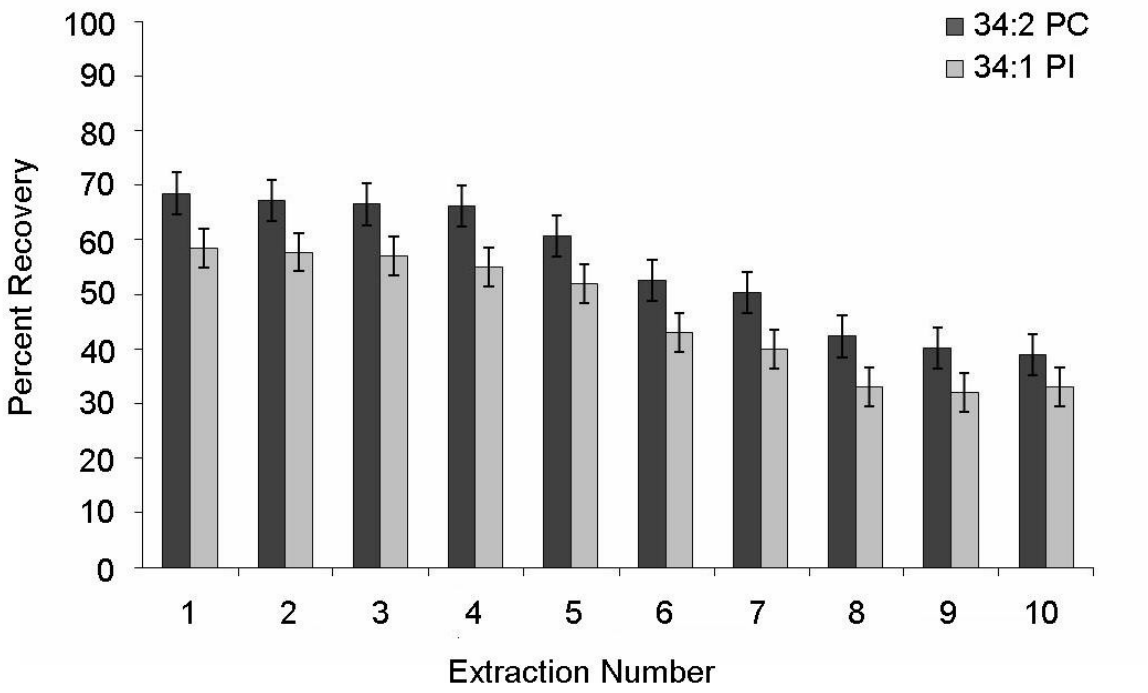

Figure 1-13 Phospholipid recovery rate on the microchip over ten successive extractions. Standard mixtures of 5 μM 34:2 PC (black) and 34:1 PI (gray) were used. Values represent mean ± S.E. of ten successive measurements in triplicate determinations.

1.4.5 Extraction Profile

To ensure that phospholipids were eluted from cells only when the eluent was applied, fractions were collected and analyzed for a phospholipid elution profile during extraction and the results are shown in Figure 1-14. During this extraction step, a sample of 10 μL cells sandwiched with 20 μL of lysing agent was loaded onto the silica bed at a flow rate of 10 μL/min. After a wash with 20 mM Tris HCl buffer (100 μL, pH 7.5), during which any nonlipid materials were removed, the lipids were eluted in methanol. A total of 18 fractions of the eluate (20 μL each) were collected at the outlet of the device

during each step of the extraction (cells loading/lysing, nonlipid materials washing, and lipids elution). The phospholipid 34:1 PI was chosen for lipid quantification during the extraction process by the nanoESI Q-TOF mass spectrometer. As shown in Figure 1-14, the major elution of 34:1 PI occurred in the first 80 μL of the elution phase, with negligible concentrations of lipid detected in other steps. This result indicates that there was no significant loss of lipid during the loading and washing steps, and most of the extracted 34:1 PI was eluted from the first several tens of microliters. These results are consistent with the fact that 34:1 PI was eluted reproducibly in the first 80 μL of the elution phase, which suggests that the lysing agent/loading buffer did not interfere with binding of the lipid to the silica bed or impact lipid recovery negatively.

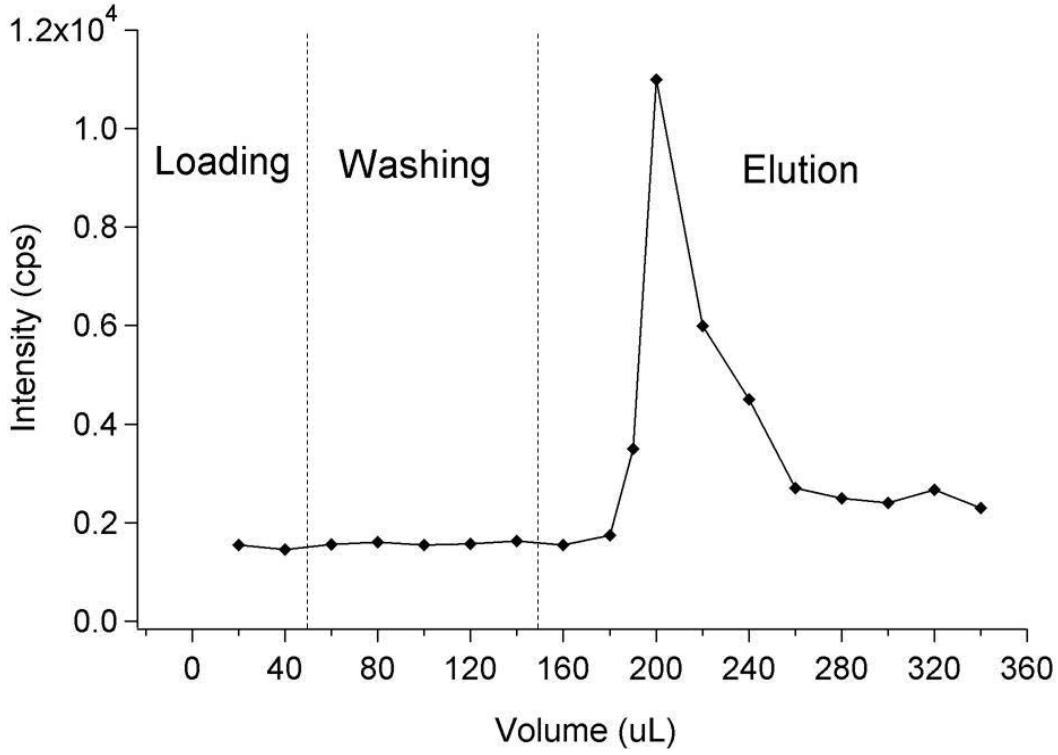

Figure 1-14 Extraction profile of 34:1 PI from the silica chip eluted by methanol. Fractions (20 μL in volume) were manually collected during loading, washing and elution steps.

1.4.6 Data Analysis

In order to identify the molecular species of phospholipids from *S. barnesii* cells, the nanoESI-Q-TOF MS/ MS was applied along with "untargeted" (discovery profiling) approaches for lipidomics research. The data analysis workflow consists of interrogation of lipid extracts data files from MS by a METLIN Personal Metabolite database and LIPID MAPS database. LIPID MAPS provides a platform that has the versatility to quantify known individual lipid molecular species and search for novel lipids affecting biological systems. With the list of possible identities significantly narrowed, phospholipid species were identified using a custom subset of the METLIN Database relevant to lipid metabolites in the mode of accurate-mass information searching. Sample data files were subsequently imported in MassHunter Qualitative Analysis software (Analyst QS) by loading the lipid database that contains the empirical formula of each lipid species. The data files were queried by each formula using a "Find by Formula" function, which finds and extracts all the coeluting isotopes, salt adducts, and dimers that belong to each empirical formula.

Six major classes of phospholipid and their lyso variants were identified with this method. Within these classes, each of the target mass identified in the profiling processes was searched against the METLIN database over a 10 ppm mass window. A mass error window of 5 ppm was set for the empirical formula calculation. Three major lipid classes, PC, PS, and PE, are detected in positive ionization mode (+ESI) [49-52], while

four major lipid classes, PI, PS, PG, and PA, are detected in negative ionization mode (-ESI) [53-55]. Their representative diagnostic ions are illustrated in Table 1-3. In addition, the lyso variants for all these phospholipids (LPE, LPC, LPA, LPI, LPS, and LPG) can be detected in both modes. Finally, the results from METLIN searches were incorporated into Excel spreadsheets for further interpretation.

Lipid Class	Diagnostic ion	Ionization mode
Phosphatidylcholine	184	Positive
Phosphatidylethanolamine	141	Positive
	196	Negative
Phosphatidic acid	153	Negative
Phosphatidylinositol	241	Negative
Phosphatidylserine	185	Positive
	87	Negative
Phosphatidylglycerol	172	Negative

Table 1-3 Diagnostic ions used for identification of major lipid classes in MS/MS

A link to the LIPID MAPS database was also provided to predict possible phospholipids species present in the cell extracts. This application allows for input of the m/z value of an unknown lipid ion or a batch of lipids to predict the most possible molecular species, based on internally generated lists of side-chains and head groups of glycerophospholipids and sphingophospholipids. The parameters used were listed as follows: intensity threshold of 1000, mass tolerance of ±0.01 amu, and ion mode of $[M + H]^+$ or $[M - H]^-$.

Low mass peaks (below m/z 350) were assigned to free fatty acid as a result of in-source collision-induced fragmentation. Peaks of lyso variants for all kinds of phospholipids were in the range of m/z 350-600. Most of the major phospholipid classes (PE, PC, PG, PS, PA, and PI) fell in the range between m/z 600 and 1000, which consisted of about 70% (about 380 peak envelopes) of the MS peaks (Figure 1-15A and 15B). As shown in Figure 1-15C and 15E, 34:2 PC was detected with $[M + H]^+$ = 758.561, and a characteristic phosphocholine headgroup peak at m/z 184.073 was shown in the MS/MS spectrum by applying 20 eV on the extracted parent ion. Relatively small peaks of lysophosphotidylcholines ($[LPC + H]^+$ and $[LPC - H_2O + H]^+$) correspond to the loss of one fatty acyl substitute as a ketene $[M - R_2CH=C=O]^+$. In Figure 1-15D and 15F, the peak of m/z 835.585 was assigned to 34:1 PI and its parent ion was extracted for fragmentation at 45 eV. Lysophosphotidylinositols ($[LPI - H]^-$ and $[LPI - H_2O - H]^-$), lysophosphatidic acids ($[LPA - H_2O - H]^-$), and the characteristic headgroup fragments including glycerophosphoinositols ($[GPI - H_2O - H]^-$ and $[GPI - 2H_2O - H]^-$), fatty acid ($[FA - H]^-$), inositolphosphate ($[IP - H_2O - H]^-$ and $[IP - 2H_2O - H]^-$), and glycerophosphate ($[GP - H_2O - H]^-$) were observed for the specific PIs identification. Fragmentation of these phospholipid species in both ionization modes yielded a wealth of structural information. In each case, the lipid identification process was aided by headgroup fragmentation, lyso-lipid formation, and fatty acid fragments. With the use of the LIPID MAPS mass prediction tool, many possible phospholipids species and their structures (double bonds, carbon numbers of fatty acyl chains, and head groups) were determined. Table A-2 in the Appendix II shows a summary of the proposed phospholipids based on METLIN database [56] and LIPID MAPS database matches of

the measured mass of the parent ions with their theoretical mass over complementary approach for identification of phospholipid isomers.

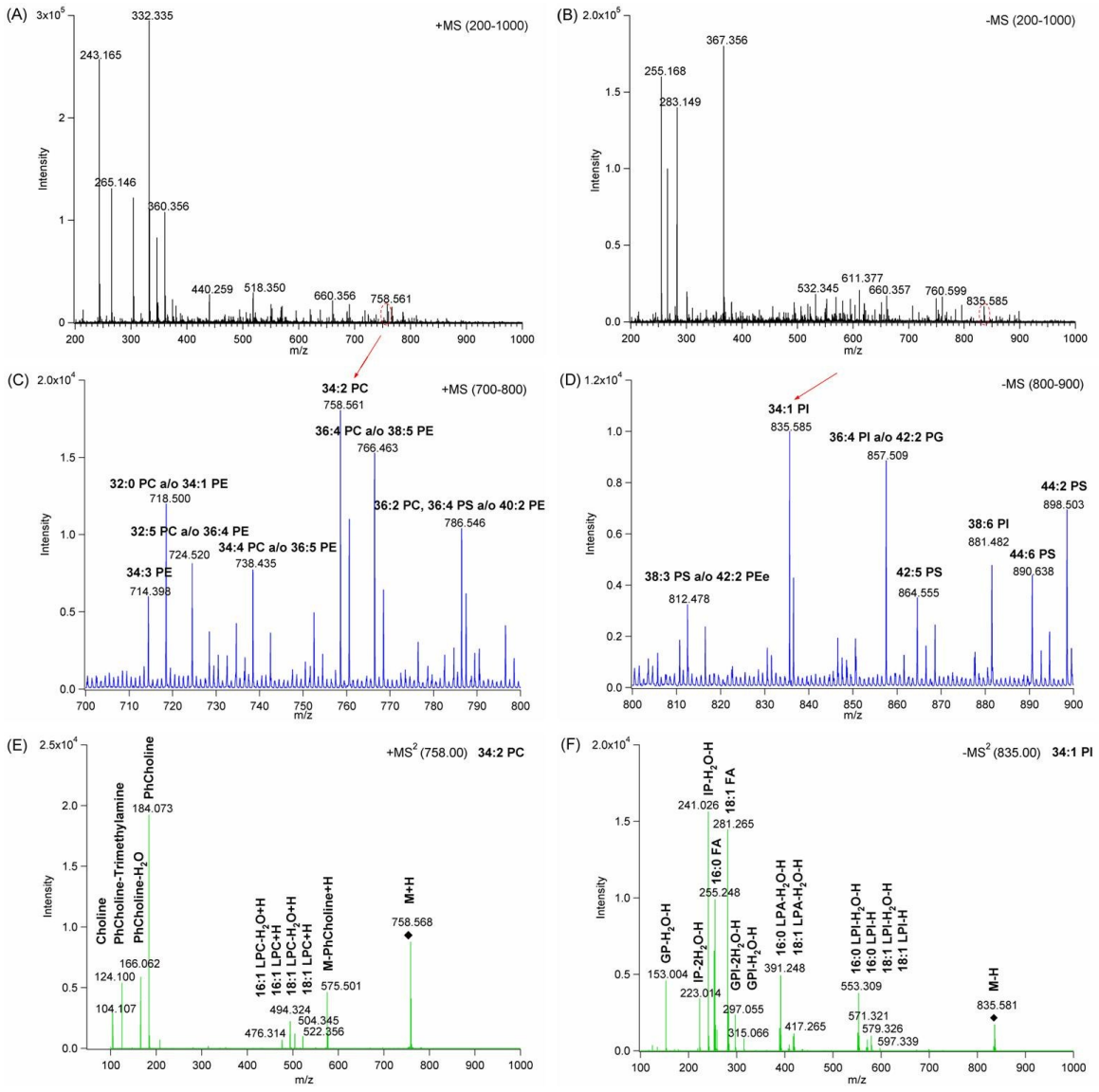

Figure 1-15 Mass spectra of phospholipid extracts from *S. barnesii* cells eluted from silica bed of microchip by methanol. Six major lipid classes were detected in positive (A) and negative (B) ionization modes, e.g. 34:2 PC (C) and 34:1 PI (D) were detected and their structures were identified with corresponding tandem mass spectra (E, F).

Empirical formulae prediction software (Analyst QS) was used to support the stages of data processing. To the information of the mass to charge ratios of molecular ions provided by the MS spectrum data, the criteria for filtering the most possible ions were as follows: possible elements C, H, P, O; adducts $[M+H]^-$, $[M+NH_4]^+$, $[M-H]^-$; mass tolerance 10 ppm. Within 10 ppm in mass error window, empirical formulae of the analytes were independently matched to the predicted values. Over 170 of identified phospholipids and lysophospholipids with 12-44 total carbons were comprised by peaks that matched the criteria. Some peaks had more than one possible lipid species that matched the empirical formulae in the same error score. These peaks were identified by the corresponding fragmentation patterns using the tandem mass spectrometry in order to obtain detailed information of the molecular ions. With this "untargeted" lipidomics approach, as many as 173 phospholipid species were identified from on-chip bacterial cell extracts (See Appendix II).

1.5 Conclusions

A microscale solid phase extraction method was developed for the extraction of glycerophospholipids from bacteria cells with integration to analysis by small scale lipidomics. A buffer solution of 20 mM Tris HCl at pH 7.5 containing 20 mg of omnipur egg white lysozyme was demonstrated to work effectively as a lysing agent for *Sulfurospirillum barnesii* strain SES-3 cells on microfluidic devices. Among different types of stationary phase and elution solvent for lipid capture tested, the best extraction

was obtained by using a silica phase with methanol as the eluent with the efficiency of 83.3% (Figure 1-16). Lipids purified with the developed method were suitable for subsequent lipidomics analysis and compared favorably with lipids extracted by a commonly utilized Bligh-Dyer method. By incorporation of both fast and robust peak finding algorithms and visualization software, many phospholipids were found to have matches to the METLIN and LIPID MAPS databases. In summary, this work presents a highly efficient method for microchip based solid phase extraction for use with microscale lipidomics.

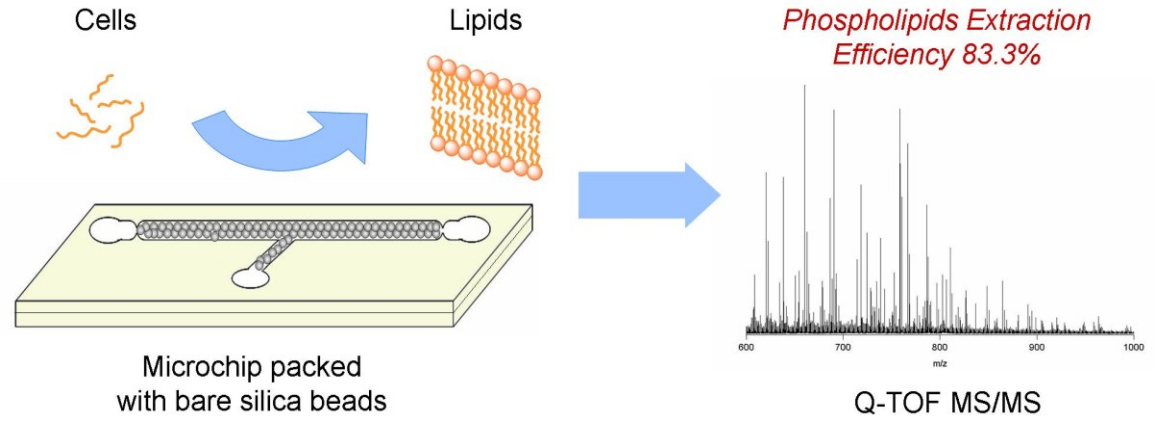

Figure 1-16 Scheme of on-chip lipid extraction with lipidomics study by Q-TOF MS.

1.6 Acknowledgements

This research is funded by National Science Foundation (Grant 0821401) and National Institutes of Health/National Institute of Neurological Disorder and Stroke (Grant R15- NS038443). We thank Dr. Partha Basu (Duquesne University, Department

of Chemistry and Biochemistry) for providing *Sulfurospirillum barnesii* samples. We also acknowledge Dr. Jana Patton-Vogt (Duquesne University, Department of Biological Sciences) and Dr. Stephanie J. Wetzel (Duquesne University, Department of Chemistry and Biochemistry) for their constructive comments, which improved the quality of the manuscript. We also have to thank the principle investigator of this project, Dr. Mitchell E. Johnson.

1.7 References

1. Brasaemle, D. L., Thematic review series: Adipocyte Biology. The perilipin family of structural lipid droplet proteins: stabilization of lipid droplets and control of lipolysis. *Journal of Lipid Research* **2007,** 48, (12), 2547-2559.

2. van Meer, G.; Voelker, D. R.; Feigenson, G. W., Membrane lipids: where they are and how they behave. *Nat. Rev. Mol. Cell Biol.* **2008,** 9, (2), 112-124.

3. Wymann, M. P.; Schneiter, R., Lipid signalling in disease. *Nat. Rev. Mol. Cell Biol.* **2008,** 9, (2), 162-176.

4. Kulinski, A.; Rustaeus, S.; Vance, J. E., Microsomal Triacylglycerol Transfer Protein Is Required for Lumenal Accretion of Triacylglycerol Not Associated with ApoB, as Well as for ApoB Lipidation. *Journal of Biological Chemistry* **2002,** 277, (35), 31516-31525.

5. Small, D. M.; Craven, B. M., Handbook of Lipid Research. *Handbook of Lipid Research* **1986,** 4, 149-182.

6. Maclouf, J.; Murphy, R. C.; Henson, P. M., Transcellular sulfidopeptide leukotriene biosynthetic capacity of vascular cells. *Blood* **1989,** 74, (2), 703-707.

7. Fischer, M.; Bueeler, H.; Lang, Y.; Bluethmann, H.; Lipp, H. P.; DeArmond, S. J.; Prusiner, S. B.; Aguet, M.; Weissmann, C., Normal development and behaviour of mice lacking the neuronal cell-surface PrP protein. *Nature* **1992,** 356, 577-582.

8. Peret, J.; Lpez-Garca, P.; Moreira, D., Ancestral lipid biosynthesis and early membrane evolution. *Trends in Biochemical Sciences* **2004,** 29, (9), 469-477.

9. Han, X.; Gross, R. W., Shotgun lipidomics: Electrospray ionization mass spectrometric analysis and quantitation of cellular lipidomes directly from crude extracts of biological samples. *Mass Spectrometry Reviews* **2005,** 24, (3), 367-412.

10. Schiller, J.; S, R.; Arnhold, J.; Fuchs, B.; Leig, J.; Mller, M.; Petkovi, M.; Spalteholz, H.; Zschrnig, O.; Arnold, K., Matrix-assisted laser desorption and ionization time-of-flight (MALDI-TOF) mass spectrometry in lipid and phospholipid research. *Progress in Lipid Research* **2004,** 43, (5), 449-488.

11. Bevers, E. M.; Comfurius, P.; Dekkers, D. W.; Harmsma, M.; Zwaal, R. F., Transmembrane phospholipid distribution in blood cells: control mechanisms and pathophysiological significance. *Biological chemistry* **1998,** 379, (8-9), 973-86.

12. Wenk, M. R., The emerging field of lipidomics. *Nat. Rev. Drug Discov.* **2005,** 4, (7), 594-610.

13. Han, X., Neurolipidomics: challenges and developments. *Front. Biosci.* **2007,** 12, 14.

14. Fahy, E.; Subramaniam, S.; Brown, H. A.; Glass, C. K.; Merrill, A. H.; Murphy, R. C.; Raetz, C. R. H.; Russell, D. W.; Seyama, Y.; Shaw, W.; Shimizu, T.; Spener, F.; van Meer, G.; VanNieuwenhze, M. S.; White, S. H.; Witztum, J. L.; Dennis, E. A., A comprehensive classification system for lipids. *Journal of Lipid Research* **2005,** 46, (5), 839-862.

15. Axelsen, P. H.; Murphy, R. C., Quantitative analysis of phospholipids containing arachidonate and docosahexaenoate chains in microdissected regions of mouse brain. *Journal of Lipid Research* **2010,** 51, (3), 660-671.

16. Yan, K.-P.; Hao, J.; Dan, N.; Chen, C., A Simple and Improved Method for Extraction of Phospholipids from Hemoglobin Solutions. *Artificial Cells, Blood Substitutes and Biotechnology* **2008,** 36, (1), 19-33.

17. Ivanova, P. T.; Milne, S. B.; Myers, D. S.; Brown, H. A., Lipidomics: a mass spectrometry based systems level analysis of cellular lipids. *Current Opinion in Chemical Biology* **2009,** 13, (5-6), 526-531.

18. Han, X.; Gross, R. W., Global analyses of cellular lipidomes directly from crude extracts of biological samples by ESI mass spectrometry. *Journal of Lipid Research* **2003,** 44, (6), 1071-1079.

19. Paglia, G.; Ifa, D. R.; Wu, C.; Corso, G.; Cooks, R. G., Desorption Electrospray Ionization Mass Spectrometry Analysis of Lipids after Two-Dimensional High-Performance Thin-Layer Chromatography Partial Separation. *Analytical Chemistry* **2010,** 82, (5), 1744-1750.

20. Rohlfing, A.; Müthing, J.; Pohlentz, G.; Distler, U.; Peter-Katalinić, J.; Berkenkamp, S.; Dreisewerd, K., IR-MALDI-MS Analysis of HPTLC-Separated Phospholipid Mixtures Directly from the TLC Plate. *Analytical Chemistry* **2007,** 79, (15), 5793-5808.

21. Chen, X.; Cui, D.; Liu, C.; Li, H.; Chen, J., Continuous flow microfluidic device for cell separation, cell lysis and DNA purification. *Analytica Chimica Acta* **2007,** 584, (2), 237-243.

22. Reyes, D. R.; Iossifidis, D.; Auroux, P.-A.; Manz, A., Micro Total Analysis Systems. 1. Introduction, Theory, and Technology. *Analytical Chemistry* **2002,** 74, (12), 2623-2636.

23. Jacobson, S. C.; Hergenroder, R.; Koutny, L. B.; Ramsey, J. M., High-Speed Separations on a Microchip. *Analytical Chemistry* **1994,** 66, (7), 1114-1118.

24. Jacobson, S. C.; Hergenroder, R.; Moore, A. W., Jr.; Ramsey, J. M., Precolumn Reactions with Electrophoretic Analysis Integrated on a Microchip. *Analytical Chemistry* **1994,** 66, (23), 4127-4132.

25. Jacobson, S. C.; Hergenroeder, R.; Koutny, L. B.; Ramsey, J. M., Open Channel Electrochromatography on a Microchip. *Analytical Chemistry* **1994,** 66, (14), 2369-2373.

26. Jacobson, S. C.; Koutny, L. B.; Hergenroeder, R.; Moore, A. W.; Ramsey, J. M., Microchip Capillary Electrophoresis with an Integrated Postcolumn Reactor. *Analytical Chemistry* **1994,** 66, (20), 3472-3476.

27. Seiler, K.; Harrison, D. J.; Manz, A., Planar glass chips for capillary electrophoresis: repetitive sample injection, quantitation, and separation efficiency. *Analytical Chemistry* **1993,** 65, (10), 1481-1488.

28. Jemere, A. B.; Oleschuk, R. D.; Harrison, D. J., Microchip-based capillary electrochromatography using packed beds. *Electrophoresis* **2003,** 24, (17), 3018-3025.

29. Bligh EG, D. W., A rapid method of total lipid extraction and purification. *Can J Biochem Physiol* **1959,** 37, (8), 7.

30. Smith, C. A.; Maille, G. O.; Want, E. J.; Qin, C.; Trauger, S. A.; Brandon, T. R.; Custodio, D. E.; Abagyan, R.; Siuzdak, G., METLIN: A Metabolite Mass Spectral Database. *Therapeutic Drug Monitoring* **2005,** 27, (6), 747-751.

31. Fahy, E.; Subramaniam, S.; Murphy, R. C.; Nishijima, M.; Raetz, C. R. H.; Shimizu, T.; Spener, F.; van Meer, G.; Wakelam, M. J. O.; Dennis, E. A., Update of the LIPID MAPS comprehensive classification system for lipids. *Journal of Lipid Research* **2009,** 50, (Supplement), S9-S14.

32. Jacobson, S. C.; Hergenroder, R.; Koutny, L. B.; Warmack, R. J.; Ramsey, J. M., Effects of Injection Schemes and Column Geometry on the Performance of Microchip Electrophoresis Devices. *Analytical Chemistry* **1994,** 66, (7), 1107-1113.

33. Ko, W. H.; Suminto, J. T., *Semiconductor Integrated Circuit Technology and Micromachining*. Wiley-VCH Verlag GmbH: 2008; p 107-168.

34. Jemere, A. B.; Oleschuk, R. D.; Ouchen, F.; Fajuyigbe, F.; Harrison, D. J., An integrated solid-phase extraction system for sub-picomolar detection. *Electrophoresis* **2002,** 23, (20), 3537-3544.

35. Yuen, P. K.; Kricka, L. J.; Fortina, P.; Panaro, N. J.; Sakazume, T.; Wilding, P., Microchip Module for Blood Sample Preparation and Nucleic Acid Amplification Reactions. *Genome Research* **2001,** 11, (3), 405-412.

36. Finster, K.; Liesack, W.; Tindall, B. J., Sulfurospirillum arcachonense sp. nov., a New Microaerophilic Sulfur-Reducing Bacterium. *International Journal of Systematic Bacteriology* **1997,** 47, (4), 1212-1217.

37. Luijten, M. L. G. C.; de Weert, J.; Smidt, H.; Boschker, H. T. S.; de Vos, W. M.; Schraa, G.; Stams, A. J. M., Description of Sulfurospirillum halorespirans sp. nov., an anaerobic, tetrachloroethene-respiring bacterium, and transfer of Dehalospirillum multivorans to the genus Sulfurospirillum as Sulfurospirillum multivorans comb. nov. *International Journal of Systematic and Evolutionary Microbiology* **2003,** 53, (3), 787-793.

38. Loew, L. M.; Simpson, L. L., Charge-shift probes of membrane potential: a probable electrochromic mechanism for p-aminostyrylpyridinium probes on a hemispherical lipid bilayer. *Biophysical journal* **1981,** 34, (3), 353-365.

39. Skipski, V. P.; Smolowe, A. F.; Sullivan, R. C.; Barclay, M., Separation of lipid classes by thin-layer chromatography. *Biochimica et Biophysica Acta (BBA) - Lipids and Lipid Metabolism* **1965,** 106, (2), 386-396.

40. Yu, R. K.; Ariga, T.; Alfred H. Merrill, J. Y. A. H., Ganglioside analysis by high-performance thin-layer chromatography. In *Methods in Enzymology*, Academic Press: 2000; Vol. Volume 312, pp 115-134.

41. Weerheim, A. M.; Kolb, A. M.; Sturk, A.; Nieuwland, R., Phospholipid Composition of Cell-Derived Microparticles Determined by One-Dimensional High-Performance Thin-Layer Chromatography. *Analytical Biochemistry* **2002,** 302, (2), 191-198.

42. Johnson, M. E., Rapid, Simple Quantitation in Thin-Layer Chromatography Using a Flatbed Scanner. *Journal of Chemical Education* **2000,** 77, (3), 368.

43. Moura, S. P.; Carmona-Ribeiro, A. M., Cationic Lipid Modulates Phospholipid Adsorption on Silica. *MRS Proceedings* **2005,** 900, 98-104.

44. Goyne, K. W.; Zimmerman, A. R.; Newalkar, B. L.; Komarneni, S.; Brantley, S. L.; Chorover, J., Surface Charge of Variable Porosity Al2O3(s) and SiO2(S) Adsorbents. *Journal of Porous Materials* **2002,** 9, (4), 243-256.

45. Kobayashi, M.; Juillerat, F.; Galletto, P.; Bowen, P.; Borkovec, M., Aggregation and Charging of Colloidal Silica Particles: Effect of Particle Size. *Langmuir* **2005,** 21, (13), 5761-5769.

46. Stumm, W., and Morgan, J. J.,, Aquatic Chemistry, 3rd edn. *John Wiley and Sons, New York,* **1996**.

47. Christie, W. W., Lipid Analysis: Isolation, Separation, Identification and Structural Analysis of Lipids, 3rd ed. *The Oily Press: Bridgwater, U.K.* **2003**.

48. Van Horne, K. C., Sorbent Extraction Technology. *Analytichem International: Harbor City, CA,* **1985**.

49. Ekroos, K.; Ejsing, C. S.; Bahr, U.; Karas, M.; Simons, K.; Shevchenko, A., Charting molecular composition of phosphatidylcholines by fatty acid scanning and ion trap MS3 fragmentation. *Journal of Lipid Research* **2003,** 44, (11), 2181-2192.

50. Hong, J.; Cho, K.; Kim, Y. H.; Cheong, C.; Lee, K.-S.; Jung, J. H., Structural determination of lysophosphatidylcholines extracted from marine sponges by fast atom bombardment tandem mass spectrometry. *Rapid Communications in Mass Spectrometry* **2001,** 15, (13), 1120-1126.

51. Hsu, F.-F.; Turk, J., Structural determination of sphingomyelin by tandem mass spectrometry with electrospray ionization. *Journal of the American Society for Mass Spectrometry* **2000,** 11, (5), 437-449.

52. Hsu, F.-F. u.; Turk, J., Electrospray ionization/tandem quadrupole mass spectrometric studies on phosphatidylcholines: the fragmentation processes. *Journal of the American Society for Mass Spectrometry* **2003,** 14, (4), 352-363.

53. Hsu, F.-F.; Turk, J., Charge-driven fragmentation processes in diacyl glycerophosphatidic acids upon low-energy collisional activation. A mechanistic proposal. *Journal of the American Society for Mass Spectrometry* **2000,** 11, (9), 797-803.

54. Hsu, F.-F.; Turk, J., Charge-remote and charge-driven fragmentation processes in diacyl glycerophosphoethanolamine upon low-energy collisional activation: a mechanistic proposal. *Journal of the American Society for Mass Spectrometry* **2000,** 11, (10), 892-899.

55. Hsu, F.-F.; Turk, J., Studies on phosphatidylglycerol with triple quadrupole tandem mass spectrometry with electrospray ionization: fragmentation processes and structural characterization. *Journal of the American Society for Mass Spectrometry* **2001,** 12, (9), 1036-1043.

56. Sana, T. R.; Roark, J. C.; Li, X.; Waddell, K.; Fischer, S. M., Molecular Formula and METLIN Personal Metabolite Database Matching Applied to the Identification of Compounds Generated by LC/TOF-MS. *Journal of Biomolecular Techniques* **2008,** 19(4): 258-266.

Chapter 2

Analysis of Glycerophosphoinositol Uptake in Candida albicans by Liquid Chromatography-Electrospray Ionization Tandem Mass Spectrometry[1]

[1]The application of the approach described in this Chapter has contributed to the following publication:

Bishop, A. C.; **Sun, T.**; Johnson, M. E.; Bruno, V. M.; Patton-Vogt, J. Robust utilization of phospholipase-generated metabolites, glycerophosphodiesters, by *Candida albicans*: Role of the CaGit1 permease, *Eukaryotic Cell*, 2011, 10 (12), 1618-27.

2.1 Abstract

The phosphatidylinositol (PI) metabolite, glycerolphosphoinositol (GroPIns), which results from phospholipase B-mediated cleavage of phosphatidylinositol, exits and enters the yeast, *Saccharomyces cerevisiae*. In *S. cerevisiae*, GroPIns is transported across the plasma membrane via a transport protein encoded by the *GIT1* gene. GroPIns transport has not been addressed in the pathogenic yeast, *Candida albicans*, but the *C. albicans* genome has four potential *GIT1* homologs. In order to investigate and identify the role of *CaGIT1* as a GroPIns permease in *C. albicans*, a liquid chromatography-tandem mass spectrometry based method (hydrophilic interaction liquid chromatography-MS/MS rather than reverse phase liquid chromatography-MS/MS) for quantification of GroPIns is described. GroPIns is eluted at retention time of 13.06 ± 0.15 min with total run time of 15 min. Quantification was performed by generation of an external calibration curve. The developed approach was employed to monitor the levels of GroPIns in the medium. Our results show that while a wild type *C. albicans* strain transports exogenously supplied GroPIns into the cell, a strain lacking the CaGit1 permease does not.

2.2 Introduction

Phosphatidylinositol, which accounts for up to approximately 10% of membrane phospholipids, is widely distributed among the different cellular membranes. Phosphatidylinositol has been reported to be degraded by at least four distinct routes [1, 2]. The fatty acid esterified at the *sn*-1 and the *sn*-2 positions of the glycerol moiety are removed by phospholipase A_1 and phospholipase A_2, respectively, thus providing an important source of fatty acid. Phospholipase B refers to an enzyme that is able to hydrolyze the fatty acyl ester bond at both the *sn*-1 and *sn*-2 positions on glycerol. By far the most widely studied pathway for metabolism of phosphatidylinositol involves cleavage of the diacylglycerol-phosphate bond by phsopholipase C. Alternatively, phosphatidylinositol appears to be hydrolyzed by cleavage of the inositol-phosphate bond by phospholipase D to phosphatide and inositol.

The extracellular glycerophosphodiesters, such as glycerophosphoinositol (GroPIns), are the products resulting from hydrolysis of both fatty acid chains of phospholipids via phospholipase B-mediated deacylation. Most fungal cells including *Candida albicans* contain multiple phospholipase B (PLB)-encoding genes that have deacylation activity [3]. Although PLBs play a potential role as virulence factors, the metabolic fate and function of the products of PLB turnover, the glycerophosphodiesters, remain an open question [4-8]. This stands in stark contrast to our understanding of the inositol-phosphates resulting from phospholipase C-mediated cleavage, for which numerous kinases and phosphatases have been identified, and many metabolic conversions clearly documented [9]. In addition, not all of the cell's

glycerophosphodiesters appear to be produced via *C. albicans* PLB activity and there is growing evidence that this metabolic segregation, especially GroPIns and GroCho, may be achieved by the occurrence of host phospholipase activity in organism [10-19].

In *S. cerevisiae*, GroPIns is transported into the cell via the transport protein, ScGit1, encoded by the *GIT1* gene. Four open reading frames (orfs) in *C. albicans, CaGIT1-4* contain significant sequence homology to *ScGIT1* [20]. ScGit1 and CaGit1-4 are between 400-600 amino acids in length and contain either 12 or 14 membrane spanning segments [21]. The *C. albicans* genome contains five PHS (phosphate: H^+ symporter) family member: CaGit1-4 and Pho84, the homolog of the *S. cerevisiae* high affinity phosphate transporter. Notably, none of these family members has been characterized in *C. albicans*.

The method described here was developed to accurately determine the occurance of GroPIns at nanogram levels or below in the media of *C. albicans*. In a biological matrix, analytes can have different sizes, charges, polarities and hydrophobicities. Chromatography techniques provide control of separation through changes in the mobile-phase solvent content, the ionic strength, the pH, and the salt additives. Options for optimal separations can be achieved through chromatographic mode, such as normal-phase liquid chromatography (NPLC), reversed-phase liquid chromatography (RPLC), hydrophilic interaction liquid chromatography (HILIC), and ion-exchange liquid chromatography (IEX-LC). Approximately 80-90% of all HPLC analytical separations apply RPLC as the separation mode. However, small polar compounds are often very challenging to biological analysis. It is difficult to analyze polar analytes by RPLC due to the lack of sufficient retention ability on reverse-phase columns. Although NPLC and

IEX-LC can retain polar and charged compounds, their organic solvent contents in the mobile phase have either high ionic strength or are not amenable to the electrospray ionization environment in mass spectrometry. Moreover, ion pair separation of both acid and a base in the same analysis is difficult.

HILIC is a viable complementary method to RPLC, NPLC, and IEX-LC and is widely used for the separation of biologically active polar substances, such as amino acids, peptides, carbohydrates, oligosaccharides, etc. The stationary phase of HILIC column is composed of polar materials such as silica, amino or mixed mode, and its mobile phase is mainly organic with aqueous solvent. Its mechanism of separation is based on the ability of a polar analyte to partition into and out of adsorbed water and the addition of a charged polar analyte to undergo cation exchange with charged silanol groups. The combination of these mechanism results in enhanced polar retention while lack of either of the mechanisms results in no polar retention [22-25]. Table 2-1 summaries the different methods for GroPIns separation. The separations of GroPIns have mainly been done on anion-exchange columns [26, 27]. A microchip based separation of phosphoinositides by micellar electrokinetic capillary chromatography method was reported [28]. An amino-phase column was also applied to separate GroPIns and other inositol phosphates using an acetate buffer in the mobile phase [29]. The above techniques have the non-negligible disadvantage of being a multi-step procedure in which the isotopic equilibrium of radiolabelled products is difficult to achieve. Recently, a LC-MS/MS method using a β-cyclodextrin-bonded column was described for the quantitative analysis of internal GroPIns in rat cell lines, but extracellular GroPIns was not included in this method [30]. Another study used normal phase LC-MS to quantitate several

water-soluble metabolites, including GroPIns and GroPCho, from rat brain tissue [31]. Our study differs from previous studies in that we use HILIC chromatography coupled with MS/MS to detect GriPIns in the extracellular medium which has a high concentration of other small molecules, including free phosphate.

Method	Analyte	Sample	Detector	Reference
Anion-Exchange column with Cation-Exchange column	GroPCho, GroPEth	Hamster ovary cells	Liquid Scintillation Counting	[27]
Amino-Normal phase column	GroPIns, Inositol phosphates	Human platelets	Liquid Scintillation Counting	[29]
Phenomenex NH_2 Normal Phase column	GroPIns, GroPCho	Mice brain tissue	Q-TOF MS	[30]
Nucleodex β-OH Silica column	GroPIns	Mice cell lines	Triple Quadrupole MS	[31]
Waters Xbridge HILIC column	GroPIns, GroPCho, GroP, Inositol, Choline	Yeast extracellular medium	Triple Quadrupole MS	Patton-Vogt et al (accepted)

Table 2-1 Summary of methods for separating and detecting GroPIns and GroPCho.

HILIC overcomes the shortcomings of some of the other retention mechanisms for extremely polar compound analysis. It retains highly polar analytes that would not be retained by RPLC, and using a highly organic mobile phase promotes enhanced ESI-MS response. In the tandem mass spectrometer, the analyte, GroPIns was dissociated by collision gas to produce various product ions that could be monitored at the same time. Liquid chromatography combined with tandem mass spectrometric detection was the preferred method for quantitative analysis due to its intrinsic selectivity, sensitivity, and speed in "omics" studies [33-36]. The expected fragmentation patterns of GroPIns are shown in Figure 2-1. Although there are other methods available to study GroPIns, the published methods mainly include radioactive analysis and have not added the absolute quantification of the metabolites in the extracellular medium of a cell culture [37-39]. Our aim was to develop a novel HILIC-MS/MS method for quantification of GroPIns in the extracellular medium of *Candida albicans* to monitor its uptake as a function of growth.

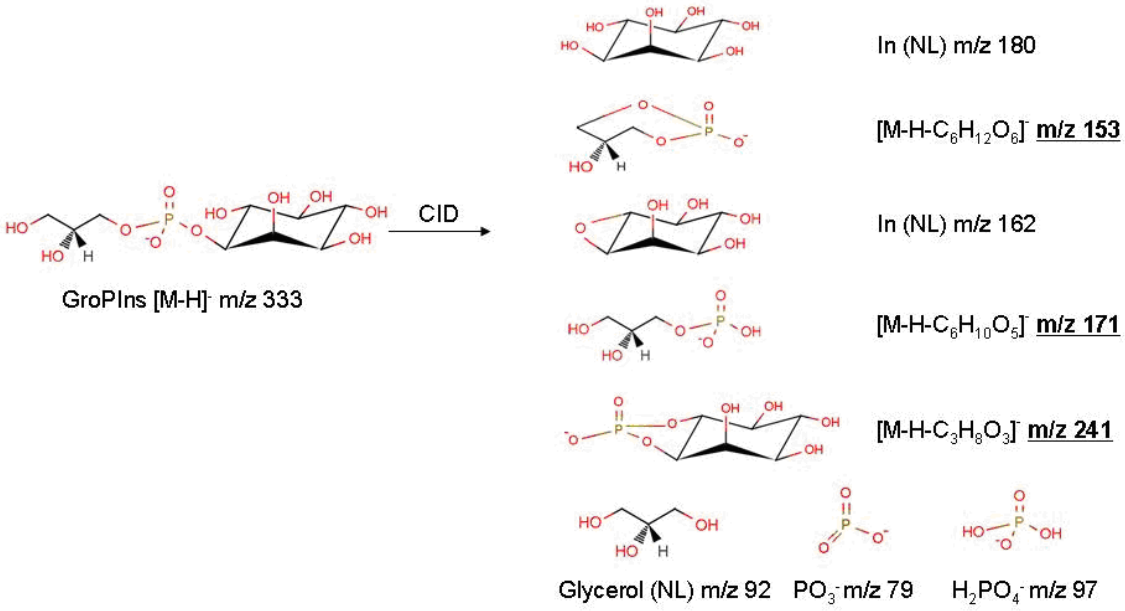

Figure 2-1 Expected fragmentation patterns of GroPIns by tandem mass spectrometry.

2.3 Materials and Methods

2.3.1 Reagents

The methanol and acetonitrile used for the LC-MS/MS analysis were Optima grade from either Thermo Fisher Scientific (Pittsburgh, PA) or J.T. Baker (Phillipsburgh, NJ). Distilled water was deionized with Barnstead Nanopure water system (Dubuque, IA). The water was filtered with 0.22 μm Nylon membrane filters from either Millipore (Billerica, MA) or Whatman International (Maidstone, England) prior to use. The mobile phase for the HPLC analysis contained ammonium acetate (99% pure) from Thermo Fisher Scientific in both acetonitrile and water. These solutions were made up fresh each day and sonicated for 15 min in a 2210 Branson Ultrasonic cleaner (Danbury, CT) to mix

and degas before use. Glycerophosphoinositol (L-α-glycerophospho-D-myo-inositol) was from Sigma-Aldrich (St. Louis, MO).

2.3.2 Strains, Media and Culture Conditions

A wild type *C. albicans* strain DAY185 (*ura3*Δ*::*λ*imm434/ura3*Δ*::*λ*imm434 pARG4::URA3::arg4::hisG/arg4::hisG pHIS1::his1::hisG/his1::hisG*) was used in this study. The strain in which the *CaGIT1* gene was deleted was constructed in strain DAY185 to produce *git1::UAU1/git1::URA3* (JPV484). For insertional complementation, plasmid pDDB78GIT1 was linearized and transformed into JPV484 to produce JPV512 (*git1::UAU1/git1::URA3* + pDDB78GIT1). Empty plasmid pDDB78 was also linearized and transformed into JPV484 to produce JPV526 (*git1::UAU1/git1::URA3* + pDDB78). Insertional complementation or reintegration delivers the *GIT1* gene back into the mutant strain to test for reoccurrence of the wild type transport function. The strains were grown aerobically over night at either 30°C or 37°C with shaking in low phosphate (P_i) yeast nitrogen base (YNB) media. Growth was monitored by measuring the optical density at 600 nm (OD600) on a Biomate 3 Thermo Spectronic spectrophotometer. Low P_i media were made by replacing the KH_2PO_4 (1 gm/liter) in YNB media with KCl (1gm/liter) and adding KH_2PO_4 to 0.2 mM. The cultures to be analyzed by MS grew in medium lacking KH_2PO_4 that contained 200 μM (≈ 67 μg/mL) GroPIns. Immediately after inoculation, 1 mL of the samples were removed in duplicate to obtain T=0 time point. Once the cultures were started, samples

were taken at T=6 hours and T=24 hours. At each time point, 1 mL of the cultures was removed, centrifuged to pellet the cells, and the supernatant filtered through the 0.22 μm filters.

2.3.3 Standards and Sample Preparation

The primary solution of glycerophosphoinositol (13.4 mM) was diluted in water to obtain aliquots of the standard compound at the concentration of 2 mM as stock solutions. A working standard solution of GroPIns in 100 μg/mL was prepared from the stock solution by dilution in water. The working standard solution was further serially diluted in water to obtain eight calibration standard solutions of 2.5, 5, 10, 50, 100, 500, 1000 and 10000 ng/mL (approximately 7.5-30000 nM).

For the media samples from the above conditions, culture aliquots were centrifuged at 3000 rpm for 5 min, and the resulting supernatant was filtered. 250 μL of each media sample was then transferred into centrifuge tube and was diluted with 5 fold volume of methanol/water, 90:10 (v/v) for centrifugation at 10,000 rpm for 5 min. The supernatant was collected and dried under a stream of nitrogen. The residue was resuspended in 250 μL of acetonitrile/methanol, 3:1 (v/v). Because the calibration curve ranges over 2.5-10000 ng/mL (approximately 7.5-30000 nM) and 200 μM GroPIns was in the media, was diluted the analyte in 1:100 fold volumes prior to analysis. Typically, an injection volume of 10 μL was used and each sample was run in triplicate.

2.3.4 Equipment and Experimental Parameters

The liquid chromatography with tandem mass spectrometry system (LC-MS/MS) was composed of an Agilent 1200 Rapid Resolution LC system and an Agilent 6440 Triple Quadrupole Mass Spectrometer (Santa Clara, CA). The Mass Hunter software package was used for the acquisition and processing of data. Quantification was performed using Qualitative Analysis B1.0.82.2 as implemented in the Mass Hunter software.

Electrospray ionization-tandem mass spectrometry (ESI-MS/MS) for characterization, identification as well as quantification was performed in positive and negative mode using product ion scan (PIS) and multiple-reaction monitoring (MRM) respectively with a triple quadrupole mass spectrometer. PIS is a scan mode in which all product ions fragmented from the selected molecular ion are detected in one run. MRM was used to monitor the mass to charge ratios corresponding to the selected precursor and product ions of interest; the program was set up to monitor several targeted ions at different time segments in one run. The targeted ion dissociation pathway (Figure 2-2)

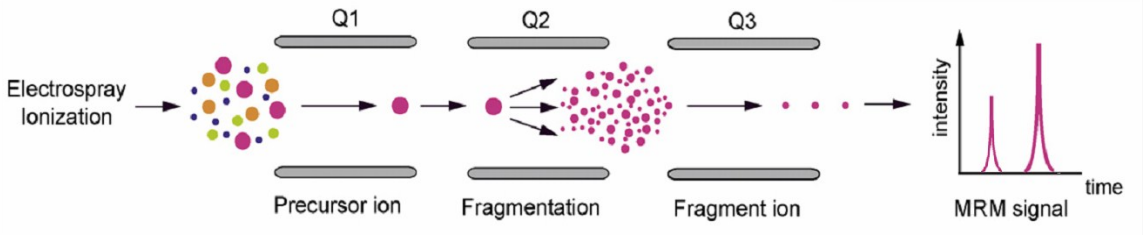

Figure 2-2 Scheme of collision induced dissociation of ions in triple quadrupole mass spectrometer.

for the above scan modes was optimized with regard to collision energy to minimize variations in relative ion abundance due to differences in rates of dissociation. The capillary voltage was maintained at 3.0 kV. The drying gas temperature was 300 °C and the sheath gas temperature was 325 °C. The drying gas flow rate was set to 4 liters/min, and the nebulizer pressure was 50 psi. The mass spectrum was acquired from *m/z* 50-1000 with the acquisition time same as the chromatography. The fragmentor voltage and collision energy were optimized from 10-150 V and 0-100 eV. The optimal value of the fragmentor voltage was manually adjusted to 90 V. The collision energy was optimized to be 35 eV. The dwell time was set to be 200 ms for GroPIns.

The LC system, consisting of an Agilent binary pump and an Agilent high-performance autosampler, was used to provide the mobile phase and to inject samples. For separation, a 5 μm XBridge column (150 x 4.60 mm, Waters, Milford, MA) was used for hydrophilic interaction liquid chromatography (HILIC). The chromatography was performed in isocratic elution at a flow rate of 0.5 mL/min when the mobile phase was acetonitrile/water, 50:50 (v/v) with 10 mM ammonium acetate at pH 7.19. The relative concentration of GroPIns in the media was selectively measured by multiple-reaction monitoring and calculated by normalizing its peak area to the peak area of the relevant external standards on calibration curve. All separations were carried out at the room temperature (25 °C).

2.4 Results and Discussion

2.4.1 Tandem Mass Spectrometry Optimization

In order to obtain lower detection limit of the analyte without compromising the reliability of this method, a high selective MS/MS strategy rather than traditional approaches such as UV detection was employed to ensure the specificity of detection. The following conditions were applied for optimization experiments unless otherwise noted. 10 μL of 1000 ng/mL GroPIns was loaded onto the column. A 20 min isocratic elution was applied where the column was equilibrated in 50:50 acetonitrile/water before each injection. After elution, the mobile phase was ramped linearly to 90:10 acetonitrile/water and was held over 10 min before returning to the initial conditions (5 min ramp). The mobile phase was then held at the initial conditions for 10 min before doing the next injection. Ammonium acetate (10 mM) was in both the acetonitrile and the water. The most relevant parameters in mass spectrometer to optimize are the capillary voltage, source temperature and drying gas flow. The starting ESI-MS parameters were as follows: capillary voltage 1.5 kV, drying gas temperature 100 °C, and drying gas flow 2 liters/min. A high pressure liquid nitrogen dewar was used as the nitrogen gas source. Once one of the above parameters had been optimized, its setting was applied to optimize the other MS parameters in subsequent experiments. For these experiments, the mass to charge ratio corresponding to the GroPIns being analyzed was monitored throughout the analysis.

The capillary voltage is used at the entrance of the capillary and it is relative to the nebulizer and spray chamber that are at ground potential. In order to optimize the

setting for the capillary voltage, the rest of the MS parameters were held constant. The capillary voltage was varied from 1.5 to 3.5kV. Analyte at 1000 ng/mL (≈ 3 μM) was injected in triplicate at each voltage setting. The values of capillary voltage are slightly different in positive and in negative ionization mode. The results in Figure 2-3 indicate that a capillary voltage of 3.0 kV gave the largest signal as the optimum value.

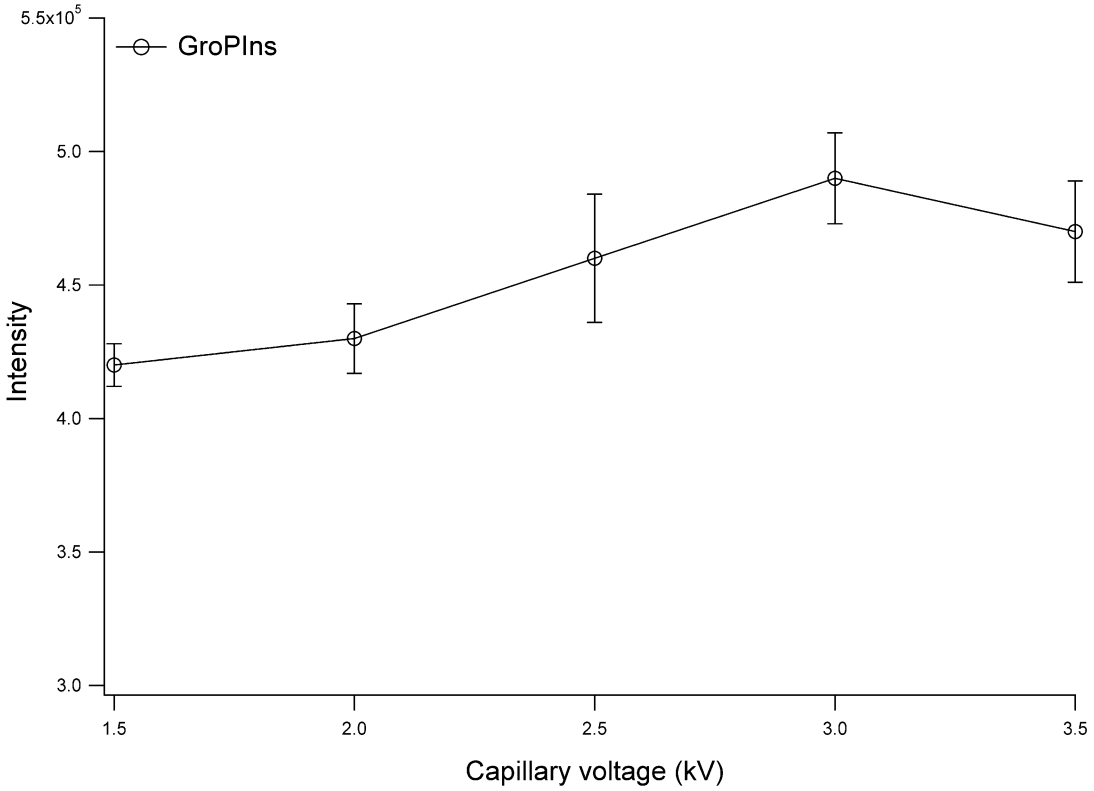

Figure 2-3 Resulting peak intensities from injecting 1000 ng/mL (≈ 3 μM) of GroPIns into the mass spectrometer while varying the capillary voltage setting. Results are the average of three injections with the standard deviation.

A series of injections were conducted where all the parameters were held constant except for the temperature of drying gas varying from 100 to 300 °C. Three replicates of injections were done at each temperature setting. Results from varying the temperature

are shown in Figure 2-4 that signal intensity increased with increasing drying gas temperature. By comparing at the intensities, it was determined that 300 °C was the optimal setting for the ESI source.

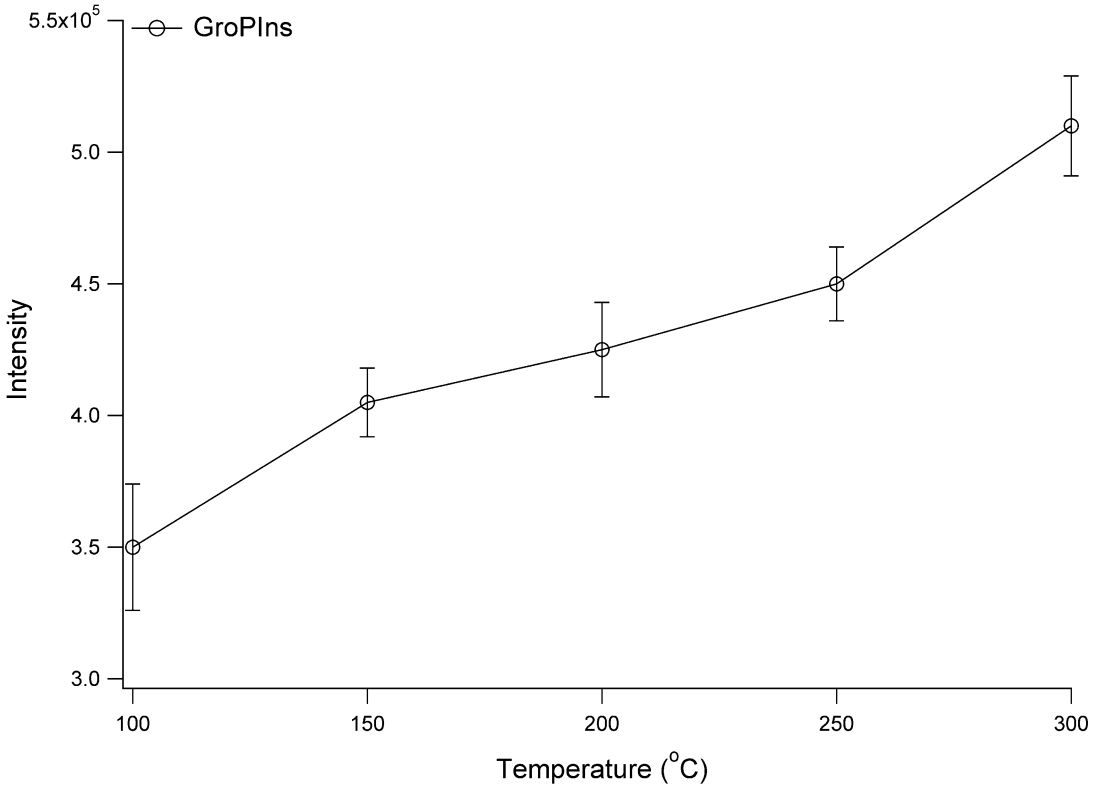

Figure 2-4 Resulting peak intensities from injecting 1000 ng/mL of GroPIns into the mass spectrometer while varying the drying gas temperature setting. Results are the average of three injections with the standard deviation.

An experiment was performed to optimize the drying gas flow; all the parameters were held constant except for the drying gas flow. Three injections of 1000 ng/mL analyte were done at each gas flow setting. The results are shown in Figure 2-5. This experiment shows that the optimal drying gas flow setting was 4 liters/min. With these conditions the analyte was detected by multiple reaction monitoring (MRM).

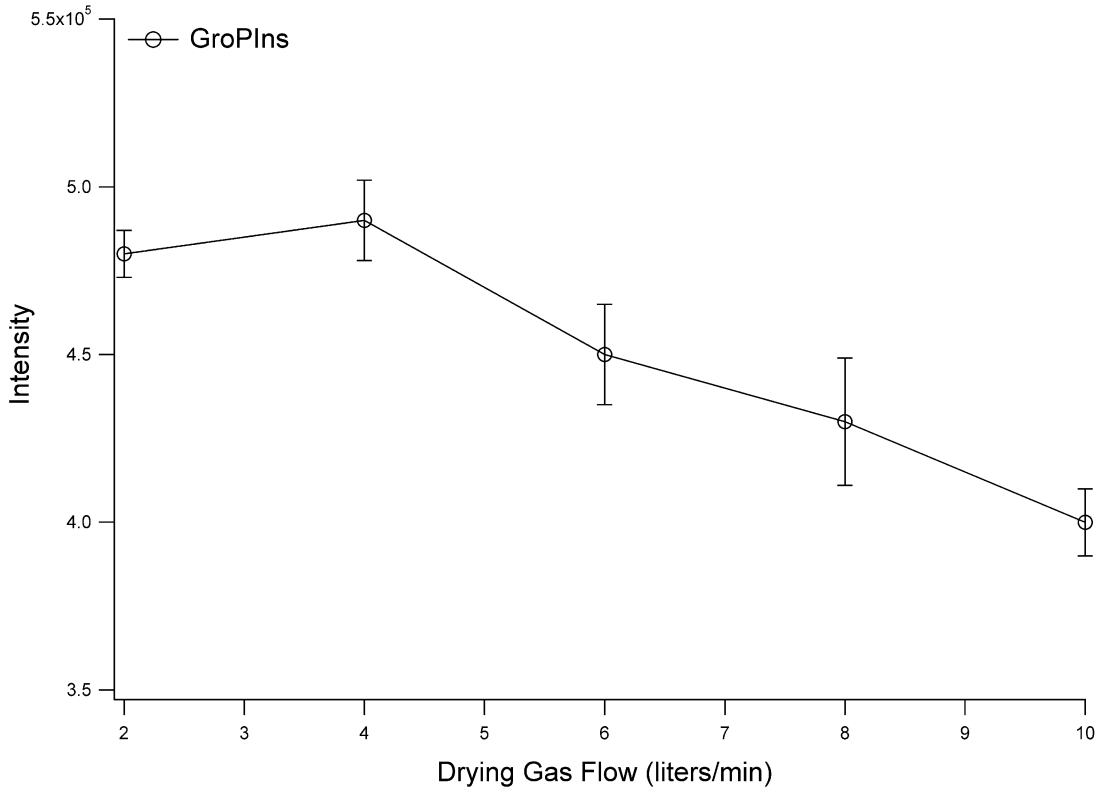

Figure 2-5 Resulting peak intensities from injecting 1000 ng/mL of GroPIns into the mass spectrometer while varying the drying gas flow setting. Results are the average of three injections with the standard deviation.

The nebulizer pressure was optimized by varying the setting from 30 to 50 psi, while the other MS parameters were held constant. GroPIns (1000ng/mL) was injected in triplicate at each pressure setting. The results are shown in Figure 2-6. The experiment shows that the optimal nebulizer pressure setting was 50 psi and to some extend was flow dependent.

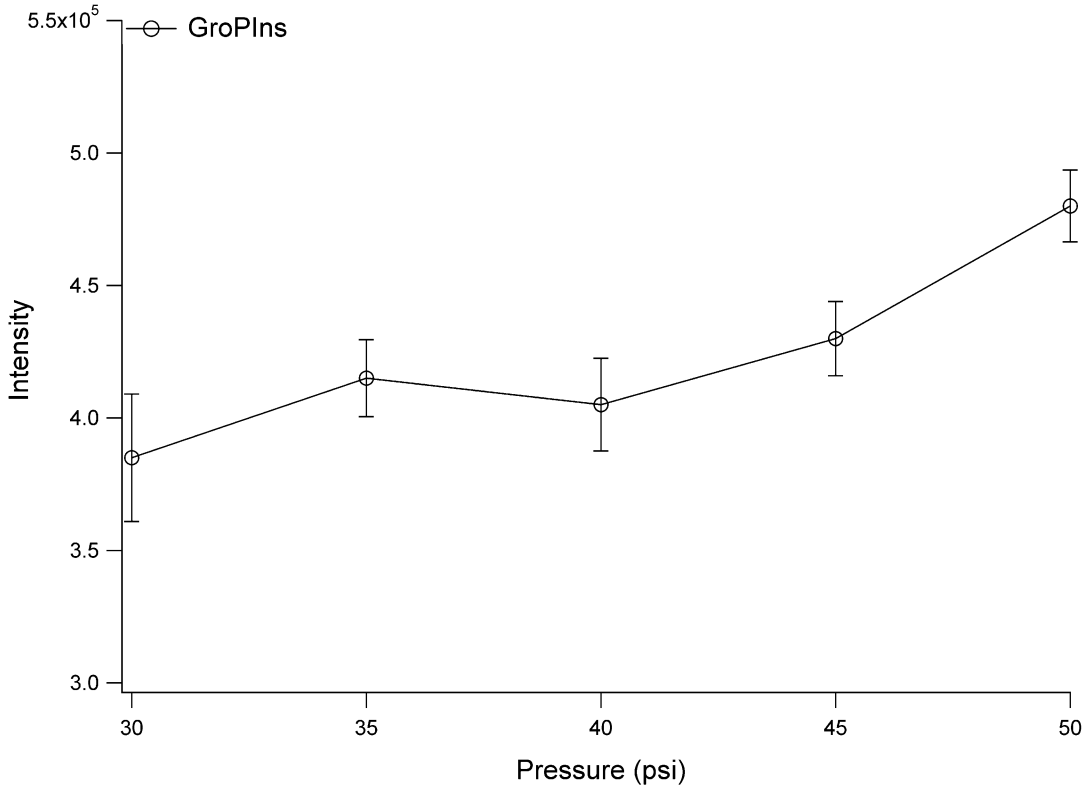

Figure 2-6 Resulting peak intensities from injecting 1000 ng/mL of GroPIns into the mass spectrometer while varying the nebulizer pressure setting. Results are the average of three injections with the standard deviation.

In order to assess the usefulness of ESI-MRM-MS/MS techniques for GroPIns analysis, experiments were first conducted to establish the most efficient transition for MRM. Electrospray ionization mass spectrometry in positive (+ESI) and negative (-ESI) modes was performed for selective and sensitive detection. Full scan spectra were acquired over the mass to charge ratio range of 50-1000. The precursor ion of GroPIns ($[M-H]^-$) was detected at *m/z* 333.0 in –ESI (Figure 2-7).

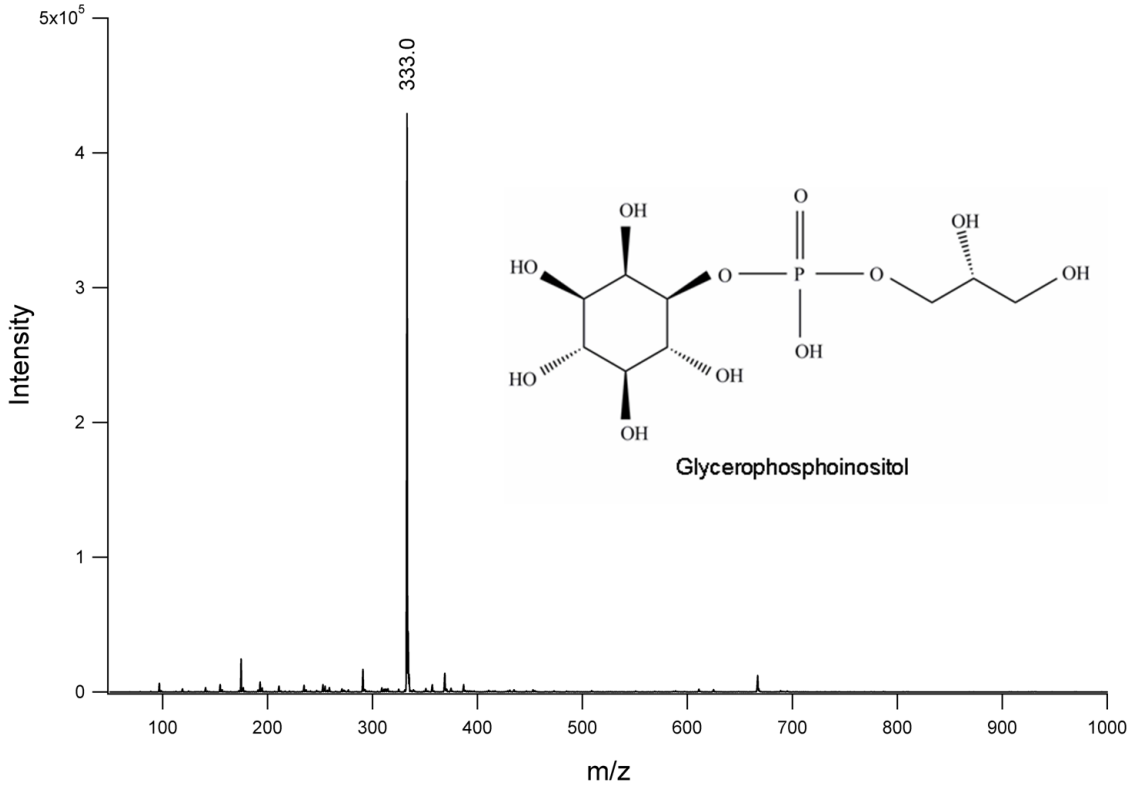

Figure 2-7 Mass spectrum of the GroPIns in negative mode with total ion scan. GroPIns at 1000 ng/mL was injected.

To investigate the fragmentation of the analyte, product ion scan spectra were acquired over the *m/z* range of 50-1000 for GroPIns (Figure 2-8). The most intense fragment for GroPIns was selected for MRM analysis quantification with the following parameters: *m/z* 333.0 → 153.0 for GroPIns ([M-Inositol-H]$^-$), with a screen of corresponding standards at 1000 ng/mL. To further improve MRM conditions, the effect of fragmentor and collision energies over a range of different values were investigated by separate loop injections with no column connected for best response of the most intense precursor and product ions, respectively. The fragmentor voltage affects the transmission and fragmentation of precursor ions. It helps the ions traverse the relatively high pressure area between the exit of the capillary and skimmer. The maximum structural information

is achieved at higher voltage values. The analyte was first injected in the mobile phase (50:50 acetonitrile/water with 10 mM ammonium acetate) and MS spectra were acquired with a total cycle time of 500 ms and a dwell time of 200 ms.

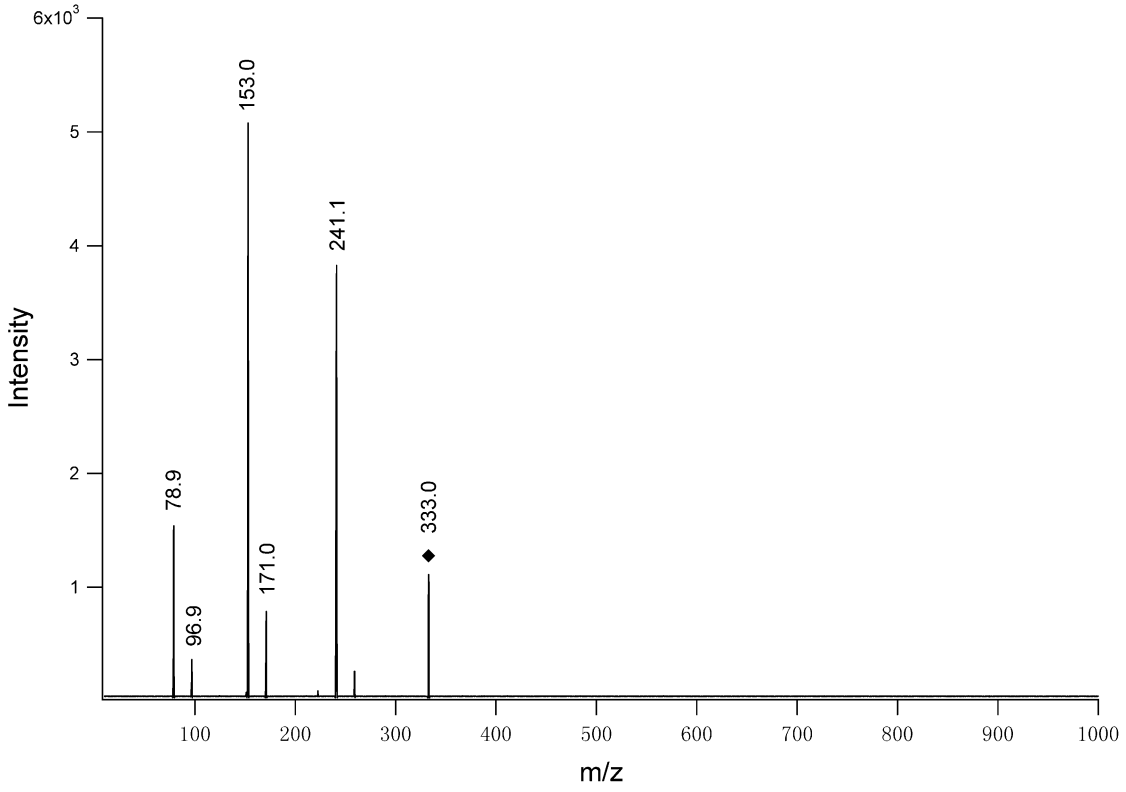

Figure 2-8 Tandem mass spectrum of the GroPIns by product ion scan in negative mode. 1000 ng/mL of GroPIns was injected.

With the above settings of total cycle time and dwell time, an accurate evaluation of a wide range of fragmentor voltage (10-150 V) in steps of 20 V for the studied analyte were performed. Three injections of 1000 ng/mL GroPIns was done at each voltage setting. The fragmentor voltage was optimized for best response of the precursor ion of GroPIns, and the optimal fragmentor voltage was transferred to an MRM method for the particular analyte (Figure 2-9). While the optimal fragmentor voltage was determined at

90 V, values for collision energy varied for the studied analyte and needed to be analyzed as well.

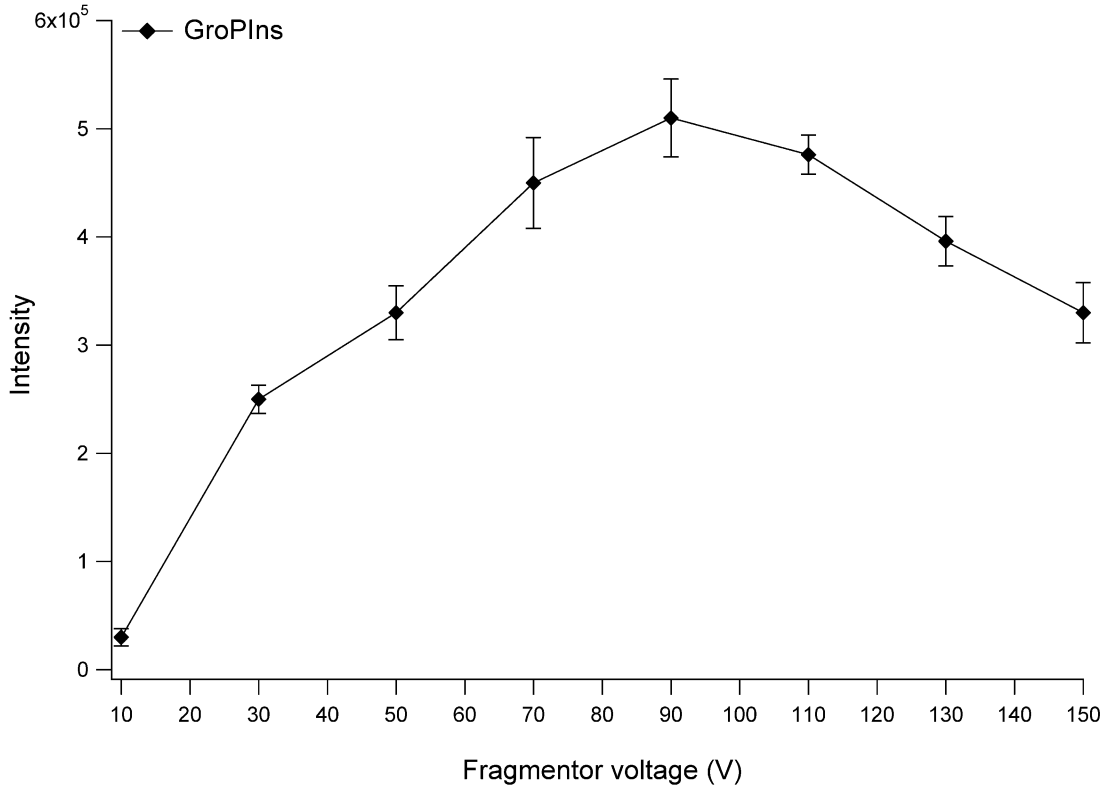

Figure 2-9 Resulting peak intensities from injecting 1000 ng/mL of GroPIns into the mass spectrometer while varying the fragmentor voltage setting. Results are the average of three injections with the standard deviation.

A second injection was made to optimize the collision energy. Since different precursor ions have different collision stabilities, good product ion yields are achieved with minimum losses in the overall ion current. The precursor ion was transmitted through the first quadrupole (Q1) into the collision cell (Q2), fragmented and corresponding fragments were monitored through third quadrupole (Q3). The product ion spectra were acquired at different collision energies ranging from 0 to 100 eV in steps

of 10 eV. The collision energy was evaluated for best response of the most intense product ion. As shown in Figure 2-10, the intensities of the precursor ions of the analyte decreased when the collision energy increased. At the meantime, the signals of its product ions increased at first and then decreased. The optimal collision energy was selected and also transferred to the MRM. This process for optimization was repeated for GroPIns and the MRM conditions were stored before sample acquisition.

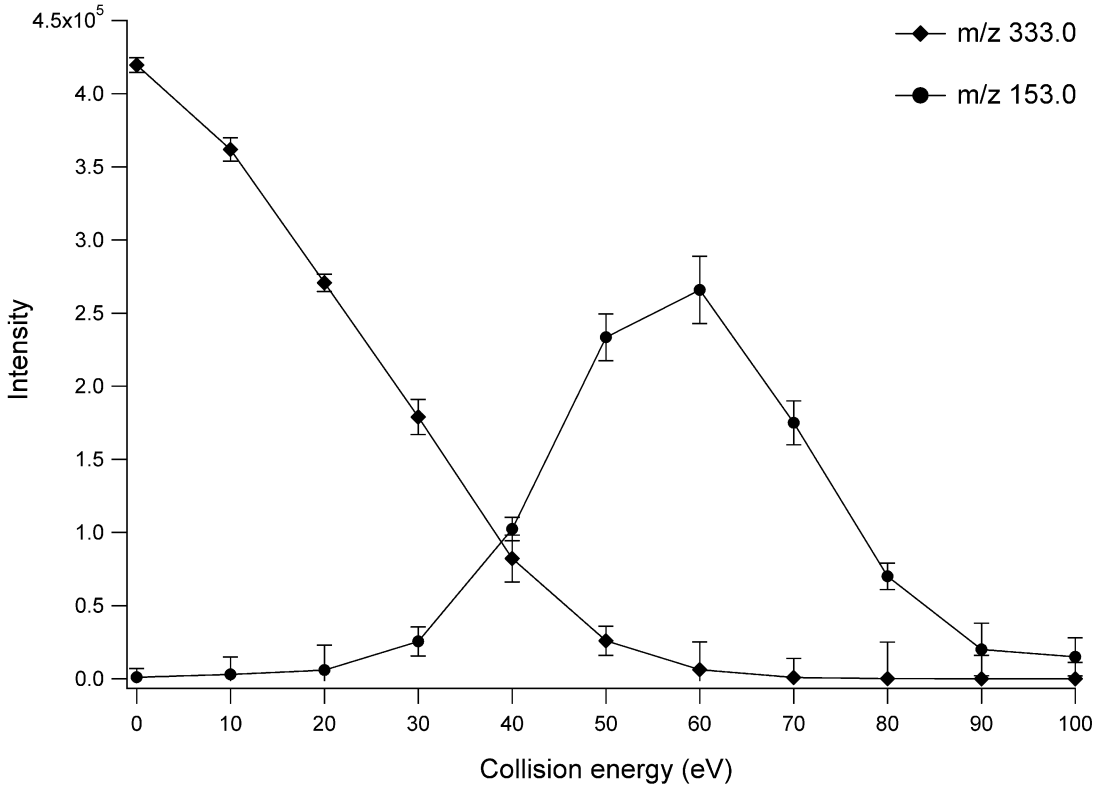

Figure 2-10 Resulting peak intensities from injecting 1000 ng/mL of GroPIns into the mass spectrometer while varying the collision energy setting. Results are the average of three injections with the standard deviation.

The optimized MS parameters for GroPIns detection were as follows: capillary voltage 3.0 kV, fragmentor voltage 90 V, collision energy 35 eV, drying gas temperature

300 °C, sheath gas temperature 325 °C, drying gas flow 4 liters/min, and the nebulizer pressure 50 psi. More analytes were added once the MS parameters had been optimized in order to evaluate the separation conditions on the HILIC column.

2.4.2 Liquid Chromatography Optimization

Chromatographic conditions, especially composition and nature of the mobile phase is crucial for LC separation as this has significant impact on retention time of the analyte, peak shapes, sensitivity and therefore on the overall separation efficiency. Base on literature survey water was selected as the strong solvent that is more polar than acetonitrile to elute polar analytes as the polarity of the mobile phase was increased by increasing the percentage of water. Analysis of analytes was initiated under isocratic conditions with an aim to develop a simple separation process with a short time. Separation was optimized using various combinations of mobile phase between water and acetonitrile. Unless otherwise noted, the optimized MS/MS parameters were applied.

According to the manufacture's instruction, the new column was at first flushed for 50 column volumes (125 mL) of 50:50 acetonitrile/water (v/v) with 10 mM ammonium acetate. The column was then equilibrated with 20 column volumes (50 mL) of initial mobile phase conditions prior to making first injection. Other conditions were also considered for best results. At least 5% water was maintained in the mobile phase to ensure that column particle is always hydrated, which could greatly reduce the column equilibration time and thus ensure stable retention times. For best reproducibility, a

blank sample at the beginning of each sample set was injected. Additionally when using an autosampler, a needle wash step with acetonitrile was incorporated.

Mobile phase combination with acetonitrile: water was performed with different ratios (90:10, 80:20, 70:30, 50:40, 50:50 v/v) in isocratic mode. The initial elution was 20 min long with constant flow rate at 0.5 mL/min and after that the column was equilibrated in 90:10 acetonitrile/water for 10 min. The mobile phase was then ramped linearly to the initial conditions over 5 min and was held at the initial conditions for 10 min before doing the next injection. Ammonium acetate (10 mM) was in both the acetonitrile and the water. Figure 2-11 shows the retention time increased as the composition of acetonitrile in the mobile phase increased. As more acetonitrile was added to the mobile phase, the elution time for GroPIns was slowed down. In other words, by adding more water to the initial conditions (50:50 acetonitrile/water) the peak was obtained at retention time of 13.06 ± 0.15 min for GroPIns with total run time of 20 min (Figure 2-12).

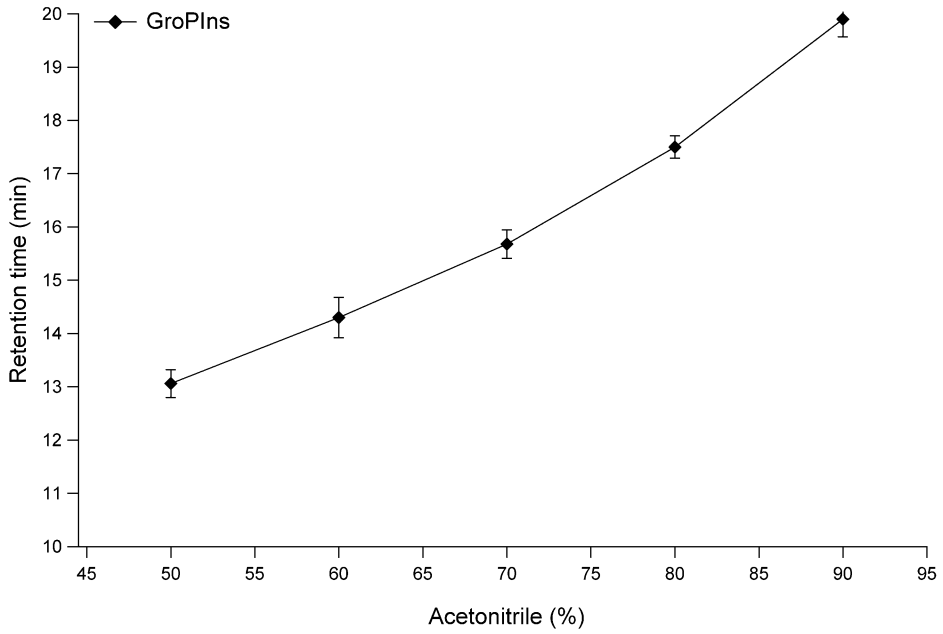

Figure 2-11 Changes of the retention time of GroPIns on the XBridge HILIC column while varying the composition of acetonitrile in the mobile phase. Results are the average of three injections with the standard deviation.

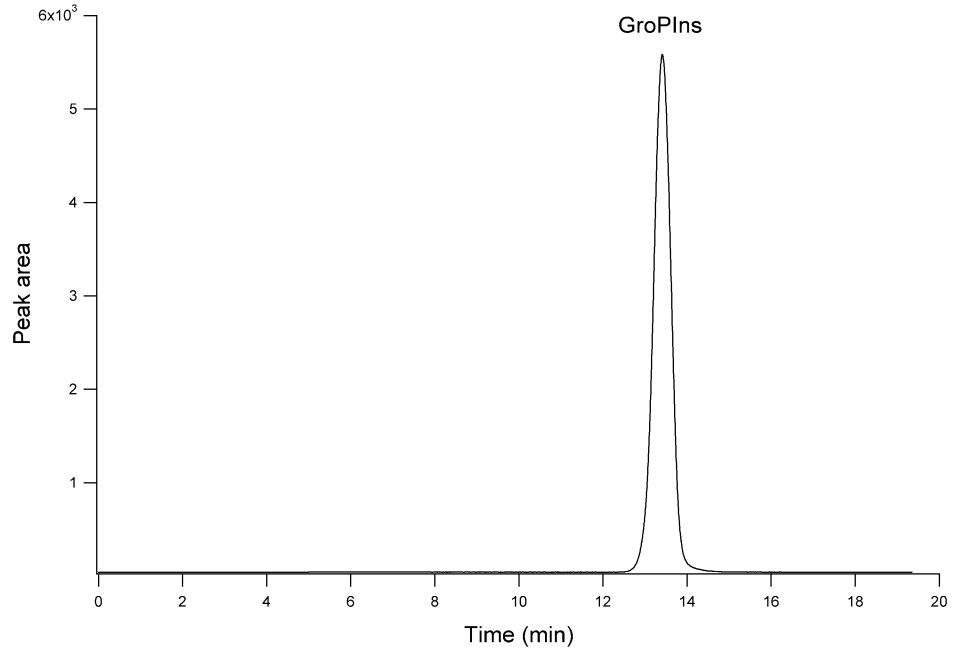

Figure 2-12 LC-MS/MS separation and detection of GroPIns. 10 µL of the analyte at 1000 ng/mL was injected. *m/z* 333.0 → 153.0 for GroPIns was monitored in MRM mode.

In order to evaluate the effect of buffer in the mobile phase, injections of the GroPIns at 1000 ng/mL were conducted in triplicate for the varying concentrations of ammonium acetate (2.5, 5, 7.5, 10, 15 and 20 mM) in the mobile phase. The concentration of ammonium acetate had to be optimized to improve the ionization of the metabolites in the ESI-MS/MS source. For these experiments, the peak areas of GroPIns were monitored. Figure 2-13 shows the resulting peak areas as the concentration of ammonium acetate was changed for the analyte. The experiments conclude that 10 mM ammonium acetate in the mobile phase gave the best ionization efficiency of the analyte when using ESI source. The mobile phase was required to be prepared daily to prevent the degradation of the buffer.

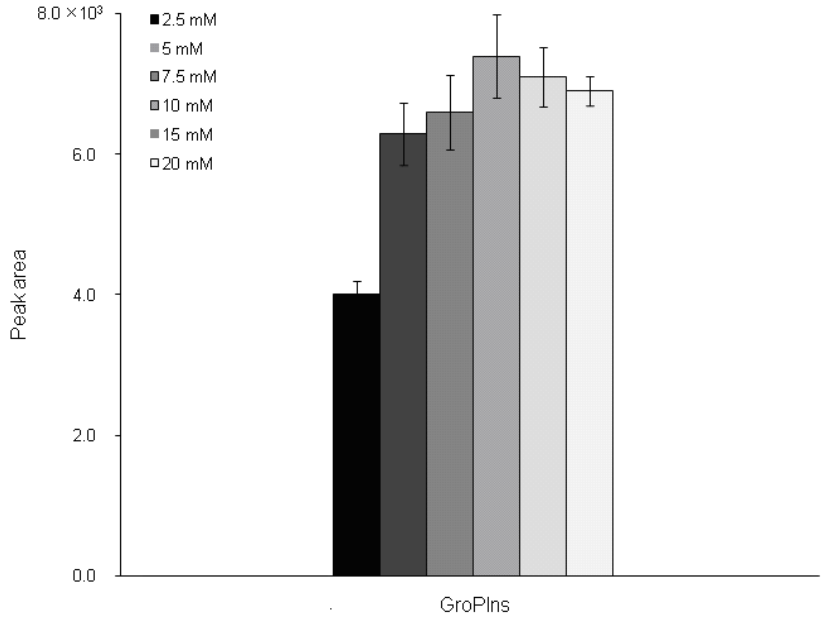

Figure 2-13 Resulting peak areas from injecting 1000 ng/mL of GroPIns on the XBridge HILIC column while varying concentration of ammonium acetate in the mobile phase. Results are the average of three injections with the standard deviation.

After the buffer in the mobile phase had been optimized, the detection limit was investigated using 10 mM ammonium acetate in the mobile phase. The isocratic elution was the same as above with the flow rate of 0.5 mL/min directed into the MS. A series of injections were conducted, varying the concentrations of GroPIns loaded over two orders of magnitude. Representative chromatograms at the lowest standard injected are presented in Figure 2-14. The results indicate that the detection limit for GroPIns was generally 2.5 ng/mL (≈ 7.5 nM) when using this method. Adequate sensitivity was observed for the lowest calibration standard. From running these experiments, it was shown that the cleanness of the capillary, the chamber vacuum seal, and the gas flow affected the ionization of the lipid metabolites. It was also important for the mobile phase with ammonium acetate to be prepared daily to prevent the buffer from degrading.

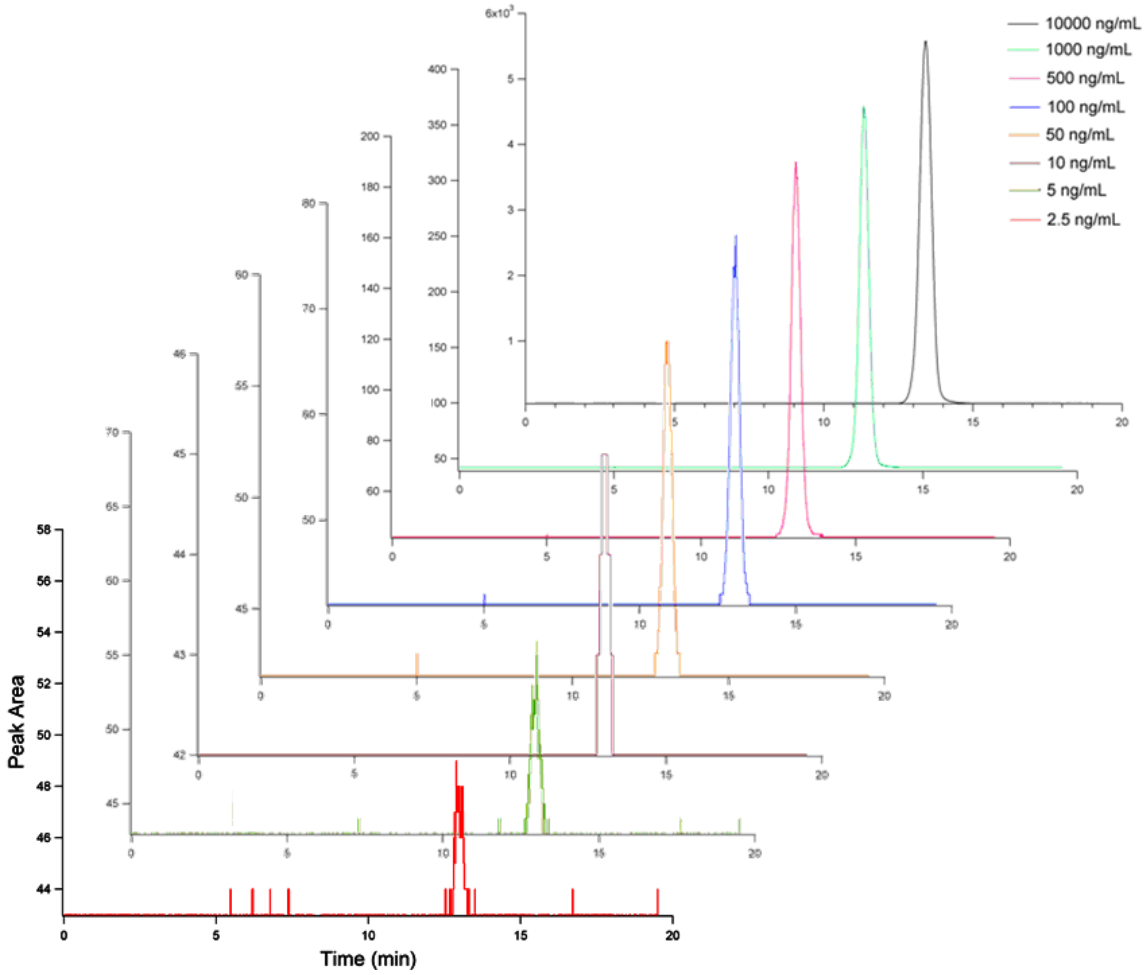

Figure 2-14 LC-MS/MS separation and detection of GroPIns. 10 µL of the analyte from 2.5 to 10000 ng/mL was injected. Eight chromatograms are shown where the same isocratic elution was used, but the concentration of the analyte was varied.

2.4.3 Method Performance

Quantification was performed by comparison of the analyte peak area versus an external calibration curve. The external calibration curves were generated by using eight calibration standards with different concentrations ranging from 2.5 to 10000 ng/mL.

The calibration curve standards were prepared in three replicates for analysis. The results were fitted to least-squares linear regression analysis. Figure 2-15 shows that the analyte has good linearity. Correlation coefficient of the calibration curves for GroPIns is 0.9962.

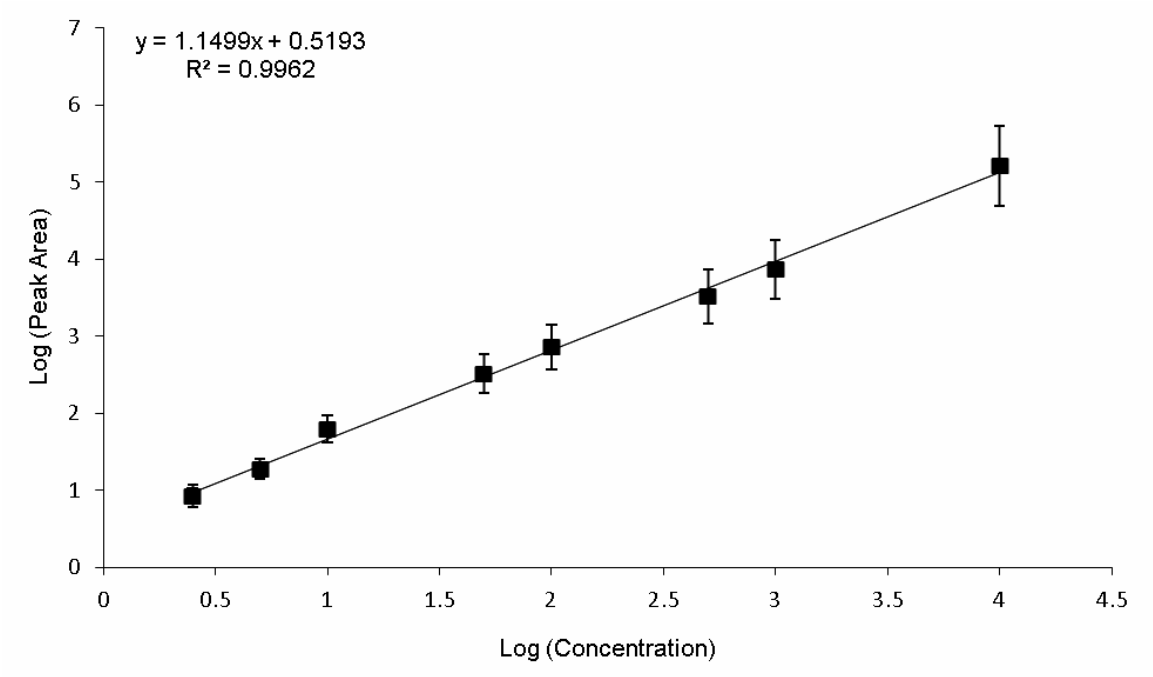

Figure 2-15 Calibration curve of the log of the average peak area of GroPIns standard versus the log of the corresponding concentration (ng/mL).

In order to evaluate the reproducibility of the results from run to run, 10 successive injections of GroPIns at 1000 ng/mL were conducted on one day. Results are shown in Figure 2-16. The coefficient of variation (relative standard deviation) in the peak was calculated to be 3.1% for GroPIns.

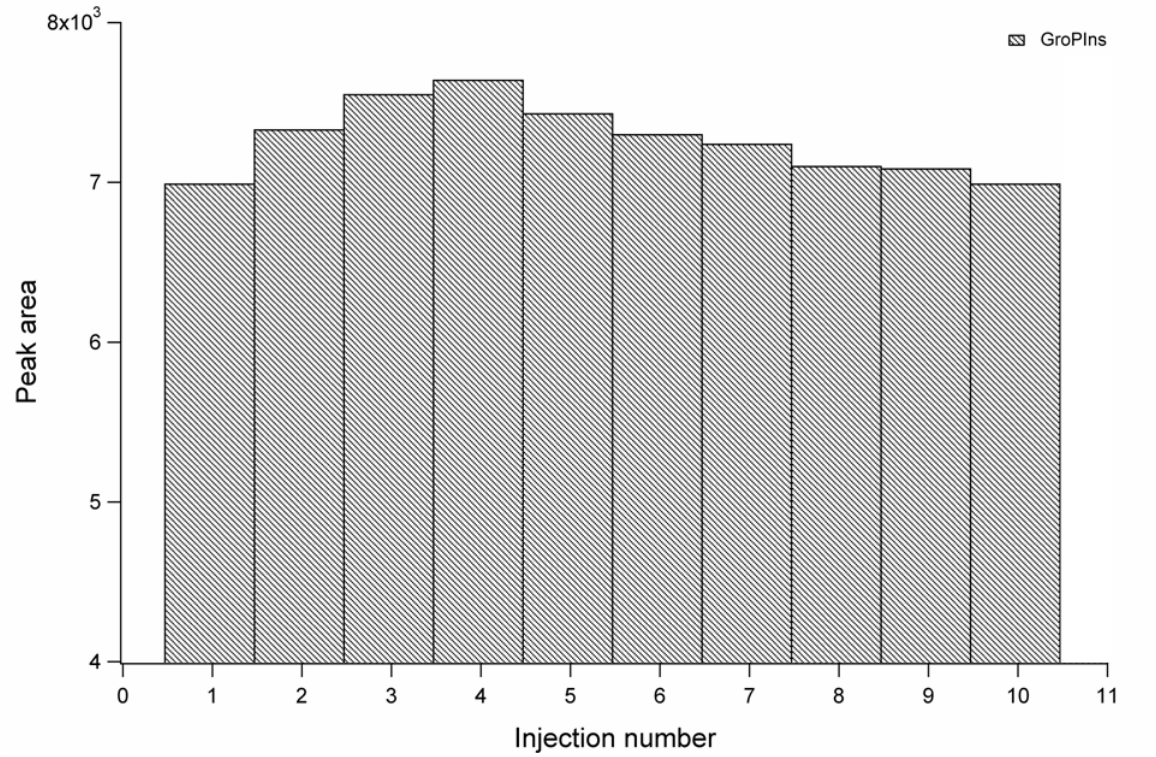

Figure 2-16 Plot of the peak areas from GroPIns over the course of 10 successive injections.

The extraction recovery of the analyte was evaluated by comparing the peak areas of medium spiked with standards at the concentrations of 500 and 1000 ng/mL in three replicates to those of blank medium extracts spiked with standards at equivalent concentrations after a single step liquid-liquid extraction. The mean extraction recovery was 82.3% for GroPIns. No significant degradation occurred under experimental conditions. These results indicate the adequate reliability and reproducibility of this method within the analytical range.

2.4.4 Determination of GroPIns Uptake in *Candida albicans*

The developed LC-MS/MS method was employed to monitor the levels of GroPIns in the medium as a function of growth in *Candida albicans* in order to obtain evidence for the transport of GroPIns across the plasma membrane. A wild type strain DAY185 (JPV484), a homozygous insertional mutant of *CaGIT1* (JPV526), and a homozygous insertional mutant bearing reintegrated *CaGIT1* (JPV512) were grown over 24 hours. 1 mL of media samples from each strain were taken in triplicate during the culture processes at T=0, 6 and 24 hours. Samples were prepared as described in section 2.2.3 and were analyzed using the optimized LC-MS/MS method. We first monitored the culture media spiked with 200 μM GroPIns to get a zero time reading and again after 6 and 24 hours of growth, at which points the GroPIns remaining in the media were monitored (Figure 2-17). A decrease in GroPIns levels in wild type strain (85.17 ± 0.93 μM at 6 hours and 1.3± 0.01 μM at 24 hours) and a decrease in GroPIns levels in homozygous insertion mutant bearing a reintegrated copy of *CaGIT1* (125.5 ± 1.05 μM at 6 hours and 1.3 ± 0.01 μM at 24 hours) were observed in Figure 2-17. In contrast, there was no decrease in the GroPIns peak for the homozygous *git1-/git1-* mutant (162.33 ± 0.96 μM at 6 hours and 178.43 ± 1.50 μM at 24 hours). The fact that the levels of GroPIns in the medium decreased or remained the same depending on the presence of the *CaGIT1* gene indicates that the depletion of GroPIns levels from the medium is dependent upon *CaGIT1*.

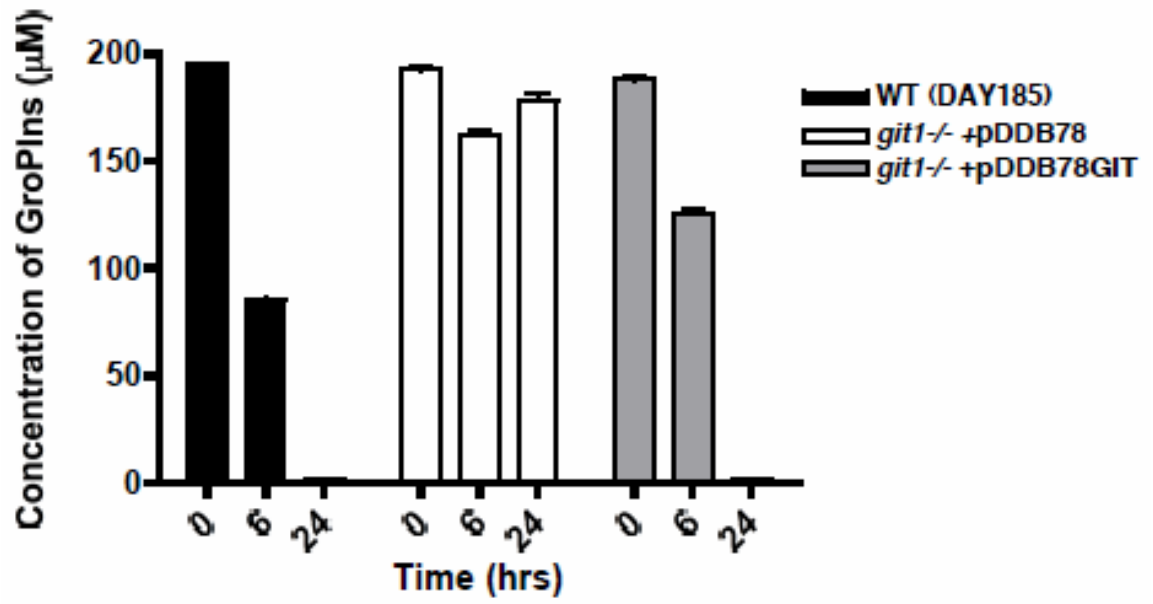

Figure 2-17 Determination of GroPIns concentrations from extracellular media of *Candida albicans* in wild type cells, a homozygous insertional mutant of *CaGIT1* (*git1-/-* +pDDB78), and a homozygous insertional mutant bearing reintegrated *CaGIT1* (*git1-/-* +pDDB78GIT) after 0, 6, and 24 hours. Because the analytes were diluted in 1:100 fold volumes before injection, the concentrations of GroPIns in the figure were calculated by multiplying the values detected in the MS by 100. Values represent mean ± S.E. of triplicate determinations.

2.5 Conclusions

A new chromatographic method was developed for analyzing a small polar lipid-related metabolite, glycerophosphoinositol, in extracellular medium of *C. albicans*. The developed method has high reproducibility, a low limit of detection, and high selectivity. It requires standard instrumentation with an isocratic HPLC system and a HILIC column which is readily adapted to tandem mass spectrometry detection. The time for a single

run analysis is less than 15 min. The analysis time could be reduced through automation and by using a gradient elution for HPLC. This method was successfully applied in a metabolic study for the determination of GroPIns uptake in *C. albicans*. The application of the approach described in this Chapter has contributed to the publication in the *Eukaryotic Cell* journal (Bishop *et al*., 2011).

2.6 Acknowledgments

This work is supported by National Science Foundation MRIDBI-0821401. Andrew C. Bishop prepared the strains and provided technical assistance. We also acknowledge the principle investigator of the NSF funding, Dr. Mitchell E. Johnson.

2.7 References

1. Henry, S. A.; Patton-Vogt, J. L.; Kivie, M., Genetic Regulation of Phospholipid Metabolism: Yeast as a Model Eukaryote. In *Progress in Nucleic Acid Research and Molecular Biology*, Academic Press: 1998; Vol. Volume 61, pp 133-179.

2. Angus, W. W.; Lester, R. L., Turnover of inositol and phosphorus containing lipids in Saccharomyces cerevisiae; extracellular accumulation of glycerophosphorylinositol derived from phosphatidylinositol. *Archives of Biochemistry and Biophysics* **1972,** 151, (2), 483-495.

3. Kohler, G. A.; Brenot, A.; Haas-Stapleton, E.; Agabian, N.; Deva, R.; Nigam, S., Phospholipase A2 and Phospholipase B activities in fungi. *Biochimica et Biophysica Acta (BBA) - Molecular and Cell Biology of Lipids* **2006,** 1761, (11), 1391-1399.

4. Hoover, C. I.; Jantapour, M. J.; Newport, G.; Agabian, N.; Fisher, S. J., Cloning and regulated expression of the Candida albicans phospholipase B (PLB1) gene. *FEMS Microbiology Letters* **1998,** 167, (2), 163-169.

5. Leidich, S. D.; Ibrahim, A. S.; Fu, Y.; Koul, A.; Jessup, C.; Vitullo, J.; Fonzi, W.; Mirbod, F.; Nakashima, S.; Nozawa, Y.; Ghannoum, M. A., Cloning and Disruption of caPLB1, a Phospholipase B Gene Involved in the Pathogenicity of Candida albicans. *Journal of Biological Chemistry* **1998,** 273, (40), 26078-26086.

6. Mukherjee, P. K.; Chandra, J.; Kuhn, D. M.; Ghannoum, M. A., Differential expression of Candida albicans phospholipase B (PLB1) under various environmental and physiological conditions. *Microbiology* **2003,** 149, (1), 261-267.

7. Mukherjee, P. K.; Seshan, K. R.; Leidich, S. D.; Chandra, J.; Cole, G. T.; Ghannoum, M. A., Reintroduction of the PLB1 gene into Candida albicans restores virulence in vivo. *Microbiology* **2001,** 147, (9), 2585-2597.

8. Jana, P.-V., Transport and metabolism of glycerophosphodiesters produced through phospholipid deacylation. *Biochimica et Biophysica Acta (BBA) - Molecular and Cell Biology of Lipids* **2007,** 1771, (3), 337-342.

9. Di Paolo, G.; De Camilli, P., Phosphoinositides in cell regulation and membrane dynamics. *Nature* **2006,** 443, (7112), 651-657.

10. Backshall, A.; Alferez, D.; Teichert, F.; Wilson, I. D.; Wilkinson, R. W.; Goodlad, R. A.; Keun, H. C., Detection of Metabolic Alterations in Non-tumor

Gastrointestinal Tissue of the ApcMin/+ Mouse by 1H MAS NMR Spectroscopy. *Journal of Proteome Research* **2009,** 8, (3), 1423-1430.

11. Corda, D.; Iurisci, C.; Berrie, C. P., Biological activities and metabolism of the lysophosphoinositides and glycerophosphoinositols. *Biochimica et Biophysica Acta (BBA) - Molecular and Cell Biology of Lipids* **2002,** 1582, (1-3), 52-69.

12. Gallazzini, M.; Burg, M. B., What's New About Osmotic Regulation of Glycerophosphocholine. *Physiology* **2009,** 24, (4), 245-249.

13. Gallazzini, M.; Ferraris, J. D.; Burg, M. B., GDPD5 is a glycerophosphocholine phosphodiesterase that osmotically regulates the osmoprotective organic osmolyte GPC. *Proceedings of the National Academy of Sciences* **2008,** 105, (31), 11026-11031.

14. Klein, J.; Gonzalez, R.; Koppen, A.; Loffelholz, K., Free choline and choline metabolites in rat brain and body fluids: sensitive determination and implications for choline supply to the brain. *Neurochemistry International* **1993,** 22, (3), 293-300.

15. Paban, V.; Fauvelle, F.; Alescio-Lautier, B., Age-related changes in metabolic profiles of rat hippocampus and cortices. *European Journal of Neuroscience* 31, (6), 1063-1073.

16. Senar, S.; Recio, M. N.; Perez-Albarsanz, M. A., Lindane affects phosphoiniositide turnover through a different mechanism of the phosphatidylinositol synthesis inhibition in rat renal proximal tubule cell culture. *Cellular Signalling* **1994,** 6, (4), 433-438.

17. Walter, A.; Korth, U.; Hilgert, M.; Hartmann, J.; Weichel, O.; Hilgert, M.; Fassbender, K.; Schmitt, A.; Klein, J., Glycerophosphocholine is elevated in cerebrospinal fluid of Alzheimer patients. *Neurobiology of Aging* **2004,** 25, (10), 1299-1303.

18. Wang, Y.; Holmes, E.; Comelli, E. M.; Fotopoulos, G.; Dorta, G.; Tang, H.; Rantalainen, M. J.; Lindon, J. C.; Corth 茅 sy-Theulaz, I. E.; Fay, L. B.; Kochhar, S.; Nicholson, J. K., Topographical Variation in Metabolic Signatures of Human Gastrointestinal Biopsies Revealed by High-Resolution Magic-Angle Spinning 1H NMR Spectroscopy. *Journal of Proteome Research* **2007,** 6, (10), 3944-3951.

19. Wang, Y.; Tang, H.; Holmes, E.; Lindon, J. C.; Turini, M. E.; Sprenger, N.; Bergonzelli, G.; Fay, L. B.; Kochhar, S.; Nicholson, J. K., Biochemical Characterization of Rat Intestine Development Using High-Resolution Magic-Angle-Spinning 1H NMR Spectroscopy and Multivariate Data Analysis. *Journal of Proteome Research* **2005,** 4, (4), 1324-1329.

20. Braun, B. R.; van het Hoog, M.; d'Enfert, C.; Martchenko, M.; Dungan, J.; Kuo, A.; Inglis, D. O.; Uhl, M. A.; Hogues, H.; Berriman, M.; Lorenz, M.; Levitin, A.; Oberholzer, U.; Bachewich, C.; Harcus, D.; Marcil, A.; Dignard, D.; Iouk, T.; Zito, R.; Frangeul, L.; Tekaia, F.; Rutherford, K.; Wang, E.; Munro, C. A.; Bates, S.; Gow, N. A.; Hoyer, L. L.; Kohler, G.; Morschhauser, J.; Newport, G.; Znaidi, S.; Raymond, M.; Turcotte, B.; Sherlock, G.; Costanzo, M.; Ihmels, J.; Berman, J.; Sanglard, D.; Agabian, N.; Mitchell, A. P.; Johnson, A. D.; Whiteway, M.; Nantel, A., A Human-Curated Annotation of the Candida albicans Genome. *PLoS Genet* **2005,** 1, (1), e1.

21. Gaur, M.; Puri, N.; Manoharlal, R.; Rai, V.; Mukhopadhayay, G.; Choudhury, D.; Prasad, R., MFS transportome of the human pathogenic yeast Candida albicans. *BMC Genomics* **2008,** 9, (1), 579.

22. Andrew J, A., Hydrophilic-interaction chromatography for the separation of peptides, nucleic acids and other polar compounds. *Journal of Chromatography A* **1990,** 499, (0), 177-196.

23. Hemström, P.; Irgum, K., Hydrophilic interaction chromatography. *Journal of Separation Science* **2006,** 29, (12), 1784-1821.

24. Zhu, B.-Y.; Mant, C. T.; Hodges, R. S., Hydrophilic-interaction chromatography of peptides on hydrophilic and strong cation-exchange columns. *Journal of Chromatography A* **1991,** 548, (0), 13-24.

25. Ikegami, T.; Tomomatsu, K.; Takubo, H.; Horie, K.; Tanaka, N., Separation efficiencies in hydrophilic interaction chromatography. *Journal of Chromatography A* **2008,** 1184, (1 欽?), 474-503.

26. Morse, M. J.; Crain, R. C.; Satter, R. L., Phosphatidylinositol Cycle Metabolites in Samanea saman Pulvini. *Plant Physiolgy* **1987,** 83, (3), 640-644.

27. Mazzola, G.; Kent, C., Separation of choline- and ethanolamine-labeled metabolites by ion-exchange high-pressure liquid chromatography. *Analytical Biochemistry* **1984,** 141, (1), 137-142.

28. Lin, S.; Fischl, A. S.; Bi, X.; Parce, W., Separation of phospholipids in microfluidic chip device: application to high-throughput screening assays for lipid-modifying enzymes. *Analytical Biochemistry* **2003,** 314, (1), 97-107.

29. Binder, H.; Weber, P. C.; Siess, W., Separation of inositol phosphates and glycerophosphoinositol phosphates by high-performance liquid chromatography. *Analytical Biochemistry* **1985,** 148, (1), 220-227.

30. Dragani, L. K.; Berrie, C. P.; Corda, D.; Rotilio, D., Analysis of glycerophosphoinositol by liquid chromatography-electrospray ionisation tandem

mass spectrometry using a beta-cyclodextrin-bonded column. *Journal of Chromatography B* **2004,** 802, (2), 283-289.

31. Kopp, F.; Komatsu, T.; Nomura, D. K.; Trauger, S. A.; Thomas, J. R.; Siuzdak, G.; Simon, G. M.; Cravatt, B. F., The Glycerophospho Metabolome and Its Influence on Amino Acid Homeostasis Revealed by Brain Metabolomics of GDE1(-/-) Mice. *Chemistry & Biology* 17, (8), 831-840.

32. Kopp, F.; Komatsu, T.; Nomura, D. K.; Trauger, S. A.; Thomas, J. R.; Siuzdak, G.; Simon, G. M.; Cravatt, B. F., The Glycerophospho Metabolome and Its Influence on Amino Acid Homeostasis Revealed by Brain Metabolomics of GDE1(/) Mice. *Chemistry & biology* **2010,** 17, (8), 831-840.

33. Hsieh, Y., Potential of HILIC-MS in quantitative bioanalysis of drugs and drug metabolites. *Journal of Separation Science* **2008,** 31, (9), 1481-1491.

34. Weng, N., Bioanalytical liquid chromatography tandem mass spectrometry methods on underivatized silica columns with aqueous/organic mobile phases. *Journal of Chromatography B* **2003,** 796, (2), 209-224.

35. Lin, Z. J.; Li, W.; Dai, G., Application of LC-S for quantitative analysis and metabolite identification of therapeutic oligonucleotides. *Journal of Pharmaceutical and Biomedical Analysis* **2007,** 44, (2), 330-341.

36. Zhou, S.; Song, Q.; Tang, Y.; Naidong, W., Critical Review of Development, Validation, and Transfer for High Throughput Bioanalytical LC-MS/MS Methods *Current Pharmaceutical Analysis* **2005,** 1, (1), 3-14.

37. Dowd, S. R.; Bier, M. E.; Patton-Vogt, J. L., Turnover of Phosphatidylcholine in Saccharomyces cerevisiae. *Journal of Biological Chemistry* **2001,** 276, (6), 3756-3763.

38. Patton, J. L.; Pessoa-Brandao, L.; Henry, S. A., Production and reutilization of an extracellular phosphatidylinositol catabolite, glycerophosphoinositol, by Saccharomyces cerevisiae. *Journal of Bacteriology* **1995,** 177, (12), 3379-85.

39. Fernandez-Murray, J. P.; McMaster, C. R., Glycerophosphocholine Catabolism as a New Route for Choline Formation for Phosphatidylcholine Synthesis by the Kennedy Pathway. *Journal of Biological Chemistry* **2005,** 280, (46), 38290-38296.

Chapter 3

Simultaneous Quantification of Lipid-Related Extracellular Metabolites in Saccharomyces cerevisiae using HILIC-MS/MS: Application in Metabolomic Study[1]

[1]The work described in this Chapter is presented in the following manuscript:

Sun, T.; Wetzel, S. J.; Johnson, M. E.; Surlow, B. A.; Patton-Vogt, J. Development and validation of a hydrophilic interaction liquid chromatography-tandem mass spectrometry method for the quantification of lipid-related extracellular metabolites in *Saccharomyces cerevisiae*, *Journal of Chromatography B*, 2012, Accepted pending revisions.

3.1 Abstract

In this Chapter, a highly sensitive hydrophilic interaction liquid chromatography-tandem mass spectrometry (HILIC-MS/MS) method was developed and validated for the quantification of glycerophosphoinositol (GroPIns), glycerophosphocholine (GroPCho), glycerol 3-phosphate (GroP), inositol, and choline in the extracellular medium of *Saccharomyces cerevisiae*. The media samples were pretreated with a single two-phase liquid extraction. Chromatographic separation was achieved on a Waters Xbridge HILIC (150×4.6 mm, 5 μm) column under isocratic conditions using a mobile phase composed of acetonitrile/water, 70:30 (v/v) with 10 mM ammonium acetate at a flow-rate of 0.5 mL/min. Using a triple quadrupole tandem mass spectrometer, samples were detected in multiple reaction monitoring (MRM) mode via an electrospray ionization (ESI) source. The calibration curves were linear ($r^2 \geq 0.995$) over the range of 0.5-150 nM, with the lower limit of quantitation validated at 0.5 nM for all analytes. The intra- and inter-day precision ranged from 1.24 to 5.88% and 2.46 to 9.77% (CV%), respectively, and intra- and inter-day accuracy was between -8.42 to 8.22% and -9.35 to 6.62% (RE%), respectively, at all quality control levels. The extracellular metabolites were stable throughout various storage stability studies. The fully validated method was successfully applied to determine the extracellular levels of phospholipid-related metabolites in *S. cerevisiae*.

3.2 Introduction

The metabolome represents the full collection of low-molecular weight chemical species within a cell or biological system, and is considered the endpoint of "omics analysis" [1-3]. Current research on metabolomic investigation consists of four complementary approaches: target analysis, metabolic profiling, metabolic fingerprinting, and metabolic footprinting [4-6]. All of these approaches are usually applied to investigate differences in metabolite concentrations after alterations in the biological environment or upon genetic modification. The measurement of extracellular metabolites secreted from the intracellular volume into the growth medium is termed "metabolic footprinting". Footprinting analysis offers important technical advantages over the analysis of intracellular compounds, referred to as "metabolic fingerprinting" [7-9]. First of all, the extracellualar metabolome is generally quite stable owing to the relative lack of enzymes that can convert the metabolites into other products. Therefore, the time-consuming quenching steps associated with the analysis of intracellular metabolites are not required when extracellular metabolites are analyzed. In addition, the extracellular metabolome is generally simplified in terms of the number of metabolites present and their concentration ranges as compared to the intracellular metabolome, but can still provide important insight into cellular metabolism [7]. Metabolic footprinting has been used in the classification of microbial mutants for functional genomics studies by employing mass spectrometry (MS) [3, 10-12] or nuclear magnetic resonance (NMR) analysis [13]. For yeast and mammalian cells, metabolic footprinting has been performed

under a limited number of conditions, and has primarily focused on central carbon metabolites [14-18]. To our knowledge, no metabolic footprinting study has focused on lipid metabolites.

The simple eukaryote, *Saccharomyces cerevisiae*, has been used as a model to study many aspects of cell biology, including lipid metabolism [19-23]. We have chosen to monitor five major phospholipid metabolites in the media of *S. cerevisiae*: inositol, choline, glycerol 3-phosphate, glycerophosphoinositol, and glycerophosphocholine (Table 3-1). The lipid precursors inositol and choline regulate phospholipid biosynthesis at the transcriptional level in *S. cerevisiae* [24]. Thus, they are frequently added to and removed from medium to study and manipulate the biosynthetic pathways. In addition, inositol and choline can be produced by the cell via lipid turnover events. We chose to monitor GroP as it represents a metabolite that could be produced through phospholipid turnover, and is also a metabolic precursor involved in phospholipid biosynthesis. Finally, extracellular GroPIns and GroPCho are produced through the hydrolytic cleavage of both acylester bonds of plasma membrane-associated glycerophospholipids by phospholipase B type enzymes [20, 21, 25]. Thus, extracellular GroPIns and GroPCho can be monitored as an indicator of phospholipase B activity encoded by the *PLB1, PLB2,* and *PLB3* genes. Overall, the concentration of each of these metabolites in the medium is the result of two processes: their production via enzymatic activity and their uptake via plasma membrane transport.

Name	Structure
Glycerophosphoinostol	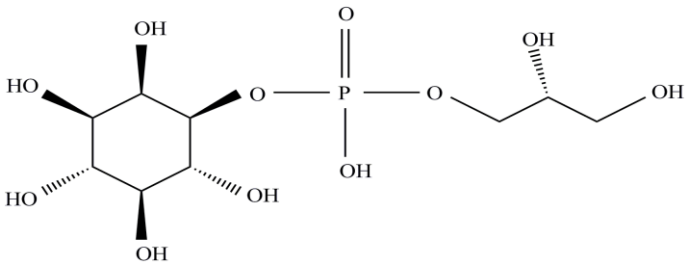
Glycerophosphocholine	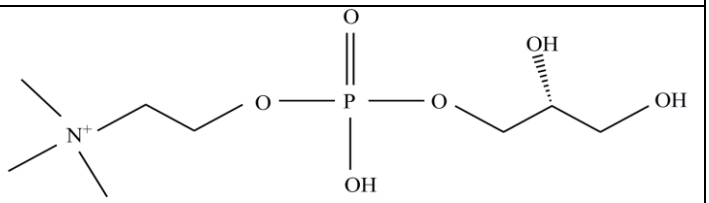
Glycerol 3-phosphate	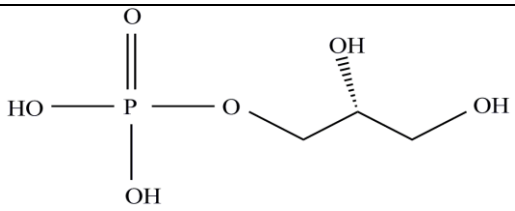
Inositol	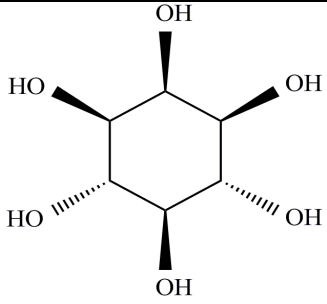
Choline	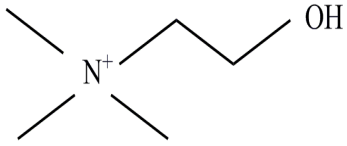
Choline-d_9	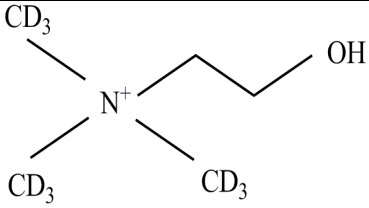

Table 3-1 Molecular structures of five lipid-related metabolites and internal standard.

This method was developed in order to create a simplified and sensitive method for the absolute and simultaneous quantitation of the levels of important phospholipid metabolites in the media of *S. cerevisiae*. Previous studies in which one or more of the compounds has been monitored usually involve the use of radioactivity, as the compounds have no UV or fluorescence detectable groups. For example, ^{3}H or ^{14}C labeled inositol or choline, and ^{32}P-H_3PO_4 are typically utilized [26-28]. However, measuring all of these compounds simultaneously with multiple radioactive compounds is technically challenging, even if a good separation system is at hand. In addition, the use of radioactive molecules can also present a quantitation problem. For example, since *S. cerevisiae* can both synthesize and import inositol and choline, radioactive labeling only allows for the discrimination of inositol and choline transported into the cell, not that derived from de novo synthesis. In contrast, MS detects all chemical species, regardless of their mode of synthesis. Finally, the method described here is an advance in terms of the LC separation of the compounds. While published procedure has described the chromatographic separation of choline-containing metabolites, and inositol-containing metabolites, we know of no published procedure for the LC separation of all five of these compounds simultaneously [29-31].

Two published studies are pertinent to the method described here. A LC-MS/MS method using a β-cyclodextrin-bonded column was described for the quantitative analysis of internal GroPIns in rat cell lines, but other metabolites were not included in this method [32]. Another study used normal phase LC-MS to quantitate several water-soluble metabolites, including GroPIns and GroPCho, from rat brain tissue [33]. Our

method differs from that of Kopp et al [33] in that we perform extensive method validation, we analyze an overlapping but different set of metabolites, and we use HILIC chromatography, which results in decreased retention times as compared to normal phase.

Here, we present a hydrophilic interaction liquid chromatography-tandem mass spectrometry (HILIC-MS/MS) method for the quantification of five lipid-related extracellular metabolites in *S. cerevisiae* cells. A liquid-liquid extraction procedure has been combined with an extensive optimization of HILIC-MS/MS methodology to provide effective and reliable chromatographic separation of analytes in the supernatant of extracellular medium. The method is highly sensitive and has been thoroughly validated according to the bioanalytical method validation guidelines for industry as specified by the US Food and Drug Administration (FDA) (www.fda.gov/downloads /Drugs/Guidance ComplianceRegulatoryInformation/Guidances/ucm070107.pdf).

3.3 Experimental

3.3.1 Materials and Regents

Standard compounds including glycerophosphoinositol (L-α–glycerophospho –D–myo-inositol), glycerophosphocholine (L-α–glycerophosphorylcholine), glycerol 3-phosphate (L-α–glycero-phosphate), myo-inositol, and choline chloride were purchased from Sigma-Aldrich (St. Louis, MO, USA). The deuterated internal standard (IS), choline chloride-d_9, was obtained from Cambridge Isotopes (Andover, MA, USA). Ammonium acetate was purchased from Fisher Scientific (Pittsburgh, PA, USA).

Optima grade methanol and acetonitrile used for LC-MS/MS analysis were also purchased from Fisher Scientific. Deionized water was obtained using a Milli-Q water purification system from Millipore (Bedford, MA, USA).

3.3.2 Preparation of Standard Solutions and Quality Control Samples

Primary stock solutions of glycerophosphoinositol (GroPIns), glycerophospho-choline (GroPCho), glycerol 3-phosphate (GroP), myo-inositol, choline chloride, and choline chloride-d_9 (IS) were prepared in methanol/water, 1:1 (v/v) at a concentration of 50 mM, respectively. Working standard solutions were made by diluting the primary stock solutions in water to a concentration of 10 μM. A working standard solution of the internal standard (choline-d_9) in 2.5 μM was prepared by diluting its primary stock solution in deionized water. Eight calibration standards were prepared by adding 25 μL aliquots of appropriate dilution of the working standard solutions and internal standard to 475 μL aliquots of the blank medium to obtain the following concentrations: 0.5, 1.5, 5, 10, 30, 60, 90 and 150 nM. Quality control (QC) samples were prepared at concentrations of 2 nM (low QC, LQC), 50 nM (middle QC, MQC), and 100 nM (high QC, HQC) by spiking the blank media with the working standard solutions. The primary stock solutions, working standard solutions and QC samples were stored at -20°C until use.

3.3.3 Culture Conditions and Sample Preparation

The *S. cerevisiae* wild type strains, BY4741 (JPV203, *MATa his3Δ1 leu2Δ0 met15Δ0 ura3Δ0*) and BY4742 (JPV399, *MATα his3Δ1 leu2Δ0 lys2Δ0 ura3Δ0*) were purchased from Open Biosystems (Thermo Scientific, Huntsville, AL, USA). The deletion strains were constructed using standard homologous recombination techniques. Drug resistant markers, *hph*, *KanMX*, and *nat1* were amplified from plasmids pAG32, pUG6, and pAG25, respectively, and were inserted in place of the target genes for deletion. The plasmids were received from Euroscarf [34, 35]. Deletion strains were constructed in JPV203 to produce *plb1::hph* (JPV617), *plb2::KanMX* (JPV618), *plb3::nat1* (JPV 619), *plb1::hph/plb2::KanMX/plb3::nat1* (JPV623), and in strain JPV399 to produce *plb1::hph* (JPV668). Strains were grown aerobically at 30°C in yeast nitrogen base (YNB) medium containing 75 μM inositol, 20 μM choline, and 2 mM KH_2PO_4 instead of normal 7.35 mM KH_2PO_4 in order to minimize ion suppression in mass spectrometry. Growth was monitored by measuring the OD 600 nm using a Biomate 3 Thermo Spectronic spectrophotometer.

To prepare medium samples, culture aliquots were centrifuged at 3000 rpm for 5 min, and the resulting supernatant was filtered. A liquid-liquid extraction approach was performed in order to separate polar lipid metabolites from the non-polar materials in the extracelluar medium. 10 μL of internal standard working solution and 100 μL aliquots of the metabolite containing supernatant were added to 890 μL of chloroform/methanol, 2:1 (v/v). This mixture was vortexed for 2 min, followed by centrifugation at 3000 rpm for 3 min. A 200 μL aliquot of the upper phase (49.3 ± 1.0% of the total analytes) was

collected and transferred into a 1.5-mL HPLC vial for evaporation under nitrogen. The residue was reconstituted in 200 μL of acetonitrile/methanol, 75:25 (v/v) and was diluted in 1:100 fold volumes before analysis. The sample injection volume to LC-MS/MS system was 10 μL.

3.3.4 Instrumentation

Chromatographic studies were performed via a 1200 series Rapid Resolution LC system coupled with a 6440 Triple Quadrupole Mass Spectrometer (Agilent, Santa Clara, CA, USA). MassHunter workstation software package was used for data acquisition and processing. Quantification was determined using Qualitative (B1.0.82.2) and Quantitative (B1.0.77.3) Analysis as implemented in the MassHunter software.

3.3.4.1 Chromatographic Conditions

The analytical column used was a Waters Xbridge HILIC (150×4.6 mm, 5 μm) column from Waters Corporation (Milford, MA, USA). Separations were performed under isocratic conditions at a flow rate of 0.5 mL/min at room temperature. Mobile phase consisted of acetonitrile/water, 70:30 (v/v) with 10 mM ammonium acetate at pH 4.5. Column effluent was then passed through the mass spectrometer for later detection.

3.3.4.2 MS Settings

Electrospray mass spectrometry (ESI-MS) was performed on a triple quadrupole mass spectrometer. Mass transitions of m/z for each metabolite and IS were optimized by direct infusion of the respective analytes in acetonitrile/water, 70:30 (v/v) with 10 mM ammonium acetate in product ion mode. Optimum settings for subsequent LC-MS analyses were manually adjusted. Metabolites were detected in both positive and negative ionization modes at different time segments in one run using multiple reaction monitoring (MRM). Other MS parameters were set as follows: capillary voltage of 3.5 KV, drying gas temperature of 300°C, fragmentor voltage of 50 V, and sheath gas temperature of 325°C. Sheath gas flow and drying gas flow rates (both are nitrogen) were set at 10 and 8 L/min, respectively. Low and high mass resolutions were fixed at 15 (arbitrary units) for both the first and third quadrupole mass analyzers. Dwell time and interchannel delay were maintained at 200 and 10 ms, respectively. Collision energy in the rf-only quadrupole cell and transitions were optimized for each metabolite on the reference compound. The starting parameters of ESI source for small molecules from the manufacture's instruction are illustrated in Table 3-2.

Flow dependent parameters		**Compound dependent parameters**	
Nebulizer pressure	30 psi	Capillary voltage	2 kV
Drying gas flow	5 L/min	Fragmentor voltage	10 V
Drying gas temperature	200 °C	Collision energy	0 eV

Sheath gas flow	8 L/min	Sheath gas temperature	250 °C

Table 3-2 Starting parameters for ESI source optimization.

3.3.5 Method Validation

The LC-MS/MS method was validated through evaluation of specificity, linearity, sensitivity, intra- and inter-day precision, accuracy, recovery, and stability in accordance with currently approved FDA bioanalytical method validation guidelines.

3.3.5.1 Specificity and Selectivity

To determine if endogenous contaminants were present in coelution with the analytes, the chromatography was developed and the MS/MS parameters were optimized to obtain separation of the analytes from potentially interfering compounds as well as the highest signal to noise ratios.

3.3.5.2 Linearity of Calibration Standards, Precision, and Accuracy

Linearity was evaluated over the concentration range of 0.5 to 150 nM. The calibration curve was constructed by plotting the peak area ratio of analyte to that of IS against the nominal concentration of calibration standards. The results were fitted to

least-squares linear regression analysis with a correlation coefficient of 0.995 or better. Intra-day and inter-day precision and accuracy were determined through analysis of six replicates at four different levels (0.5, 2, 50 and 100 nM) during the same day and on three different days. The precision was determined by calculating the coefficient of variation (CV), and the accuracy was expressed in the form of the relative error (RE), which was calculated as the percent deviation of the mean from the true value. The acceptance criteria of the data included precision within ±15% CV from the nominal values and an accuracy of within ±15% RE, except for LLOQ, where it should not exceed ±20% of accuracy as well as precision (Bioanalytical method validation guidelines of FDA).

3.3.5.3 Recovery

The extraction recoveries of analytes from medium were determined by comparing the mean peak areas of medium spiked with standards at three levels (2, 50 and 100 nM, n=6) to those of blank medium extracts spiked with standards at equivalent concentrations, corrected for the evaporated volume of organic phase. The recovery of the internal standard was determined at a concentration of 50 nM.

3.3.5.4 Matrix Effect

Matrix effects from the medium samples were evaluated by comparing the peak areas of the spiked blank medium extracts (2, 50 and 100 nM, n=6) to the peak areas from standards spiked in mobile phase of acetonitrile/water, 70:30 (v/v) with 10 mM ammonium acetate.

3.3.5.5 Stability

The stability of analytes in medium was investigated using QC samples (2 and 100 nM) stored under different temperature conditions for different periods of time. The six replicates were subjected to three freeze (12, 18 and 24 h) – thaw (2, 3 and 4 h) cycles. Short-term storage stability was evaluated at room temperature for 4 h, and long-term storage stability at -20°C for 30 days. Reinjections of QC samples (n=6) were analyzed after 24 h storage at the same concentrations in the autosampler.

3.4 Results and Discussion

3.4.1 Optimization of MS/MS Conditions

The Agilent triple quadruple mass spectrometer applies Jet stream technology, of which the super-heated sheath gas collimates the nebulizer spray and presents more ions

to the MS inlet. The source optimization for ESI-MS system is composed of two main parameters: flow dependent parameters and compound dependent parameters. The flow dependent parameters include nebulizer pressure, drying gas temperature and flow and sheath gas flow, while the compound dependent parameters consist of capillary voltage, fragmentor voltage, collision energy and sheath gas temperature. All the parameters had a substantial effect on the MS/MS determination of the analytes and thus their adjustment was crucial. The optimum conditions for the determination of the metabolites by triple quadruple MS/MS extracted from this experiment are summarized in Table 3-3.

Analyte	Capillary voltage (kV)	Fragmentor voltage (V)	Collision energy (eV)	Drying gas temperature (° C)	Sheath gas temperature (° C)	Drying gas flow (L/min)	Sheath gas flow (L/min)	Nebulizer pressure (psi)
GroPIns	3.5	50	20	300	325	8	10	45
GroPCho	3.5	50	10	300	325	8	10	45
GroP	3.5	50	10	300	325	8	10	45
Inositol	3.5	50	20	300	325	8	10	45
Choline	3.5	50	10	300	325	8	10	45
Choline-d_9	3.5	50	10	300	325	8	10	45

Table 3-3 Optimum parameter values for the determination of lipid-related metabolites by triple quadruple MS/MS technique

The standards of the analytes were first characterized by total ion scan and product ion scan through direct infusion to ascertain their precursor ions and to select product ions for use in MRM mode. Voltages and gas flow changed quickly and were optimized with series of flow injections. Temperatures including sheath gas and drying gas needed equilibration time between injections. The MS/MS parameters, specifically fragmentor voltage and collision energy, were evaluated for the best response of the parent ion and daughter ion, respectively, using the starting parameters above for ESI source and then transferred to the MRM method. Long dwell times were required for obtaining better sensitivity. GroPCho, GroP, and choline were found to give the most intense protonated molecular ions under positive ionization, while GroPIns and inositol were detected in negative ionization mode. The m/z values of precursor ions and fragment ions for each analyte are illustrated in Table 3-4.

Analyte	Ionization mode (m/z)	Precursor ion (m/z)	Transition pairs (m/z)	Main fragmentation structure
Choline	Positive	104.1	104.1→60.1	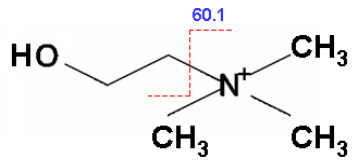
Choline-d_9	Positive	113.1	113.1→69.1	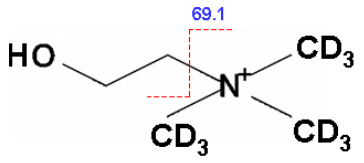
GroP	Positive	172.7	172.7→98.8	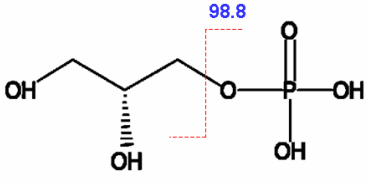

Inositol	Negative	178.7	178.7→86.8	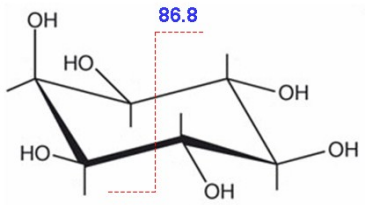
GroPCho	Positive	258.0	258.0→104.0	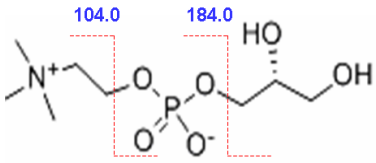
GroPIns	Negative	333.0	333.0→152.9	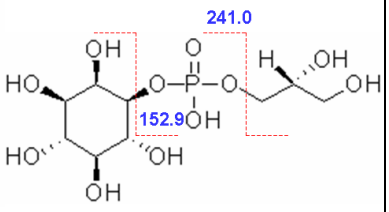

Table 3-4 Precursor ions, transition pairs and the corresponding main fragmentation structures for the analytes and internal standard.

Full scan spectra produced a predominant peak for $[M+H]^+$ at m/z 258.0 of GroPCho, 172.7 of GroP, 104.1 of choline, and 113.1 of internal standard, respectively. The deprotonated molecular ions $[M-H]^-$ of GroPIns and inositol were detected at m/z 333.0 and 178.7, respectively. Collision induced dissociation of the precursor ions produced major fragmentation for each analyte. Therefore, the transition pairs 258.0→104.0 (Figure 3-1), 172.7→98.8 (Figure 3-2), 104.1→60.1 (Figure 3-3), and 113.1→69.1 (Figure 3-4) were optimized for GroPCho, GroP, choline, and choline-d_9, respectively. Using similar procedures, the MRM transition of GroPIns and inositol were determined to be 333.0→152.9 (Figure 3-5), and 178.7→86.8 (Figure 3-6), respectively.

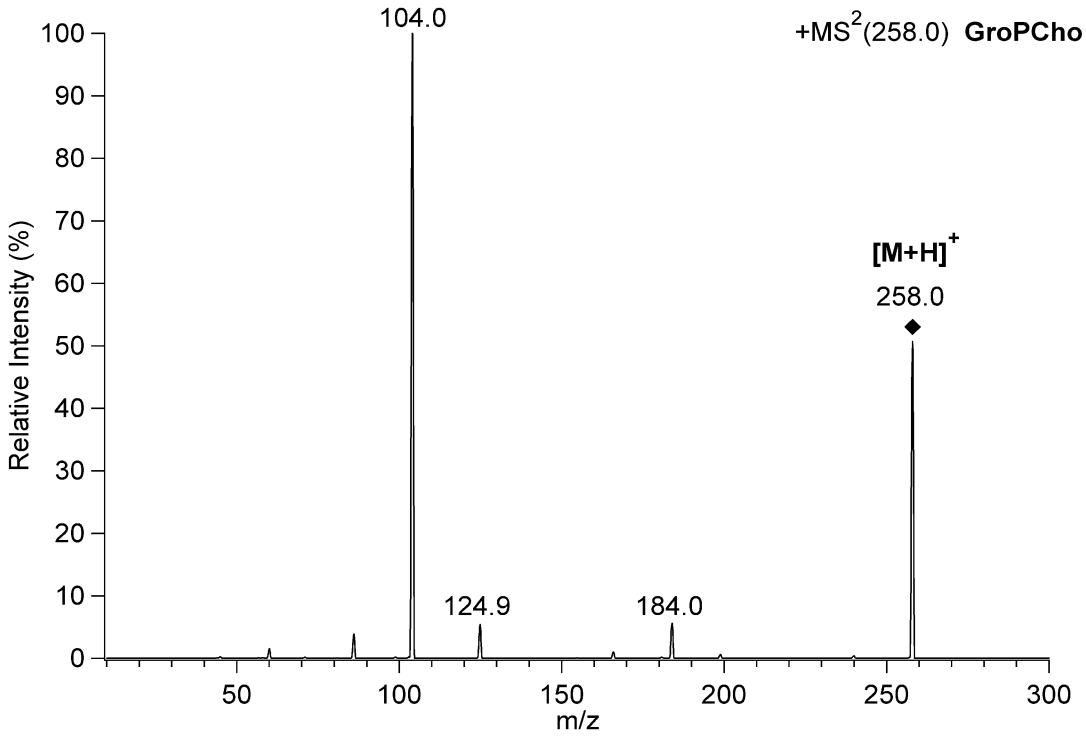

Figure 3-1 Tandem mass spectra of the GroPCho by product ion scan in positive mode.

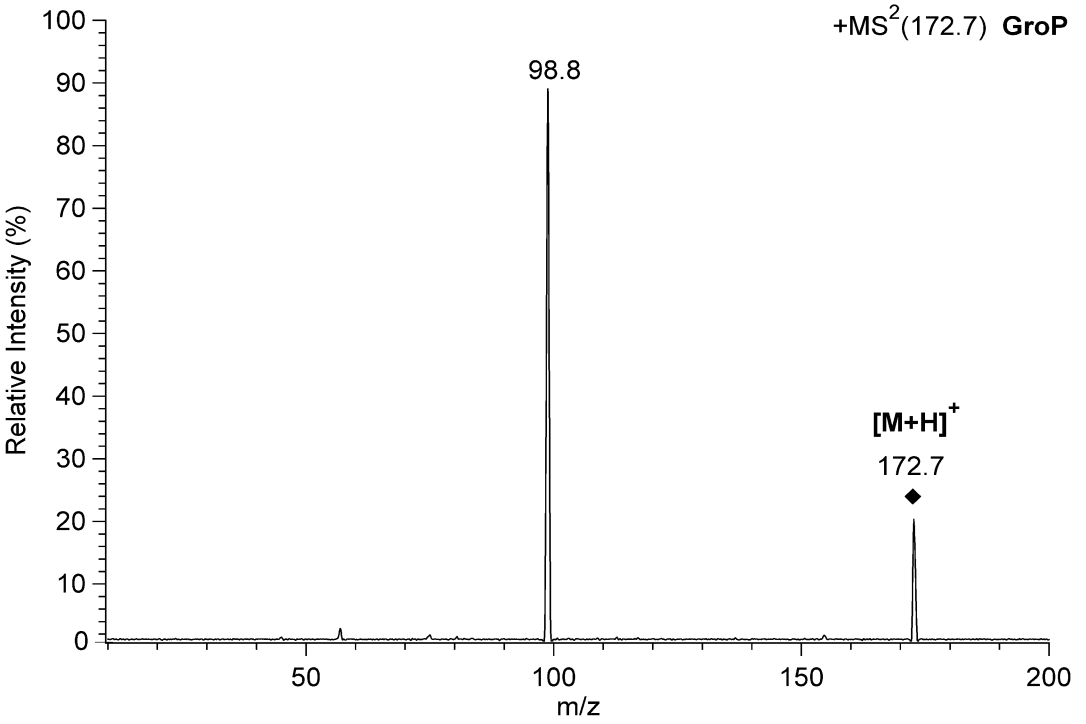

Figure 3-2 Tandem mass spectra of the GroP by product ion scan in positive mode.

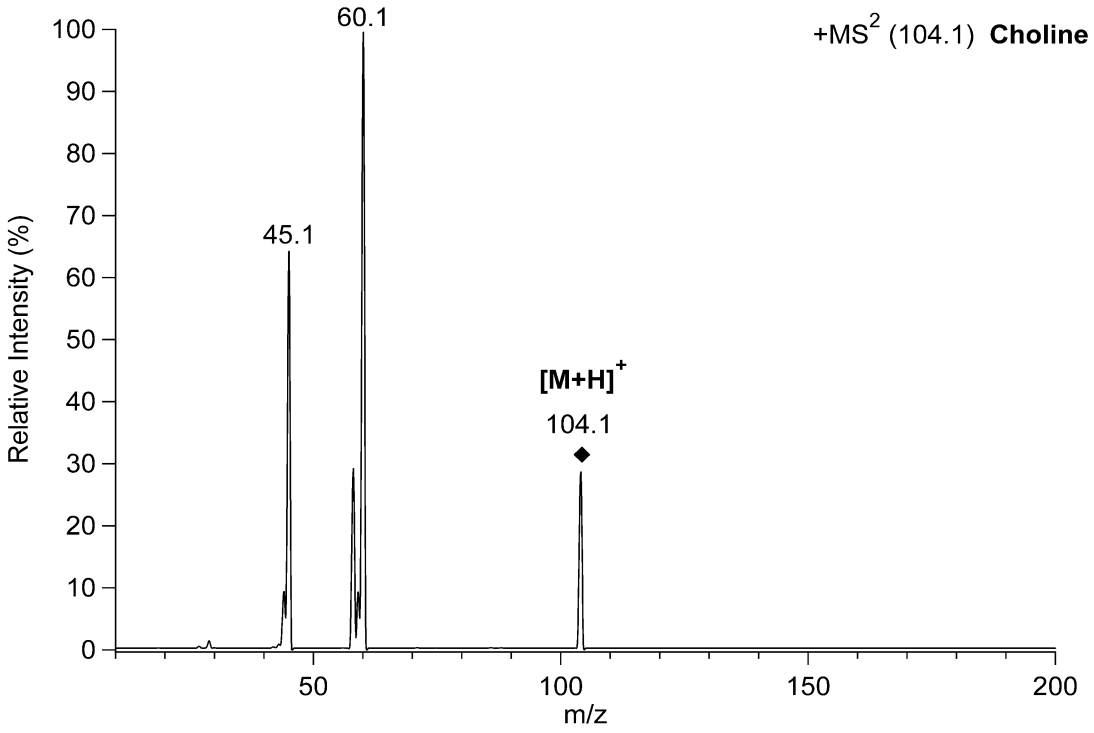

Figure 3-3 Tandem mass spectra of the choline by product ion scan in positive mode.

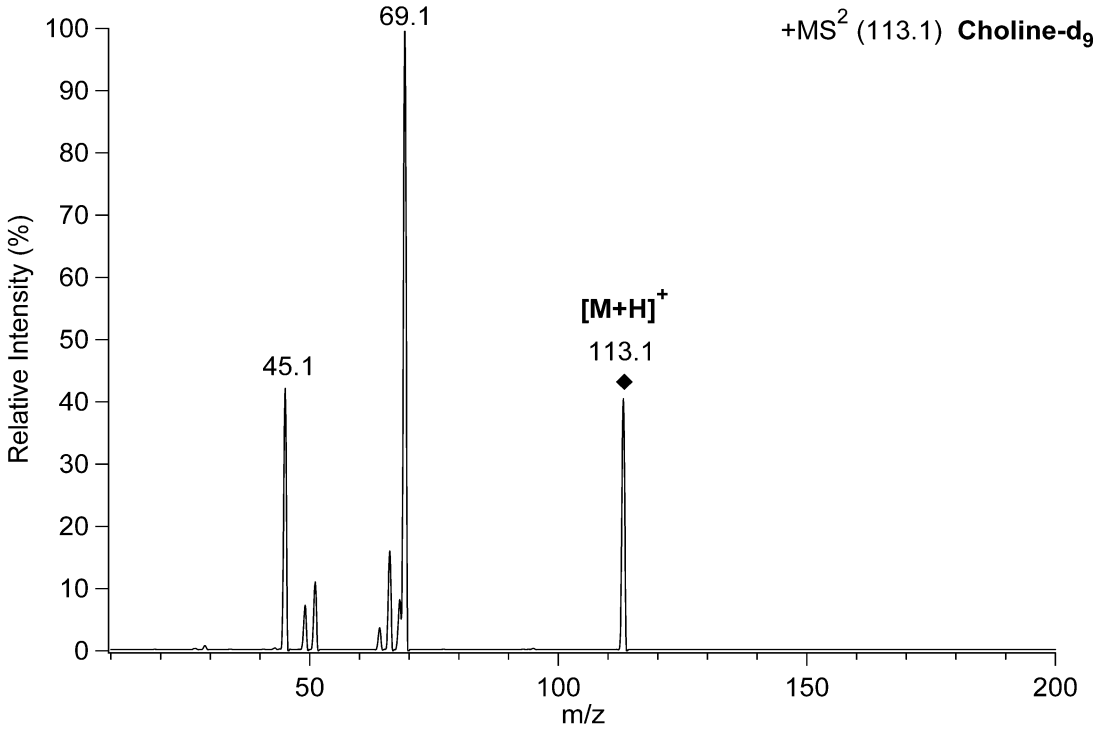

Figure 3-4 Tandem mass spectra of the choline-d_9 by product ion scan in positive mode.

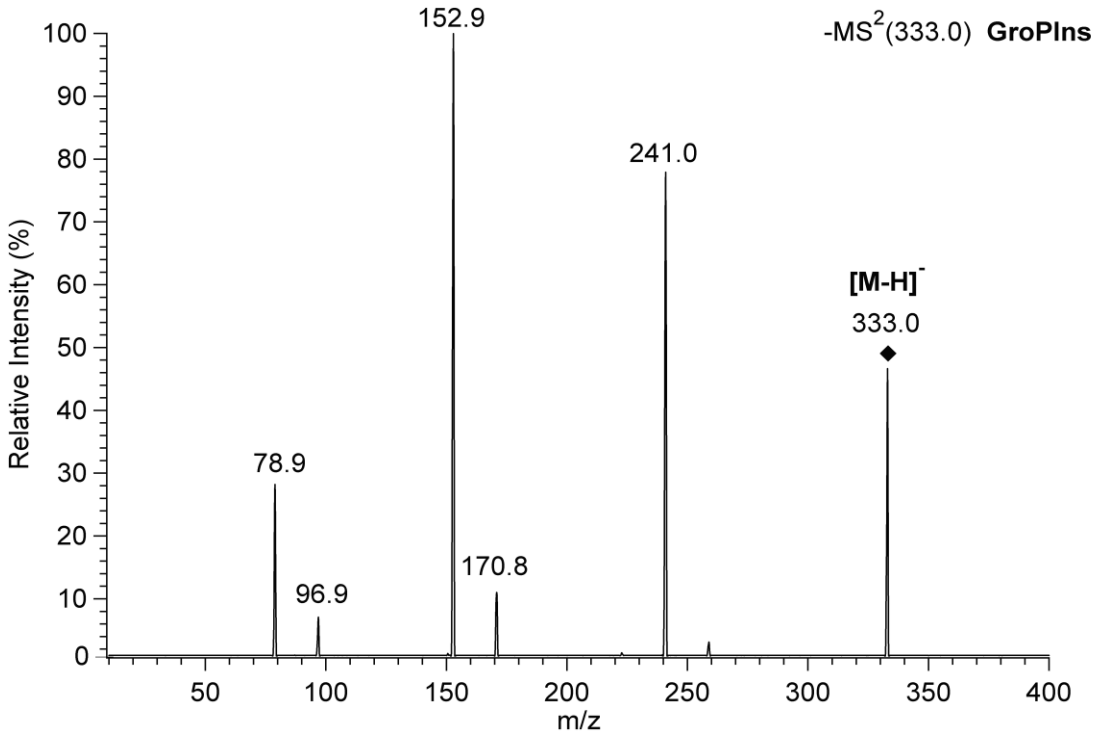

Figure 3-5 Tandem mass spectra of the GroPIns by product ion scan in negative mode.

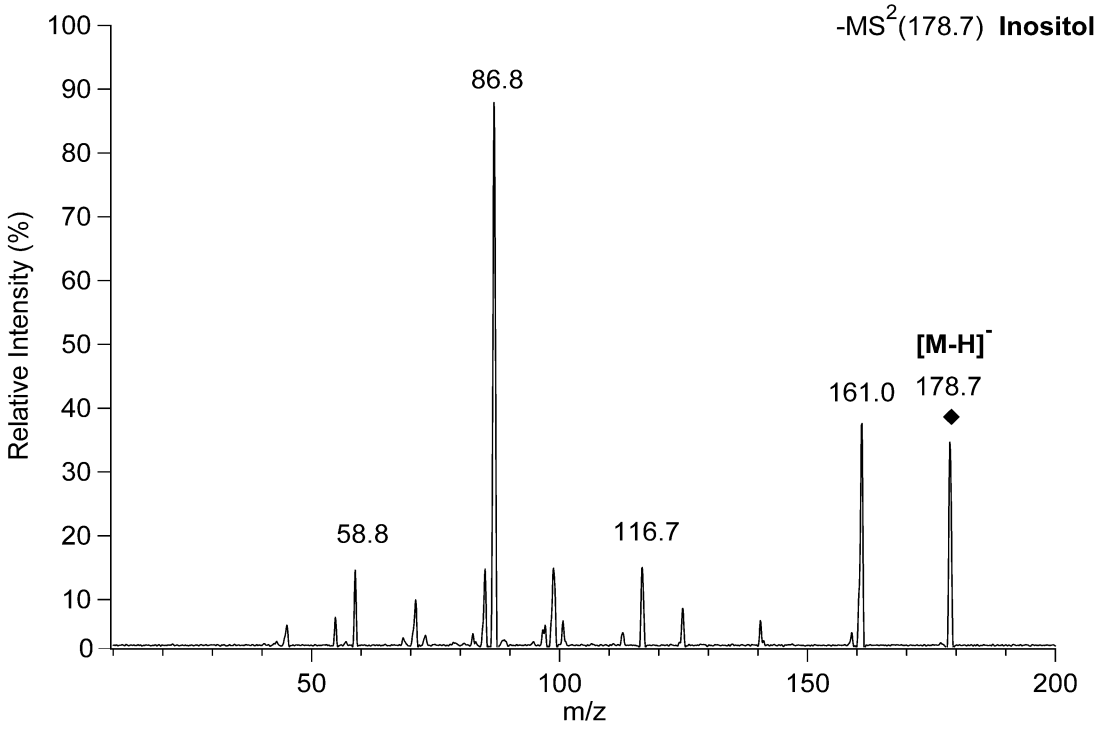

Figure 3-6 Tandem mass spectra of the inositol by product ion scan in negative mode.

3.4.2 Optimization of LC Conditions

Polar lipid-related metabolites were extracted from the extracellular medium by a liquid-liquid extraction. Chloroform/methanol, 2:1 (v/v) was used as the extraction solvent to remove non-polar compounds from the medium. The choice of a chromatography method was less straightforward since a diverse range of metabolites at widely differing concentrations are present in culture medium. A HILIC column was chosen as an appropriate approach based on a review of the literatures for smaller hydrophilic and ionizable analytes [36-45]. A Waters Xbridge HILIC (150×4.6 mm, 5 μm) column was selected to provide the best compromise between specificity and speed of analysis. With the optimum isocratic elution, the metabolites were adequately separated with retention times of 5.58 min for inositol, 15.47 min for GroP, 15.68 min for GroPIns, 5.39 min for GroPCho, and coelution of choline and choline-d_9 at 3.38 and 3.37 min, respectively (Figure 3-7B).

3.4.3 Method Validation

3.4.3.1 Specificity and Selectivity

Representative chromatograms of blank medium, a spiked medium sample, and the medium obtained after growth of a wild type strain were shown in Figure 3-7. No interference with the retention time of the analytes and internal standard (Figure 3-7B and

3-7C) was observed in the blank medium (Figure 3-7A), indicating the specificity of the present method.

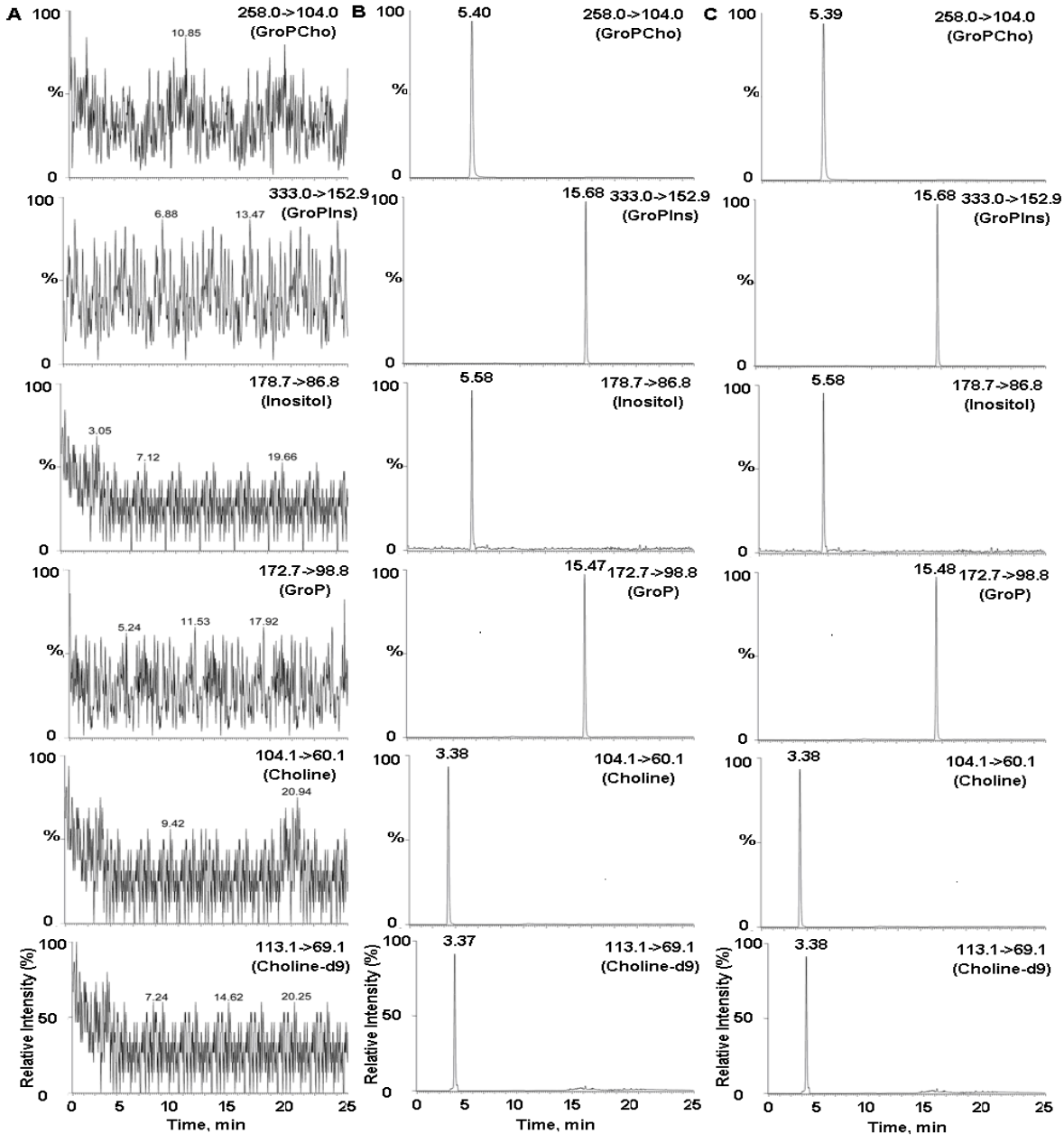

Figure 3-7 Representative LC-MS/MS chromatograms of (A) a blank medium (noise baseline), (B) medium sample spiked with analytes and internal standard at 0.5 nM (LLOQ), and (C) medium from a wild type strain (JPV203) spiked with internal standard at 0.5 nM.

3.4.3.2 Linearity of Calibration and LLOQ

The calibration curves were constructed by plotting the instrument response (peak area ratio (analyte/IS)) versus calibration standard concentration. A linear relationship was constructed over the concentration range of 0.5-150 nM. Correlation coefficients (r^2) of the calibration curves for all standards ranged between 0.995 and 0.997 (Figure 3-8, 3-9, 3-10, 3-11 and 3-12). The precisions (CV%) were less than 8.7%, and the accuracies (RE%) were within the range of -6.2 to 8.3% in Table 3-5. Using the present method, the LLOQ was validated at 0.5 nM for all analytes, which is equivalent to 186, 129, 185, 90 and 70 pg/mL for GroPIns, GroPCho, GroP, inositol, and choline, respectively. Under the present LLOQ, the concentration of analyte in the medium can be determined even 24 h after administration. As a result, this method was sensitive enough to investigate the levels of these metabolites in the exometabolome of *S. cerevisiae*.

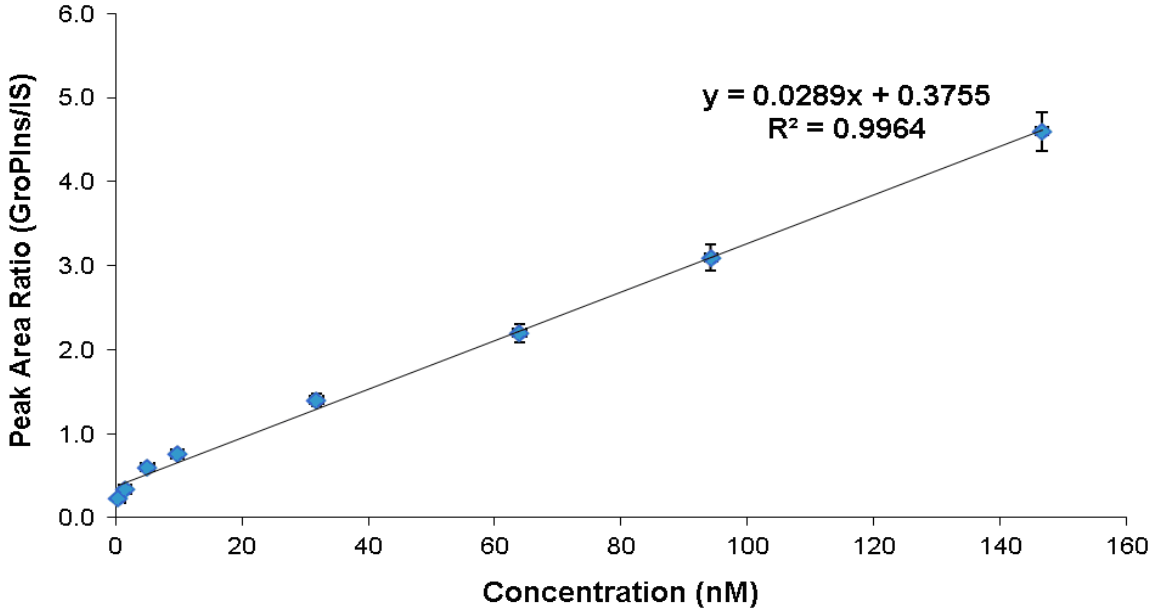

Figure 3-8 Plot of the peak area ratio of GroPIns to internal standard versus the concentration of GroPIns.

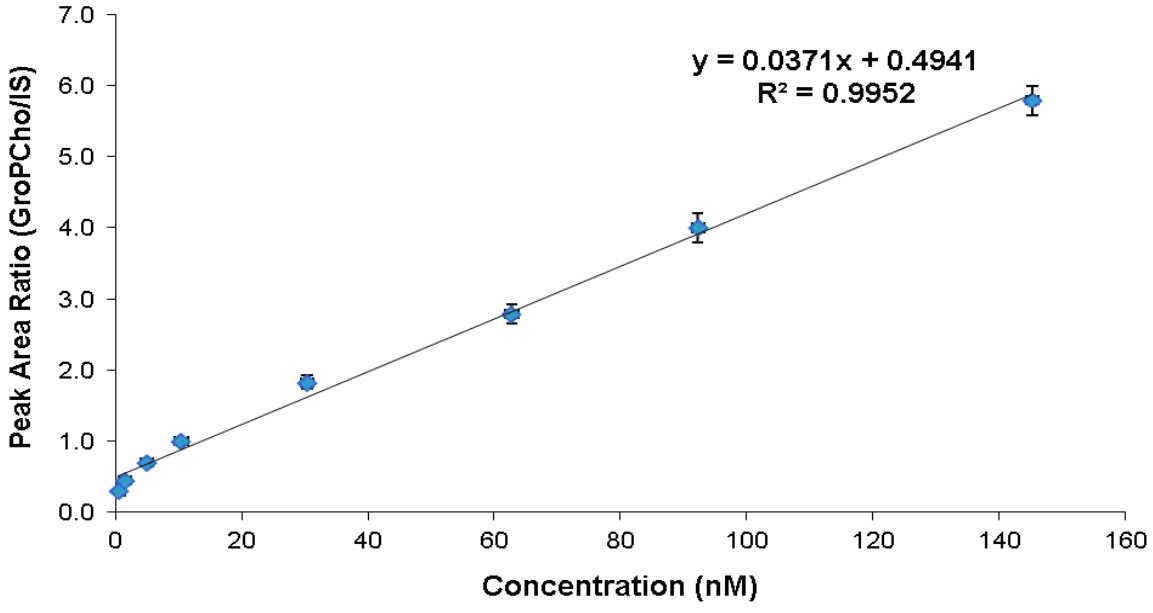

Figure 3-9 Plot of the peak area ratio of GroPCho to internal standard versus the concentration of GroPCho.

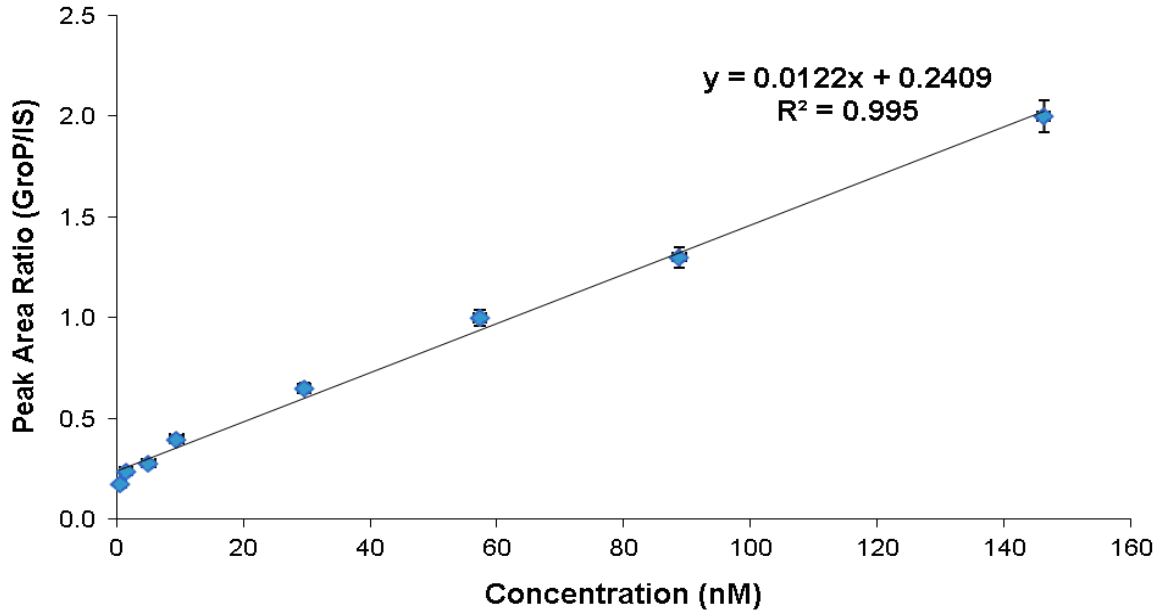

Figure 3-10 Plot of the peak area ratio of GroP to internal standard versus the concentration of GroP.

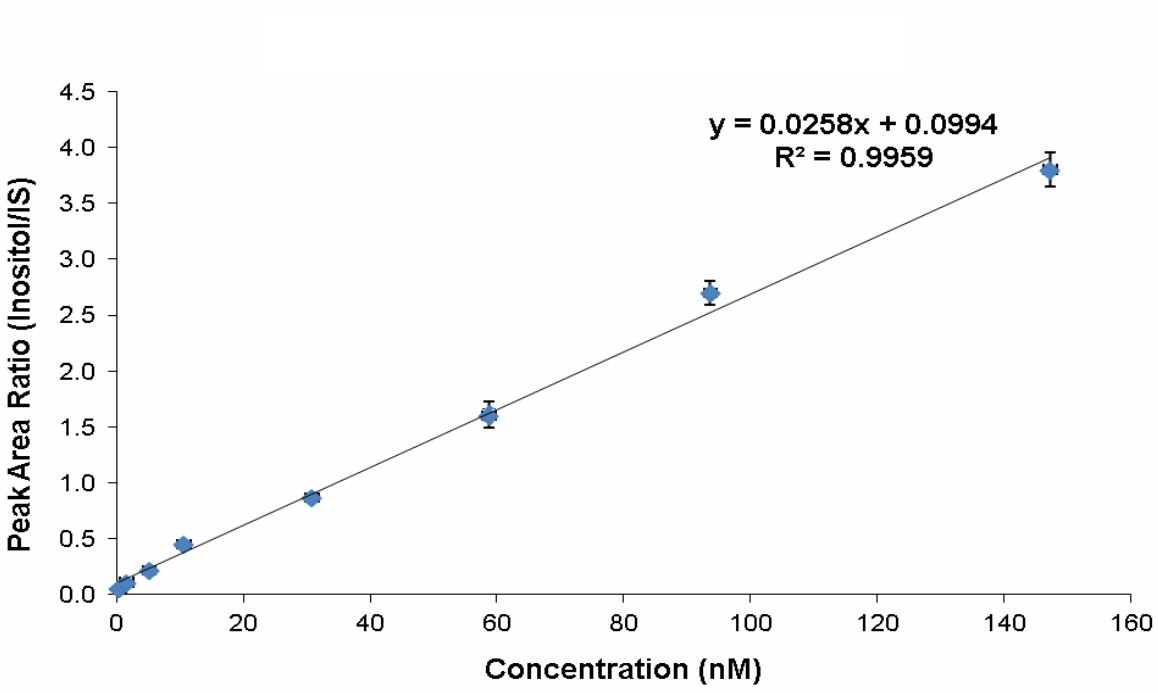

Figure 3-11 Plot of the peak area ratio of inositol to internal standard versus the concentration of inositol.

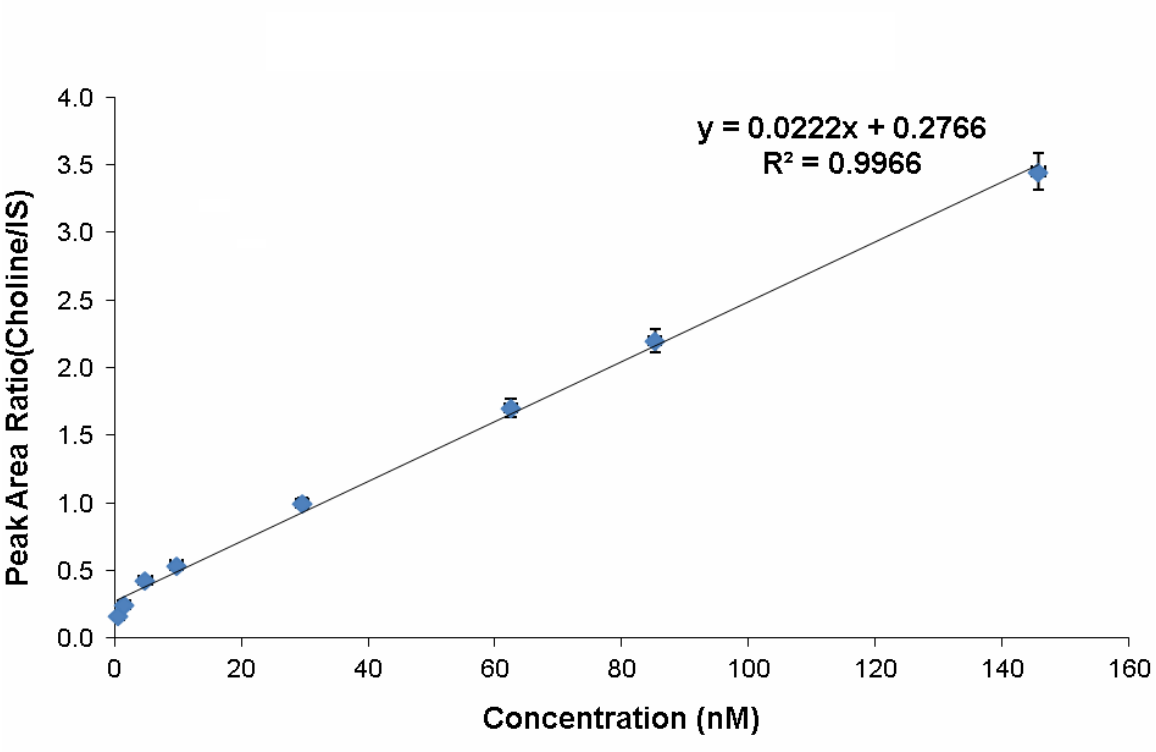

Figure 3-12 Plot of the peak area ratio of choline to internal standard versus the concentration of choline.

3.4.3.3 Recovery

The mean extraction recoveries of analytes in Table 3-7 were 74.4% for GroPIns, 72.6% for GroPCho, 80.7% for GroP, 82.5% for inositol, 75.9% for choline, and 75.5% for IS at 50 nM. The simple sample extraction procedure with 10 volumes of chloroform/methanol, 2:1 (v/v) to 1 volume of sample allowed for high sample throughputs and good recoveries. No significant degradation occurred under any experimental condition.

Analyte	Nominal concentration (nM)							
	0.5	1.5	5	10	30	60	90	150
GroPIns								
Mean	0.47	1.52	5.06	9.73	31.84	63.92	94.21	146.62
Precision (CV%)[b]	3.44	2.79	6.82	5.40	4.27	6.98	3.18	4.02
Accuracy (RE%)[c]	-6.24	1.33	1.24	-2.75	6.13	6.53	4.68	-2.25
GroPCho								
Mean	0.50	1.47	4.93	10.44	30.37	62.82	92.29	145.22
Precision (CV%)	4.29	8.70	3.37	6.13	4.28	3.27	4.91	2.47
Accuracy (RE%)	0.03	-2.73	-1.42	4.42	1.23	4.75	2.54	-3.19
GroP								
Mean	0.52	1.46	5.09	9.52	29.64	57.28	88.74	146.25
Precision (CV%)	4.25	1.57	3.81	2.39	5.07	2.73	4.20	3.31
Accuracy (RE%)	4.20	2.67	1.83	-4.88	1.21	-4.53	-1.45	-2.58
Inositol								
Mean	0.46	1.58	5.12	10.67	30.88	58.73	93.64	147.27
Precision (CV%)	2.55	4.98	6.96	3.38	5.26	3.01	2.29	4.47
Accuracy (RE%)	8.31	5.33	2.46	6.70	2.93	-2.12	4.04	-1.82
Choline								
Mean	0.51	1.54	4.85	9.82	29.64	62.49	85.26	145.72
Precision (CV%)	3.01	6.28	4.11	5.26	4.42	1.57	2.06	6.31
Accuracy (RE%)	2.11	2.67	-3.31	-1.87	-1.22	4.15	-5.27	-2.85

Table 3-5 Precision and accuracy of calibration samples (n=6 in 3 runs). The coefficient of variation (CV%) = [Standard deviation/mean concentration measured] × 100. The relative error (RE%) = [(mean concentration measured-nominal concentration)/nominal concentration] × 100.

3.4.3.4 Precision and Accuracy

Table 3-6 is a summary of the intra - and inter-day precision and accuracy validation using QC samples as described in Section 3.3.5.2. QC samples were determined in replicate (n = 6) at three different concentrations: 2, 50, and 100 nM. Within the range of 2–100 nM, the intra-day and inter-day precisions (CV%) were between 1.2 to 9.8% for each QC level of analytes. The accuracy (RE%), determined for QC samples, was within -9.3 to 8.3% for each QC level of analytes.

Analyte	Intra-day (n=6)				Inter-day (n=6)			
(nM)	Mean	SD	PRE (CV%)	ACC (RE%)	Mean	SD	PRE (CV%)	ACC (RE%)
GroPIns								
2	2.04	0.12	5.88	2.16	1.92	0.09	4.69	-4.64
50	48.37	1.46	3.02.	-3.26	53.25	3.64	6.84	6.52
100	92.66	2.27	2.45	-7.34	90.66	5.82	6.42	-9.35
GroPCho								
2	1.97	0.09	4.57	-1.58	2.05	0.11	5.37	2.51
50	52.01	2.42	4.65	4.02	47.62	1.17	2.46	-4.76
100	94.67	1.17	1.24	-5.33	92.13	3.87	4.20	-7.87
GroP								
2	1.89	0.07	3.70	-5.53	1.94	0.14	7.22	-3.68
50	51.39	1.98	3.85	2.78	53.22	4.21	7.91	6.44
100	96.64	4.61	4.77	-3.36	95.27	2.36	2.48	-4.73
Inositol								
2	2.07	0.11	5.31	3.54	1.97	0.14	7.11	-3.74
50	47.65	2.61	5.48	-4.77	47.29	4.62	9.77	-5.42
100	91.58	3.52	3.84	-8.42	94.63	3.10	3.28	-5.37
Choline								
2	1.92	0.06	3.13	-4.65	1.95	0.09	4.62	-2.52
50	54.11	1.29	2.38	8.22-	46.74	2.73	5.84	-6.53
100	94.28	4.17	4.42	-5.72	92.18	4.71	5.11	-7.82

Table 3-6 Intra- and inter-day precision and accuracy of the QC samples (n=6 in 3 runs). SD: standard deviation. PRE: precision. ACC: accuracy. The coefficient of variation (CV%) = [Standard deviation/mean concentration measured] × 100. The relative error (RE%) = [(mean concentration measured-nominal concentration)/nominal concentration] × 100.

3.4.3.5 Matrix Effect

The absolute matrix effects, the ratio of the peak areas of three-concentration level standards spiked in medium extracts to areas of the standards spiked in mobile phase (10

mM ammonium acetate in acetonitrile/water, 70:30 (v/v)), were measured to be 95.6%, 97.7%, 98.4%, 95.3%, and 97.0% for GroPIns, GroPCho, GroP, inositol, and choline, respectively (Table 3-7). The matrix effect value of <100% indicates ionization suppression. The matrix was found to have negligible impact on the ionization, as the variation in signal was less than 10% for all analytes. The absolute matrix effect value of IS at 50 nM in the medium was observed to be 96.7%.

Analyte	**Absolute matrix effect (%)**				**Recovery (%)**			
	LQC	MQC	HQC	Mean	LQC	MQC	HQC	Mean
GroPIns	97.2	94.3	95.3	95.6	72.5	75.1	75.6	74.4
GroPCho	97.4	95.9	99.8	97.7	70.5	72.9	74.4	72.6
GroP	98.5	97.6	99.0	98.4	81.7	78.4	82.0	80.7
Inositol	94.2	96.6	95.1	95.3	82.9	83.3	81.3	82.5
Choline	98.6	95.1	97.3	97.0	73.6	77.9	76.2	75.9

Figure 3-7 Absolute matrix effect and recovery of all analytes at three concentrations of 2, 50 and 100 nM (n=6 in 3 runs). Absolute matrix effect expressed as the ratio of the mean peak areas of three-concentration level standards spiked in medium extracts to those from standards spiked in the mobile phase multiplied by 100. Recovery calculated as the ratio of the mean peak areas of medium spiked with standards at three levels to those of blank medium extracts spiked with standards at equivalent concentrations multiplied by 100.

3.4.3.6 Stability

The stability of QC samples at 2 and 100 nM were determined after the following manipulations: three freeze/thaw cycles, 4-h storage at room temperature, 30-day storage at -20°C, and autosampler reinjection after 24 h (Table 3-8). QC samples were stable in

different storage conditions, as their assay values were within the acceptable limits of accuracy (±15% RE) and precision (±15% CV).

Analyte		**LQC**			**HQC**		
	Storage Condition	Mean (nM)	PRE (CV%)	ACC (RE%)	Mean (nM)	PRE (CV%)	ACC (RE%)
GroPIns	FT-3	1.97	2.72	-1.54	96.28	4.67	-3.85
	Short-T	1.99	4.63	-0.58	97.52	5.05	-2.54
	Long-T	2.02	3.57	-1.45	95.05	3.52	-5.62
	Auto-R	1.85	4.48	-7.56	89.94	4.34	-10.11
GroPCho	FT-3	1.96	5.12	-2.81	97.77	2.78	-2.36
	Short-T	1.98	4.80	-1.70	99.56	3.41	-0.58
	Long-T	1.94	4.27	-3.35	93.23	2.90	-6.84
	Auto-R	1.88	3.92	-6.12	91.02	5.33	-9.42
GroP	FT-3	1.97	3.16	-0.15	100.43	4.01	0.49
	Short-T	2.01	2.57	0.54	97.22	4.26	-2.84
	Long-T	1.90	4.43	-5.03	96.39	5.53	-3.76
	Auto-R	1.89	3.87	-5.56	88.54	3.11	-11.52
Inositol	FT-3	1.96	2.64	-2.68	94.60	2.46	-5.44
	Short-T	2.02	4.39	1.32	97.91	5.18	-2.16
	Long-T	1.98	3.61	-1.60	95.13	3.62	-4.92
	Auto-R	1.84	4.74	-7.25	90.67	4.54	-9.47
Choline	FT-3	2.03	5.89	1.59	97.92	4.36	-2.18
	Short-T	1.95	3.72	-2.52	99.36	2.91	-0.72
	Long-T	1.91	3.24	-4.52	89.63	3.83	-10.45
	Auto-R	1.87	2.67	-6.58	90.42	4.06	-9.64

Table 3-8 Stability of QC samples (n=6). FT-3: three freeze/thaw cycles. Short-T: 4-h storage at room temperature. Long-T: 30-day storage at -20°C. Auto-R: autosampler reinjection after 24 h at room temperature. The coefficient of variation (CV%) = [Standard deviation/mean concentration measured] × 100. The relative error (RE%) = [(mean concentration measured-nominal concentration)/nominal concentration] × 100.

3.4.4 Application to a Biological Analysis

To apply the developed method to a biological system, we monitored the medium of *S. cerevisiae* cultures containing wild type cells and cultures containing mutant strains in which one or more of the phospholipase B genes had been deleted. We first monitored the culture medium prior to the addition of cells in order to get a zero time reading (Figure 3-13) and again after several hours, at which point the cells had reached the stationary phase of growth (Figure 3-14).

Based on prior literature using radiolabeling, we expected to see a decrease in GroPCho levels in strains lacking the *PLB1* gene and a decrease in GroPIns levels in strains lacking the *PLB3* gene, but had no firm estimate of the absolute quantities of these metabolites [20, 21, 46]. Since we supplemented the medium with inositol and choline, we expected to see a decrease in those metabolites as a function of growth, but did dot have an estimate of the extent of uptake by the cells. With regard to GroP, we did not know if this compound would be detected extracellularly and had no expectation regarding its extracellular concentration. As shown in Figure 3-13, the mean concentrations of inositol and choline in blank medium were determined to be 61.8 μM and 15.18 μM, which are in close agreement with the supplemented concentrations of 75μ M and 20 μM when the recovery values of 82.5% and 75.9% are taken into consideration.

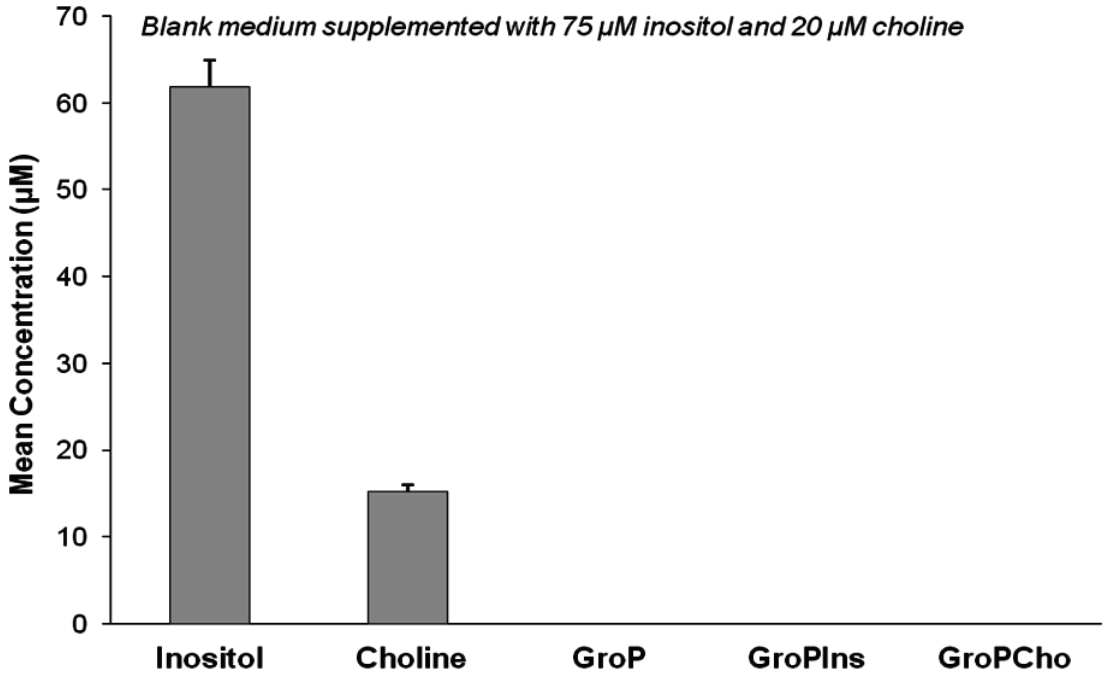

Figure 3-13 Blank medium supplemented with 75 µM inositol, and 20 µM choline was analyzed at time 0. Data represented as concentration (µM) as a function of cell growth (OD_{600}). The error bars represent the variation of three individual experiments. Values represent mean ± S.E. of triplicate determinations.

As shown in Figure 3-14, the concentration of inositol decreased in all strains to approximately 22-25 µM. Interestingly, the concentration of choline in the medium decreased to a greater extent for the wild type strain than it did for any of the strains bearing a mutated copy of a *PLB* gene. This finding suggests that either choline transport is diminished in the mutant strains or that the production and subsequent release of choline is exacerbated in the mutant strains. Further studies will be needed in order to reconcile these possibilities.

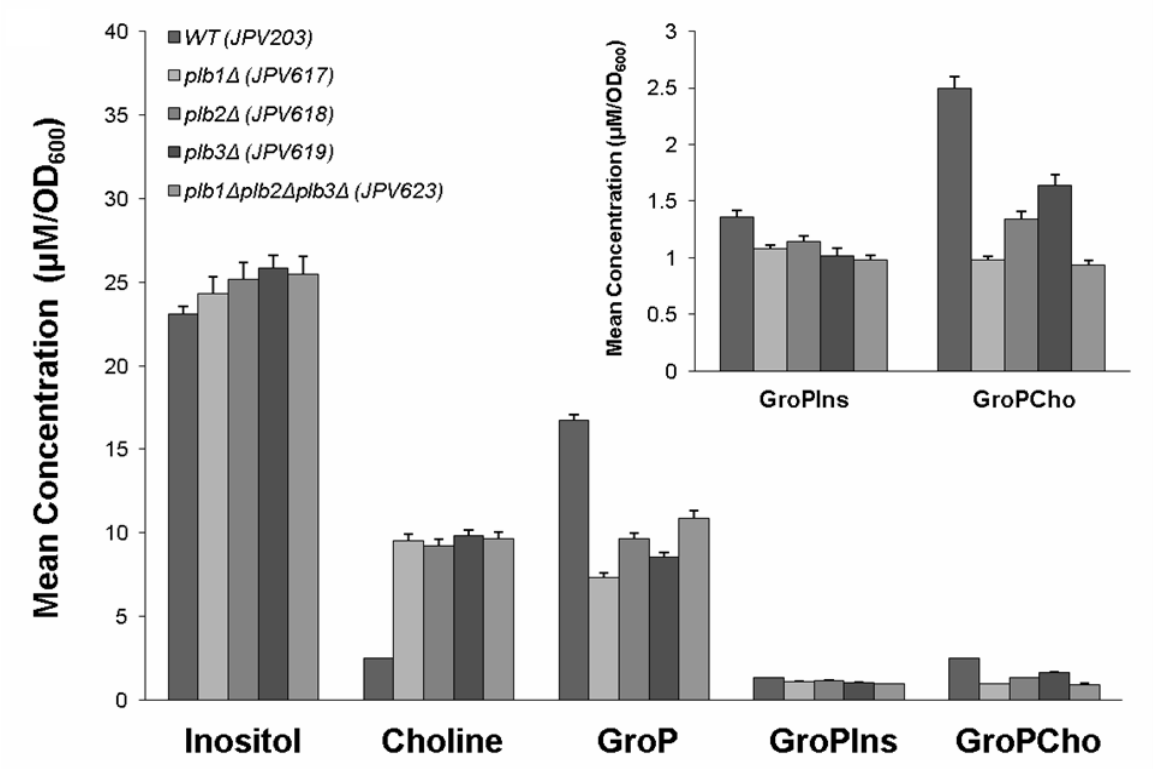

Figure 3-14 Determination of lipid-related extracellular metabolites of *S. cerevisiae* in wild cells and in response to deletion *of PLB1, PLB2,* and *PLB3* genes encoding for phospholipases B. Strains grown in medium were harvested at stationary phase after approximately 24 hours of growth for the PLB activity assays. Data represented as concentration (μM) as a function of cell growth (OD_{600}). The inset showed the mean concentrations of GroPIns and GroPCho in detail. The error bars represent the variation of three individual experiments. Values represent mean ± S.E. of triplicate determinations.

Also interesting is that not only is GroP detected in the medium, but that the level is greater in the wild type strain than in any of the mutant strains. Again, further experiments will be needed to understand the metabolic underpinnings of this result. With regard to GroPCho levels, we observed the most severe decrease in levels in the *plb1***Δ** and *plb1-3Δ* mutant as compared to the wild type strain, as expected. Somewhat surprising was that the *plb2Δ* and *plb3Δ* mutants also exhibited a decrease in GroPCho,

whereas the published data using radiolabeling saw little or no decrease in that metabolite in the *plb2Δ* and *plb3Δ* strains [20, 21, 46]. These differences may be due to the limitations associated with radiolabeling with ^{14}C-choline, since only the pool of choline taken up by the cell is labeled and not that derived from de novo synthesis. Also, genetic differences between the strain backgrounds and variations in the time of growth between the experiments may account for these differences. With regard to GroPIns levels, we did not see a decrease in the *plb3Δ* mutant strain, contrary to what we expected from the literature [20, 21, 46]. Therefore, we performed another experiment using only a wild type strain and a *plb3Δ* mutant (Figure 3-15) in which we monitored the level of metabolites at an earlier point in their growth phase, the logarithmic phase of growth, as careful examination of the published reports suggest that those studies were likely performed with logarithmically growing cells. Under those conditions, we observed the expected approximately 50% decrease in GroPIns levels in the *plb3Δ* mutant as compared to wild type (Figure 3-15).

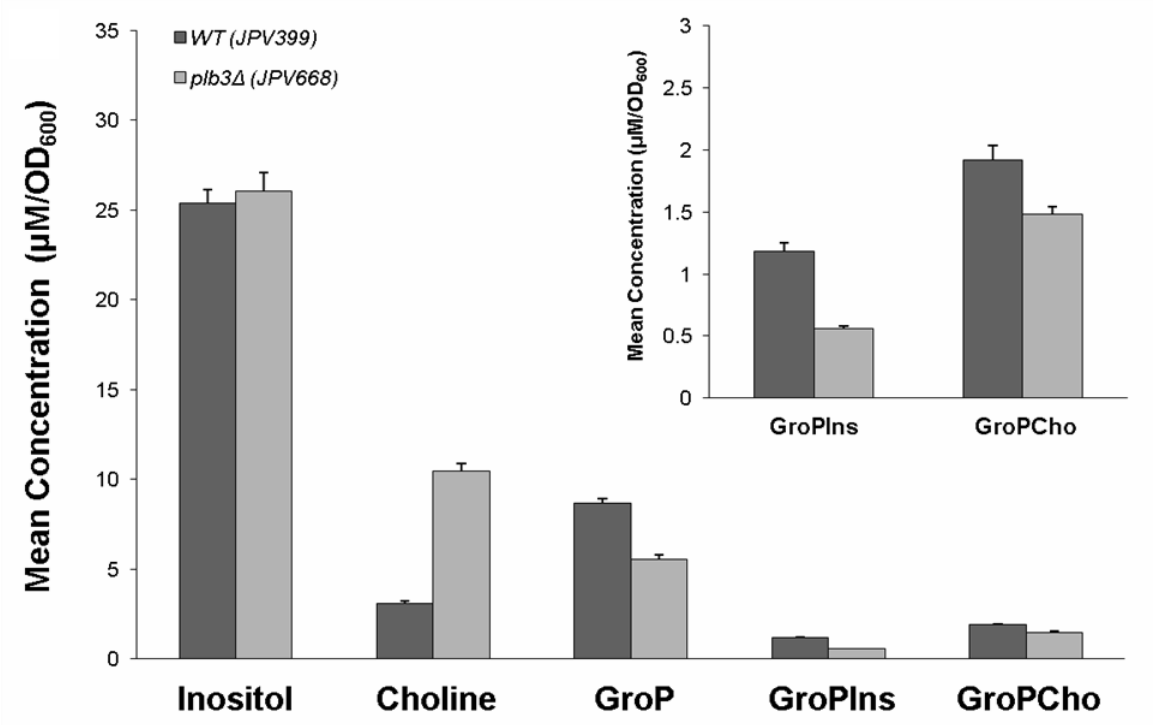

Figure 3-15 Determination of lipid-related extracellular metabolites of *S. cerevisiae* in wild cells and in response to deletion *of PLB3* genes encoding for phospholipases B. Strains grown in medium were harvested at log phase after 10-12 hours of growth for the PLB activity assays. Data represented as concentration (μM) as a function of cell growth (OD_{600}). The inset showed the mean concentrations of GroPIns and GroPCho in detail. The error bars represent the variation of three individual experiments. Values represent mean ± S.E. of triplicate determinations.

To summarize the biological application of this newly developed methodology, we were able to confirm the general trends expected for the extracellular levels of GroPIns and GroPCho in wild type and mutant strains. However, much additional information was obtained regarding the absolute levels of these metabolites and the levels of GroP, inositol, and choline in the medium as a function of growth and the absence of particular

PLB encoding genes. Thus, the application of this approach has opened up new avenues of potential research.

3.5 Conclusions

We have successfully developed and validated an efficient analytical method based on HILIC-MS/MS for the quantification of lipid-related extracellular metabolites in *S. cerevisiae*. In comparison with traditional radiolabelling methods and other LC-MS/MS methods, our approach is simple, robust, and well suited to metabolomic studies.

3.6 Acknowledgements

Mass spectrometry instrumentation was purchased in part from National Science Foundation (Grant MRI DBI-0821401). We acknowledge the principle investigator of the funding, Dr. Mitchell E. Johnson. We also thank Beth A. Surlow for preparing the strains and providing technical assistance.

3.7 References

1. Oliver, S. G.; Winson, M. K.; Kell, D. B.; Baganz, F., Systematic functional analysis of the yeast genome. *Trends in Biotechnology* **1998,** 16, (9), 373-378.

2. Bino, R. J.; Hall, R. D.; Fiehn, O.; Kopka, J.; Saito, K.; Draper, J.; Nikolau, B. J.; Mendes, P.; Roessner-Tunali, U.; Beale, M. H.; Trethewey, R. N.; Lange, B. M.; Wurtele, E. S.; Sumner, L. W., Potential of metabolomics as a functional genomics tool. *Trends in Plant Science* **2004,** 9, (9), 418-425.

3. Kell, D. B.; Brown, M.; Davey, H. M.; Dunn, W. B.; Spasic, I.; Oliver, S. G., Metabolic footprinting and systems biology: the medium is the message. *Nat Rev Microbiol* **2005,** 3, (7), 557-65.

4. Mashego, M.; Rumbold, K.; De Mey, M.; Vandamme, E.; Soetaert, W.; Heijnen, J., Microbial metabolomics: past, present and future methodologies. *Biotechnology Letters* **2007,** 29, (1), 1-16.

5. Dettmer, K.; Aronov, P. A.; Hammock, B. D., Mass spectrometry-based metabolomics. *Mass Spectrometry Reviews* **2007,** 26, (1), 51-78.

6. Schiesel, S.; Lämmerhofer, M.; Lindner, W., Multitarget quantitative metabolic profiling of hydrophilic metabolites in fermentation broths of beta-lactam antibiotics production by HILIC-ESI-MS/MS. *Analytical and Bioanalytical Chemistry* 396, (5), 1655-1679.

7. Villas-Bôas, S. G.; Højer-Pedersen, J.; Åakesson, M.; Smedsgaard, J.; Nielsen, J., Global metabolite analysis of yeast: Evaluation of sample preparation methods. *Yeast* **2005,** 22, (14), 1155-1169.

8. Villas-Bôas, S. G.; Noel, S.; Lane, G. A.; Attwood, G.; Cookson, A., Extracellular metabolomics: A metabolic footprinting approach to assess fiber degradation in complex media. *Analytical Biochemistry* **2006,** 349, (2), 297-305.

9. Villas-Bôas, S. G.; Moxley, J. F.; Akesson, M.; Stephanopoulos, G.; Nielsen, J., High-throughput metabolic state analysis: the missing link in integrated functional genomics of yeasts. *Biochem. J.* **2005,** 388, (2), 669-677.

10. Allen, J.; Davey, H. M.; Broadhurst, D.; Heald, J. K.; Rowland, J. J.; Oliver, S. G.; Kell, D. B., High-throughput classification of yeast mutants for functional genomics using metabolic footprinting. *Nat Biotechnol* **2003,** 21, (6), 692-6.

11. Allen, J.; Davey, H. M.; Broadhurst, D.; Rowland, J. J.; Oliver, S. G.; Kell, D. B., Discrimination of Modes of Action of Antifungal Substances by Use of Metabolic Footprinting. *Appl. Environ. Microbiol.* **2004,** 70, (10), 6157-6165.

12. Mas, S.; Villas-Boas, S. G.; Hansen, M. E.; Akesson, M.; Nielsen, J., A comparison of direct infusion MS and GC-MS for metabolic footprinting of yeast mutants. *Biotechnology and Bioengineering* **2007,** 96, (5), 1014-1022.

13. Kaderbhai, N. N.; Broadhurst, D. I.; Ellis, D. I.; Goodacre, R.; Kell, D. B., Functional genomics via metabolic footprinting: monitoring metabolite secretion by Escherichia coli tryptophan metabolism mutants using FT–IR and direct injection electrospray mass spectrometry. *Comparative and Functional Genomics* **2003,** 4, (4), 376-391.

14. Bedair, M.; Sumner, L. W., Current and emerging mass-spectrometry technologies for metabolomics. *TrAC Trends in Analytical Chemistry* **2008,** 27, (3), 238-250.

15. Brown, M.; Dunn, W. B.; Ellis, D. I.; Goodacre, R.; Handl, J.; Knowles, J. D.; O'Hagan, S.; Spasic, I.; Kell, D. B., A metabolome pipeline: from concept to data to knowledge. *Metabolomics* **2005,** 1, (1), 39-51.

16. Fiehn, O., Extending the breadth of metabolite profiling by gas chromatography coupled to mass spectrometry. *TrAC, Trends in Analytical Chemistry* **2008,** 27, (3), 261-269.

17. Goodacre, R.; Vaidyanathan, S.; Dunn, W. B.; Harrigan, G. G.; Kell, D. B., Metabolomics by numbers: acquiring and understanding global metabolite data. *Trends Biotechnol* **2004,** 22, (5), 245-52.

18. Weckwerth, W., *Metabolomics. Methods and Protocols*. Humana Press: Seacaucus, NJ, 2007; p 312.

19. Dickson, R. C., Thematic Review Series: Sphingolipids. New insights into sphingolipid metabolism and function in budding yeast. *Journal of Lipid Research* **2008,** 49, (5), 909-921.

20. Lee, K. S.; Patton, J. L.; Fido, M.; Hines, L. K.; Kohlwein, S. D.; Paltauf, F.; Henry, S. A.; Levin, D. E., The Saccharomyces cerevisiae PLB1 gene encodes a protein required for lysophospholipase and phospholipase B activity. *J Biol Chem* **1994,** 269, (31), 19725-30.

21. Merkel, O.; Fido, M.; Mayr, J. A.; Pruger, H.; Raab, F.; Zandonella, G.; Kohlwein, S. D.; Paltauf, F., Characterization and function in vivo of two novel phospholipases B/lysophospholipases from Saccharomyces cerevisiae. *J Biol Chem* **1999,** 274, (40), 28121-7.

22. Patton-Vogt, J. L.; Henry, S. A., GIT1, a gene encoding a novel transporter for glycerophosphoinositol in Saccharomyces cerevisiae. *Genetics* **1998,** 149, (4), 1707-15.

23. Carman, G. M.; Henry, S. A., Phosphatidic Acid Plays a Central Role in the Transcriptional Regulation of Glycerophospholipid Synthesis in Saccharomyces cerevisiae. *Journal of Biological Chemistry* **2007,** 282, (52), 37293-37297.

24. Carman, G. M.; Han, G.-S., Regulation of Phospholipid Synthesis in the Yeast Saccharomyces cerevisiae. *Annual Review of Biochemistry* **2011,** 80, (1), 859-883.

25. Jana, P.-V., Transport and metabolism of glycerophosphodiesters produced through phospholipid deacylation. *Biochimica et Biophysica Acta (BBA) - Molecular and Cell Biology of Lipids* **2007,** 1771, (3), 337-342.

26. Dowd, S. R.; Bier, M. E.; Patton-Vogt, J. L., Turnover of Phosphatidylcholine in Saccharomyces cerevisiae. *Journal of Biological Chemistry* **2001,** 276, (6), 3756-3763.

27. Patton, J. L.; Pessoa-Brandao, L.; Henry, S. A., Production and reutilization of an extracellular phosphatidylinositol catabolite, glycerophosphoinositol, by Saccharomyces cerevisiae. *Journal of Bacteriology* **1995,** 177, (12), 3379-85.

28. Patton-Vogt, J. L.; Griac, P.; Sreenivas, A.; Bruno, V.; Dowd, S.; Swede, M. J.; Henry, S. A., Role of the Yeast Phosphatidylinositol/Phosphatidylcholine Transfer Protein (Sec14p) in Phosphatidylcholine Turnover andINO1 Regulation. *Journal of Biological Chemistry* **1997,** 272, (33), 20873-20883.

29. Fernández-Murray, J. P.; McMaster, C. R., Glycerophosphocholine Catabolism as a New Route for Choline Formation for Phosphatidylcholine Synthesis by the Kennedy Pathway. *Journal of Biological Chemistry* **2005,** 280, (46), 38290-38296.

30. Cook, S. J.; Wakelam, M. J., Analysis of the water-soluble products of phosphatidylcholine breakdown by ion-exchange chromatography. Bombesin and TPA (12-O-tetradecanoylphorbol 13-acetate) stimulate choline generation in Swiss 3T3 cells by a common mechanism. *Biochem Journal* **1989,** 263, (2), 581-587.

31. Koch-Kallnbach, M. E.; Diringer, H., Isolation and separation of inositol 1-phosphate, cyclic inositol 1,2-phosphate, and glycerylphosphoinositol from tissue culture cells labeled with [3H]inositol. *Hoppe Seylers Z Physiol Chem.* **1977,** 358, (3), 367-375.

32. Dragani, L. K.; Berrie, C. P.; Corda, D.; Rotilio, D., Analysis of glycerophosphoinositol by liquid chromatography-electrospray ionisation tandem mass spectrometry using a β-cyclodextrin-bonded column. *Journal of Chromatography B* **2004,** 802, (2), 283-289.

33. Kopp, F.; Komatsu, T.; Nomura, D. K.; Trauger, S. A.; Thomas, J. R.; Siuzdak, G.; Simon, G. M.; Cravatt, B. F., The Glycerophospho Metabolome and Its Influence on Amino Acid Homeostasis Revealed by Brain Metabolomics of GDE1(/) Mice. *Chemistry & biology* **2010,** 17, (8), 831-840.

34. Sato, M.; Dhut, S.; Toda, T., New drug-resistant cassettes for gene disruption and epitope tagging in Schizosaccharomyces pombe. *Yeast* **2005,** 22, (7), 583-591.

35. Güldener, U.; Heck, S.; Fiedler, T.; Beinhauer, J.; Hegemann, J. H., A New Efficient Gene Disruption Cassette for Repeated Use in Budding Yeast. *Nucleic Acids Research* **1996,** 24, (13), 2519-2524.

36. Bajad, S. U.; Lu, W.; Kimball, E. H.; Yuan, J.; Peterson, C.; Rabinowitz, J. D., Separation and quantitation of water soluble cellular metabolites by hydrophilic interaction chromatography-tandem mass spectrometry. *Journal of Chromatography A* **2006,** 1125, (1), 76-88.

37. Barroso, B.; Bischoff, R., LC-MS analysis of phospholipids and lysophospholipids in human bronchoalveolar lavage fluid. *Journal of Chromatography B* **2005,** 814, (1), 21-28.

38. Coulier, L.; Bas, R.; Jespersen, S.; Verheij, E.; van der Werf, M. J.; Hankemeier, T., Simultaneous Quantitative Analysis of Metabolites Using Ion-Pair Liquid Chromatography,àíElectrospray Ionization Mass Spectrometry. *Analytical Chemistry* **2006,** 78, (18), 6573-6582.

39. Sun, T.; Pawlowski, S.; Johnson, M. E., Highly Efficient Microscale Purification of Glycerophospholipids by Microfluidic Cell Lysis and Lipid Extraction for Lipidomics Profiling. *Analytical Chemistry* **2011,** 83, (17), 6628-6634.

40. Cubbon, S.; Bradbury, T.; Wilson, J.; Thomas-Oates, J., Hydrophilic Interaction Chromatography for Mass Spectrometric Metabonomic Studies of Urine. *Analytical Chemistry* **2007,** 79, (23), 8911-8918.

41. Kind, T.; Tolstikov, V.; Fiehn, O.; Weiss, R. H., A comprehensive urinary metabolomic approach for identifying kidney cancer. *Analytical Biochemistry* **2007,** 363, (2), 185-195.

42. Pan, X.; Yuan, D. S.; Xiang, D.; Wang, X.; Sookhai-Mahadeo, S.; Bader, J. S.; Hieter, P.; Spencer, F.; Boeke, J. D., A robust toolkit for functional profiling of the yeast genome. *Mol Cell* **2004,** 16, (3), 487-96.

43. Piraud, M.; Vianey-Saban, C.; Bourdin, C.; Acquaviva-Bourdain, C.; Boyer, S.; Elfakir, C.; Bouchu, D., A new reversed-phase liquid chromatographic/tandem mass spectrometric method for analysis of underivatised amino acids: evaluation for the diagnosis and the management of inherited disorders of amino acid metabolism. *Rapid Communications in Mass Spectrometry* **2005,** 19, (22), 3287-3297.

44. Schlichtherle-Cerny, H.; Affolter, M.; Cerny, C., Hydrophilic Interaction Liquid Chromatography Coupled to Electrospray Mass Spectrometry of Small Polar Compounds in Food Analysis. *Analytical Chemistry* **2003,** 75, (10), 2349-2354.

45. Tolstikov, V. V.; Lommen, A.; Nakanishi, K.; Tanaka, N.; Fiehn, O., Monolithic Silica-Based Capillary Reversed-Phase Liquid Chromatography/Electrospray Mass Spectrometry for Plant Metabolomics. *Analytical Chemistry* **2003,** 75, (23), 6737-6740.

46. Merkel, O.; Oskolkova, O. V.; Raab, F.; El-Toukhy, R.; Paltauf, F., Regulation of activity in vitro and in vivo of three phospholipases B from Saccharomyces cerevisiae. *Biochem. J.* **2005,** 387, (2), 489-496.

Appendix 1

Comparison of On-chip Lipid Extraction Method Using Different Eluents on Silica or C18 Stationary Phases to Bligh and Dyer Extraction Method for Evaluating the Extraction Efficiency of Microchip

A.1 Abstract

A library for comparing the identified phospholipids extracted from microchip using different eluents: methanol, isopropanol or acetonitrile on silica stationary phase and 2:1 chloroform/methanol or 1:1 tetrahydrofuran/methanol on C18 stationary phase with the total lipid species extracted by Bligh and Dyer method. From the results, the on-chip extraction efficiency is achieved as the number of identified phospholipids species obtained using the microchip method as compared to the modified Bligh-Dyer method.

m/z	Bligh and Dyer Extraction	Silica Phase			C18 Phase	
		MeOH	IPA	ACN	2:1 Chloroform /MeOH	1:1 Tetrahydrofuran /MeOH
985.7	40:2 PIp/40:1 PIp		x		x	
983.7	40:2 PIp/40:3 PIp		x		x	
979.6	40:3 PIPp/40:4 PIPe	x		x		
973.6	38:0 PIP/44:2 PI	x	x	x		
969.6	38:2 PIP/44:4 PI	x		x		x
963.5	38:5 PIP	x		x		
959.6	38:1 PIp/38:0 PIp		x	x		
957.6	38:0 PIPp/38:1 PIPe	x	x	x		
955.6	38:1 PIPp/38:2 PIPe	x	x	x		
953.6	38:2 PIPp/38:3 PIPe	x	x		x	
945.6	42:2 PI	x		x		
935.7	42:0 PI/42:1 PI			x		
931.6	36:0 Pip/36:1 PIp		x	x		x
929.6	42:2 PIp	x		x		
923.8	42:5 Pip/42:6 PIe	x				
921.5	42:6 PIp	x		x		x
905.7	40:1PI/40:2 PI		x			x
901.5	40:2 PIp/40:3 PIe	x	x	x		
899.5	40:3 Pip/40:4 PIe	x		x		
898.6	44:2 PC/44:3 PS/44:2 PS	x		x	x	
898.5	40:5 PI/40:6 PI	x	x	x	x	x
894.7	44:4 PC/44:5 PS/44:3 PC	x		x	x	
892.6	44:6 PS/44:5 PC/44:5 PS	x	x	x		
890.6	44:6 PC/44:6 PS	x	x	x		
882.6	43:4 PS/44:10 PC			x		

m/z	Bligh and Dyer Extraction	Silica Phase			C18 Phase	
		MeOH	IPA	ACN	2:1 Chloroform /MeOH	1:1 Tetrahydrofuran /MeOH
881.5	38:6 PI	x		x	x	x
880.7	43:4 PC	x	x	x		x
879.7	38:1 PI/38:0 PI		x	x	x	x
877.6	38:0 Pip/38:1 PIe	x	x	x		
875.5	32:0 PIp/32:1 PIp			x		
869.5	38:5 PI/38:6 PI			x		
868.6	42:3 PC/42:4 PS/42:3 PS	x	x	x	x	x
866.7	42:4 PC/42:5 PS/42:4 PS	x		x	x	
865.6	37:0 PI/37:1 PI			x		
864.5	42:5 PC/42:6 PS/42:5 PS	x		x		
861.7	36:2 PI/42:0 PG	x			x	
860.6	42:7 PC/41:0 PC/44:0 PE		x	x	x	
859.6	42:2 PG/36:4 PI		x		x	
858.7	42:0 PCp/42:1 PCe/44:1 PE	x	x	x	x	x
857.5	36:4 PI/42:2 PG	x	x		x	x
856.6	42:2 PSp 44:2 PE	x	x	x		x
854.6	42:10 PC/41:4 PS		x			x
851.6	36:0 PI/36:1 PI					
850.7	44:5 PE/42:4 PCp /42:5 PCe	x			x	
850.6	44:4 PE/42:5 PSe	x				
848.6	42:6 Pce/40:0 PS /44:6 PE	x	x	x	x	x
847.6	42:0 Pge/36:1 PIp /36:2 PIe	x	x			x
846.7	40:0 PC/40:1 PS /42:6 PCp	x	x			x
846.6	42:6 PSp/40:0 PS /44:6 PE	x	x		x	x
838.6	40:5 PS/40:4 PC				x	x

m/z	Bligh and Dyer Extraction	Silica Phase			C18 Phase	
		MeOH	IPA	ACN	2:1 Chloroform /MeOH	1:1 Tetrahydrofuran /MeOH
837.6	35:0 PI/35:1 PI		x		x	x
836.6	40:5 PC/40:6 PS/40:5 PS	x	x		x	x
835.6	34:1 PI	x	x	x	x	
832.6	39:1 PS/39:0 PC/42:0 PE				x	
831.5	34:3 PI/40:1 PG	x				
830.7	40:0 PCp/40:1 Pce/40:1 PSp	x	x			x
829.5	34:5 PI					x
828.6	40:2 PS/40:3 PS				x	x
826.6	40:3 PS/40:4 PS/39:4 PS					
825.5	33:0 PI				x	
824.6	39:4 PC/42:4 PE/40:4 PS					
823.6	34:0 PI/34:1 PI		x		x	x
822.5	40:4 PCp/40:5 Pce/40:5 PSp	x	x		x	
821.6	39:0 PG/34:1 PI				x	x
820.6	38:0 PS/40:5 PCp /40:6 PS	x	x	x		
819.5	40:8 PG		x			x
818.6	38:0 PC/38:1 PS /40:6 PCp	x	x			x
816.6	38:1 PC/38:2 PS /42:0 PE/38:1 PS /42:0 PEe	x	x	x	x	x
812.6	38:3 PC/38:4 PS /42:2 Pep/38:3 PS /42:2 PEe	x			x	
810.5	38:4 PC/38:5 PS /42:4 Pee/38:4 PS/ 42:2 PEp	x	x			x
806.6	38:0 PSe/38:6 PC, 42:5 PEp /42:6 PEe	x	x		x	x
805.6	38:0 PG	x	x		x	x
802.7	38:0 PCp, 38:1 PCp/38:1 PSp/40:1 PE	x	x	x		x

m/z	Bligh and Dyer Extraction	Silica Phase			C18 Phase	
		MeOH	IPA	ACN	2:1 Chloroform /MeOH	1:1 Tetrahydrofuran /MeOH
801.5	32:5 PI		x		x	
800.7	38:1 PCp/38:2 PCe/38:2 PSp/40:2 PE	x	x	x		x
799.6	43:2 PA		x			
798.5	38:2 PCp/38:3 PCe/38:3 PSp/40:3 PE	x	x			x
797.5	31:0 PI		x			
796.5	38:3 PCp/38:4 PCe/38:4 PSp/40:4 PE	x	x			x
795.5	32:0 Pie/38:5 PG	x			x	x
794.6	38:4 PC/38:5 PS				x	
793.6	38:0 PG/32:1 PI				x	x
792.6	38:5 PC/38:6 PC					x
790.7	36:0 PC/36:1 PS /40:0 PEe	x	x	x		x
790.6	37:0 PS	x	x		x	x
786.5	36:2 PC/36:3 PS, 40:1 Pep/40:2 PEe		x	x	x	x
784.6	36:3 PC/36:4 PS, 40:2 Pep/40:3 PEe	x	x		x	x
784.5	36:3 PS/40:1 PEp /40:2 PEe	x	x	x	x	x
782.6	36:4 PC/40:4 PEe	x	x	x		x
777.6	36:1 PG	x	x			x
776.6	36:0 PCe/38:0 PE /40:6 PEp				x	x
774.5	35:2 PS/36:2 PS				x	x
772.5	35:3 PS	x	x		x	x
771.4	30:5 PI/36:3 PG	x	x	x	x	x
769.6	41:3 PA/29:0 PI		x		x	x
768.6	38:4 PE/36:3 PCp /36:4 PCe/38:3 PE	x			x	x
767.5	30:0 PIe	x			x	

m/z	Bligh and Dyer Extraction	Silica Phase			C18 Phase	
		MeOH	IPA	ACN	2:1 Chloroform /MeOH	1:1 Tetrahydrofuran /MeOH
766.6	36:4 PCp/38:5 PE/38:4 PE	x			x	
765.5	30:0 Pip/30:1 PIe	x	x	x	x	
764.6	34:0 PS/35:0 PS					
761.6	36:1 PG/36:2 PG		x		x	x
760.6	34:1 PC/38:0 PEp /38:1 Pee/38:0 PEe	x	x		x	x
758.6	34:2 PC/38:0 PEp /38:1 PEe	x	x	x		x
757.5	36:2 PGp/36:3 PGe	x				
754.5	34:4 PC/38:3 PEp /38:4 Pee/38:2 Pep/38:3 PEe	x				
753.5	28:0 PI/36:4 PGp /36:5 PGe	x			x	x
752.6	38:3 Pep/38:4 Pe/34:5 PC/38:4 Pep/38:5 PEe	x			x	x
751.6	35:0 PG/40:5 PA		x		x	x
751.3	22:0 PIp		x		x	x
750.6	33:0 PS/34:0 PS	x			x	x
749.4	28:2 PI/34:0 PG	x			x	x
746.6	34:0 PC/34:1 PC/37:0 PE		x		x	x
745.6	40:0 PA/ 40:1 PA/40:8 PA		x		x	x
742.6	34:2 PCp/34:3 PCe/36:3 PE	x	x	x	x	x
741.5	34:5 PG		x		x	x
740.5	33:4 PC/36:4 PE		x		x	x
739.4	34:6 PG		x		x	
738.4	36:4 PE/34:4/36:5 PE	x	x	x	x	
737.5	34:6 PG	x	x		x	x
736.5	36:5 PE/32:0 PS/33:0 PSe	x	x		x	x
735.5	34:0 PGe	x	x	x	x	x

m/z	Bligh and Dyer Extraction	Silica Phase			C18 Phase	
		MeOH	IPA	ACN	2:1 Chloroform /MeOH	1:1 Tetrahydrofuran /MeOH
734.5	33:0 PS/32:0 PS/36:0 PEe	x	x	x	x	x
733.5	34:0 PGp/34:1 PGe	x	x		x	x
732.6	32:1 PC/36:0 PEp /36:1 PEe	x	x	x	x	x
730.4	32:2PC/35:2 PE/36:0 Pep/36:1 PEe	x			x	x
729.4	33:4 PG	x	x		x	x
728.5	32:3 PS/36:1 PEp	x	x	x	x	x
725.4	26:1 PI	x	x		x	x
724.5	32:6 PS/32:5 PC/36:5 PE/36:3 Pep36:4 PEe	x			x	x
723.6	33:0 PG/38:5 PA		x		x	x
718.5	32:1 PC/32:0 PC/35:0 PE/34:0 PE	x	x	x	x	x
716.6	32:1 PC/35:1 PE		x		x	x
714.4	34:3 PE/31:3 PC	x	x	x	x	x
711.4	32:6 PG/38:3 PA					
708.4	34:6 PE/31:0 PS		x		x	x
707.5	32:0 PGe/38:4 Pap/38:5 PAe	x	x		x	x
706.6	31:0 PC/34:0 PE		x		x	x
704.6	34:0PE/34:1 PE		x			x
703.6	37:0 PA/37:1 PA		x		x	x
702.5	30:2 PC/33:2 PE		x		x	x
701.5	36:1 PA	x			x	x
698.4	30:5 PS/34:3 PE				x	x
697.3	24:1 PI/36:4 PA				x	x
694.5	29:0 PS/30:0 PS				x	x
692.6	30:0 PCe/30:0 PS /32:0 PE	x	x		x	x
690.5	30:0 PC/30:1 PCe /32:1 PE	x	x	x	x	x
688.5	32:2 PE/30:1 PCp	x			x	

m/z	Bligh and Dyer Extraction	Silica Phase			C18 Phase	
		MeOH	IPA	ACN	2:1 Chloroform /MeOH	1:1 Tetrahydrofuran /MeOH
686.5	32:3 PE	x	x	x	x	x
683.4	36:2 Pap/36:3 PAe	x			x	x
680.4	32:6 PE/28:0 PS				x	
679.5	30:0 PGe/36:4 PAp	x			x	x
678.5	28:0 PS/32:6 PE28:0/PC, 28:1 PS/32:0 PEe	x			x	x
677.5	34:0 PA	x			x	x
676.5	28:0 PC/28:1 PS /32:0 PEe	x			x	x
676.4	29:2 PG/28:2 PS				x	x
675.4	18:3 Pip/34:0 PA	x			x	x
674.5	28:2 PC/31:2 PE				x	x
673.4	35:2 PA/35:1 PA/34:1 PA	x	x		x	
673.4	34:2 PA	x			x	
672.4	31:3 PE/28::3 PC					
671.5	34:2 PA	x			x	x
667.4	18:0 PIp/34:5 PA				x	x
664.5	28:0 PC/30:0 PE	x			x	x
663.6	34:0 PA/33:0 PA		x		x	x
662.6	28:0 PC/30:1 PE	x	x	x	x	x
660.5	28:0 PCp/30:1 PE/30:2 PE	x			x	x
655.5	22:0 LPI/34:2 Pap/34:3 PAe	x			x	x
654.4	30:5 PE/30:4 PE	x			x	x
653.5	28:0 PG/33:5 PA		x		x	x
651.4	16:0 LPIP/22:2 LPI/28:0 PGe	x	x		x	
650.4	26:1 PS/26:0 PC		x		x	x
649.2	16:1 LPIP	x	x		x	x
647.3	22:4 LPI/32:0 PA	x	x	x	x	x
643.3	20:0 PI/21:0 PI				x	x
639.4	32:4 PA	x			x	x

m/z	Bligh and Dyer Extraction	Silica Phase			C18 Phase	
		MeOH	IPA	ACN	2:1 Chloroform /MeOH	1:1 Tetrahydrofuran /MeOH
638.4	26:1 PG/26:0 PS	x			x	x
636.5	26:0 PS/29:0 PE				x	x
634.5	26:0 PCe/28:0 PE/26:0 PCp/ 28:1 PE	x			x	x
633.5	32:0 PA/32:1 PA/31:1 PA				x	x
627.4	20:0 LPI/31:3 PA	x	x	x	x	x
623.4	26:0 PG	x			x	x
622.5	24:0 PC/28:0 PEe	x	x		x	x
620.4	24:1 PC/8:0 PEp	x			x	x
618.4	24:1 PC/28:0 PEp	x			x	x
611.4	30:5 PA/20:0 LPI/30:4 PA	x	x		x	x
608.3	23:0 PC/26:0 PE	x			x	
603.5	30:1 PA/30:0 PA	x			x	x
597.3	23:0 PG/18:1 LPI	x			x	
594.4	22:0 PC/25:0 PE				x	x
589.4	28:2 PA	x			x	x
585.4	18:0 PI/17:1 PI/28:3 PA	x			x	x
583.3	22:0 PG/18:0 LPI	x	x	x	x	
581.3	22:0 PS/22:0 PG	x	x	x	x	
580.4	24:0 PE/22:0 PC				x	x
570.4	22:6 PS/22:5 LPC	x			x	x
569.4	22:0 LPG/16:1 LPI	x			x	x
568.3	20:0 LPS/21:0 LPS/22:6 LPS/22:6 LPC	x			x	x
566.3	20:0 LPC/23:0/21:0 LPS LPE	x			x	
559.3	15:0 LPI/16:0 LPI				x	

m/z	Bligh and Dyer Extraction	Silica Phase			C18 Phase	
		MeOH	IPA	ACN	2:1 Chloroform /MeOH	1:1 Tetrahydrofuran /MeOH
555.3	16:0 LPI/21:0 LPG				x	
552.6	20:1 LPS/22:0 LPE/20:0 LPC				x	
550.4	20:2 LPS/20:1 LPS	x	x	x	x	
544.5	20:4 LPC	x	x		x	
543.3	14:1 LPI				x	
537.3	20:2 LPG/24:0 LPA				x	x
536.3	22:1 LPE/20:0 LPC				x	
535.4	24:1 LPA/20:3 LPG				x	x
532.3	13:0 LPI/22:2 LPE	x				
524.3	18:1 LPS/20:0 LPE				x	
523.3	23:0 LPA					
522.4	18:1 LPC/18:0 LPC	x	x	x	x	x
518.3	18:3 LPC/18:2 LPC	x	x		x	
510.3	17:1 LPS/18:0 LPS					
508.3	18:0 LPC/17:1 LPC					
506.3	17:2 LPC/20:2 LPE/20:1 LPE	x				
500.3	20:5 LPE	x	x		x	x
497.3	18:0 LPG/17:1 LPG					
496.6	16:1 LPS/20:0 LPE/16:0 LPC	x			x	x
495.4	22:0 LPA					
494.2	20:0 LPE/16:1 LPS/16:1 LPC	x	x		x	
481.4	21:0 LPA/20:0 LPA					
480.4	16:0 LPC					
478.3	18:2 LPE					

m/z	Bligh and Dyer Extraction	Silica Phase			C18 Phase	
		MeOH	IPA	ACN	2:1 Chloroform /MeOH	1:1 Tetrahydrofuran /MeOH
468.5	18:0 LPE/17:0 LPE	x			x	
467.3	20:0 LPA					
466.3	14:1 LPC/17:1 LPE/18:0 LPE		x		x	
465.4	20:1 LPA					
464.2	17:2 LPE					
456.3	13:0 LPS					
455.2	13:0 LPC/16:0 LPE/14:0 LPG	x				
453.4	20:0 LPA/19:0 LPA					
442.3	12:0 LPS					
440.5	16:0 LPE	x	x			
425.3	17:0 LPA/18:0 LPA		x			
412.3	10:0 LPC/13:0 LPE					
353.2	12:0 LPA	x				
327.2	10:0 LPA					

Table A-1 Library of Identified glycerophospholipd species eluted by different eluents on silica or C18 stationary phases compared to total lipid species by Bligh and Dyer method for evaluation of on-chip extraction efficiency. The matched glycerophospholipid species are marked by "x" within a mass error window of 10 ppm. Phospholipids are presented with a class abbreviation preceded by *xx:y*, where *xx* is the total fatty acid carbon number and *y* is the number of double bonds. The following abbreviations are used: PA, phosphatidic acid; PC, phosphatidylcholine; PE, phosphatidylethanolamine; PG, phosphatidylglycerol; PI, phosphatidylinositol; PS, phosphatidylserine; LPA, lysophosphatidic acid; LPC, lysophosphatidylcholine; LPE, lysophosphatidylethanolamine; LPG, lysophosphatidylglycerol; LPI, lysophosphatidylinositol; LPS, lysophosphatidylserine; PIP, phosphatidylinositol phosphate. PC, PE, PI and PIP with a lower case *e* and/or *p* refer to plasmanyl and plasmenyl (alkyl ether and plasmalogens) subspecies, respectively.

Appendix 2

Library of Identified Phospholipid Species in Sulfurospirillum barnesii Cells Extracted from the Microchip

A.2 Abstract

A library for identified glycerophospholipids extracted from *Sulfurospirillum barnesii* strain SES-3 cells based on the matches of METLIN Personal Metabolite database and LIPID MAPS database was established. The glycerophospholipids were extracted by using methanol as the eluent on microchip packed with silica stationary phase.

Measured mass	Theoretical mass	Error (ppm)	Ionization mode	
			Negative	Positive
353.177	353.173	9.6	12:0 LPA	
431.219	431.220	-2.8	18:3 LPA	
440.492	440.494	-4.5		16:0 LPE
455.245	455.242	8.3	14:0 LPG	
468.507	468.505	5.3		18:0 LPE
494.250	494.252	-5.3	16:1 LPS	
494.227	494.224	6.5		16:1 LPC
496.643	496.640	5.4		16:0 LPC
500.381	500.377	8.4		20:5 LPE
506.322	506.325	-7.5	20:1 LPE	
506.320	506.324	-8.9		20:2 LPE
518.360	518.359	1.9	18:2 LPC	
518.329	518.324	8.8		18:3 LPC
522.350	522.353	-5.6	18:0 LPC	
522.360	522.355	9.6		18:1 LPC
532.345	532.341	8.5	22:2 LPE	
544.542	544.540	3.7		20:4 LPC
550.313	550.315	-4.4	20:1 LPS	
550.382	550.386	-7.3		20:1 LPC
552.605	552.602	5.4		20:0 LPC
566.350	566.346	7.2	21:0 LPS	
568.271	568.268	4.9	22:6 LPS	
568.337	568.334	5.3		22:6 LPC
569.350	569.353	-5.1	16:1 LPI	
570.360	570.356	7.0		22:5 LPC
581.351	581.346	8.9	22:0 PG	
583.322	583.325	-6.2	18:0 LPI	
585.361	585.356	8.4	28:3 PA	
589.384	589.388	-5.4	28:1 PA	
597.301	597.305	8.7	18:1 LPI	
603.454	603.450	7.5	30:0 PA	
608.331	608.329	3.3		26:0 PE
611.363	611.357 a/o 611.369	9.9 a/o -9.9	20:0 LPI a/o 30:4 PA	
618.419	618.414 a/o 618.420	7.8 a/o -2.6	24:1 PC a/o 28:0 PEp	
620.633	620.629 a/o 620.635	6.4 a/o -3.2		24:1 PC a/o 28:0 PEp
622.492	622.494 a/o 622.489	-3.2 a/o 4.8		24:0 PC a/o 28:0 PEe
627.397	627.392 a/o 627.402	8.1 a/o -7.7	20:0 LPI a/o 31:3 PA	
634.475	634.480 a/o 634.470	-8.0 a/o 7.6	26:0 PCe a/o 28:0 PE	

Measured mass	Theoretical mass	Error (ppm)	Ionization mode	
			Negative	Positive
634.486	634.481 a/o 634.490	7.9 a/o -6.3		26:0 PCp a/o 28:1 PE
638.446	638.439	10.0		26:0 PS
639.407	639.403	5.9	32:4 PA	
647.315	647.320 a/o 647.310	-8.8 a/o 7.4	22:4 LPI a/o 32:0 PA	
649.246	649.240	9.2	16:1 LPIP	
651.357	651.355, 651.352 a/o 651.361	3.0, 7.7 a/o -6.1	16:0 LPIP, 22:2 LPI a/o 28:0 PGe	
654.416	654.414	3.1	30:4 PE	
654.418	654.413	7.6		30:5 PE
655.479	655.483, 655.476 a/o 655.476	-6.1, 4.6 a/o 4.6	22:0 LPI, 34:2 PAp a/o 34:3 PAe	
660.494	660.497 a/o 660.489	-4.5 a/o 7.6	28:0 PCp a/o 30:1 PE	
660.457	660.460	-4.5		30:2 PE
662.616	662.612 a/o 662.622	6.0 a/o -9.1		28:0 PC a/o 30:1 PE
664.527	664.528 a/o 664.531	-1.5 a/o -6.0		28:0 PC a/o 30:0 PE
671.538	671.536	3.0	34:2 PA	
673.376	673.381	-7.4	34:1 PA	
675.399	675.397	2.9	34:0 PA	
676.501	676.497, 676.504 a/o 676.504	5.9, -4.4 a/o -4.4	28:0 PC, 28:1 PS a/o 32:0 PEe	
676.497	676.491, 676.502 a/o 676.502	8.9, -7.4 a/o -7.4		28:1 PC, 32:0 PEp a/o 32:1 PEe
678.429	678.435 a/o 678.424	-8.7 a/o 7.4	28:0 PS a/o 32:6 PE	
678.511	678.507, 678.514 a/o 678.513	5.9, -4.4 a/o -2.9		28:0 PC, 28:1 PS a/o 32:0 PEe
679.487	679.492 a/o 679.481	-7.4 a/o 8.8	30:0 PGe a/o 36:4 PAp	
683.606	683.602 a/o 683.602	5.9 a/o 5.9	36:2 PAp a/o 36:3 PAe	
686.478	686.476	2.9		32:3 PE
688.501	688.495 a/o 688.508	8.7 a/o -10.0		32:2 PE a/o 30:1 PCp

Measured mass	Theoretical mass	Error (ppm)	Ionization mode	
			Negative	Positive
690.549	690.543, 690.543 a/o 690.552	8.7, 8.7 a/o -4.3		30:0 PC, 30:1 PCe a/o 32:1 PE
692.564	692.559, 692.566 a/o 692.563	7.2, -2.9 a/o 1.4		30:0 PCe, 30:0 PS a/o 32:0 PE
701.509	701.513	-5.7	36:1 PA	
707.519	707.523, 707.512 a/o 707.512	-6.0, 9.9 a/o 9.9	32:0 PGe, 38:4 PAp a/o 38:5 PAe	
714.398	714.394	5.6		34:3 PE
718.602	718.599	4.2	34:0 PE	
718.500	718.495, 718.495 a/o 718.498	9.7, 9.7 a/o 5.6		32:0 PCp, 32:1 PCe a/o 34:1 PE
724.530	724.529 a/o 724.529	1.3 a/o 1.3	36:3 Pep a/o 36:4 PEe	
724.520	724.525, 724.518 a/o 724.518	-4.1, 5.5 a/o 5.5		32:5 PC, 36:4 PEp a/o 36:5 PEe
728.457	728.451 a/o 728.460	8.2 a/o 4.4	32:3 PS a/o 36:1 PEp	
728.556	728.553 728.559 a/o 728.559	4.3, -4.0 a/o -4.0		32:3 PC, 36:2 PEp a/o 36:3 PEe
730.474	730.476 a/o 730.476	-2.7 a/o -2.7	36:0 PEp a/o 36:1 PEe	
730.440	730.438, 730.445 a/o 730.445	2.7, -6.8 a/o -6.8		32:2 PC, 36:1 PEp a/o 36:2 PEe
732.583	732.576, 732.590 a/o 732.590	9.6, -8.8 a/o -8.8		32:1 PC, 36:0 PEp a/o 36:1 PEe
733.442	733.439 a/o 733.439	4.1 a/o 4.1	34:0 PGp a/o 34:1 PGe	
734.504	734.498	4.1	32:0 PS	
734.572	734.570 a/o 734.569	2.7 a/o 4.1		32:0 PC a/o 36:0 PEe
735.461	735.455	8.2	34:0 PGe	
736.499	736.492	9.5	36:5 PE	
736.507	736.512 a/o 736.509	-6.7 a/o -2.7		32:0 PS a/o 33:0 PSe
737.543	737.540	4.1	34:6 PG	
738.402	738.408	-8.1	36:4 PE	

Measured mass	Theoretical mass	Error (ppm)	Ionization mode	
			Negative	Positive
738.435	738.430 a/o 738.437	6.8 a/o -3.3		34:4 a/o 36:5 PE
742.583	742.575, 742.575 a/o 742.588	10.0, 10.0 a/o -6.7		34:2 PCp, 34:3 PCe a/o 36:3 PE
749.429	749.425 a/o 749.434	5.3 a/o -6.7	28:2 PI a/o 34:0 PG	
752.566	752.560 a/o 752.560	7.9 a/o 7.9	38:3 PEp a/o 38:4 PEe	
752.565	752.563, 752.559 a/o 752.559	2.7, 8.0 a/o 8.0		34:5 PC, 38:4 PEp a/o 38:5 PEe
753.509	753.516, 753.508 a/o 753.508	-9.3, 1.3 a/o 1.3	28:0 PI, 36:4 PGp a/o 36:5 PGe	
754.571	754.576 a/o 754.576	-6.6 a/o -6.6	38:2 PEp a/o 38:3 PEe	
754.544	754.538, 754.545 a/o 754.545	7.9, -1.3 a/o -1.3		34:4 PC, 38:3 PEp a/o 38:4 PEe
757.542	757.539 a/o 757.539	4.0 a/o 4.0	36:2 PGp a/o 36:3 PGe	
758.711	758.707 a/o 758.707	5.3 a/o 5.3	38:0 PEp a/o 38:1 PEe	
758.561	758.568	-9.2		34:2 PC
760.728	760.723	6.6	38:0 PEe	
760.627	760.631, 760.622 a/o 760.622	-5.3, 6.6 a/o 6.6		34:1 PC, 38:0 PEp a/o 38:1 PEe
765.498	765.492 a/o 765.492	7.8 a/o 7.8	30:0 PIp a/o 30:1 PIe	
766.546	766.539	9.1	38:4 PE	
766.463	766.465 a/o 766.458	-2.6 a/o 6.5		36:4 PCp a/o 38:5 PE
767.512	767.508	5.2	30:0 PIe	
768.550	768.555	-6.5	38:3 PE	
768.449	768.454, 768.446 a/o 768.446	-6.5, 3.9 a/o 3.9		38:4 PE, 36:3 PCp a/o 36:4 PCe
771.414	771.409 a/o 771.418	6.5 a/o -5.2	30:5 PI a/o 36:3 PG	
776.565	776.558, 776,560 a/o 776.560	9.0, 6.4 a/o 6.4	36:0 PSe, 40:5 PEp a/o 40:6 PEe	

Measured mass	Theoretical mass	Error (ppm)	Ionization mode	
			Negative	Positive
776.562	776.563, 776.556 a/o 776.559	-1.3, 7.7 a/o 3.9		36:0 PCe, 38:0 PE a/o 40:6 PEp
782.579	782.573 a/o 782.586	7.7 a/o -8.9		36:4 PC a/o 40:4 PEe
784.616	784.613, 784.623 a/o 784.623	3.8, -8.9 a/o -8.9	36:3 PS, 40:1 PEp a/o 40:2 PEe	
784.623	784.628, 784.617, 784.622 a/o 784.622	-6.4, 7.6, 1.3 a/o 1.3		36:3 PC, 36:4 PS, 40:2 PEp a/o 40:3 PEe
786.546	786.541, 786.548, 786.540 a/o 786.540	6.4, -2.5, -5.1 a/o -5.1		36:2 PC, 36:3 PS, 40:1 PEp a/o 40:2 PEe
790.667	790.662, 790.659 a/o 790.668	6.3, 10.0 a/o -1.3		36:0 PC, 36:1 PS a/o 40:0 PEe
795.543	795.539 a/o 795.548	5.0 a/o -6.3	32:0 PIe a/o 38:5 PG	
796.557	796.552, 796.552, 796.549 a/o 796.555	6.3, 6.3, 10.0 a/o 2.5		38:3 PCp, 38:4 PCe, 38:4 PSp a/o 40:4 PE
798.539	798.537, 798.537, 798.544 a/o 798.541	2.5, 2.5, -6.3 a/o -2.5		38:2 PCp, 38:3 PCe, 38:3 PSp a/o 40:3 PE
800.659	800.653, 800.653, 800.652 a/o 800.666	7.5, 7.5, 8.7 a/o -8.7		38:1 PCp, 38:2 PCe, 38:2 PSp a/o 40:2 PE
802.670	802.668, 802.668, 802.676 a/o 802.672	2.5, 2.5, -7.5 a/o -2.5		38:0 PCp, 38:1 PCp, 38:1 PSp a/o 40:1 PE
805.637	805.633	5.0	38:0 PG	
806.566	806.559, 806.570, 806.569 a/o 806.569	8.7, -5.0, -3.7 a/o -3.7		38:0 PSe, 38:6 PC, 42:5 PEp a/o 42:6 PEe
810.537	810.529 a/o 810.538	9.9 a/o -1.2	38:4 PS a/o 42:2 PEp	

Measured mass	Theoretical mass	Error (ppm)	Ionization mode	
			Negative	Positive
810.533	810.531, 810.528 a/o 810.537	2.5, 6.2 a/o -4.9		38:4 PC, 38:5 PS a/o 42:4 PEe
812.478	812.473 a/o 812.482	6.2 a/o -4.9	38:3 PS a/o 42:2 PEe	
812.657	812.661, 812.649 a/o 812.653	-4.9, 9.8 a/o 4.9		38:3 PC, 38:4 PS a/o 42:2 PEp
816.579	816.576 a/o 816.585	3.7 a/o -7.3	38:1 PS a/o 42:0 PEe	
816.581	816.584, 816.575 a/o 816.584	-3.7, 7.3 a/o -3.7		38:1 PC, 38:2 PS a/o 42:0 PE
818.605	818.603, 818.597 a/o 818.606	2.4, 9.8 a/o -1.2		38:0 PC, 38:1 PS a/o 40:6 PCp
820.598	820.606, 820.602 a/o 820.595	-9.7, -4.9 a/o 3.7		38:0 PS, 40:5 PCp a/o 40:6 PS
822.539	822.537, 822.544 a/o 822.541	2.4, -6.1 a/o -2.4		40:4 PCp, 40:5 Pce a/o 40:5 PSp
830.631	830.628 a/o 830.628 a/o 830.634	3.6, 3.6 a/o -3.6	40:0 PSp, 40:1 Pse a/o 42:0 PE	
830.696	830.700, 830.700 a/o 830.693	-4.8, -4.8 a/o 3.6		40:0 PCp, 40:1 Pce a/o 40:1 PSp
831.507	831.503 a/o 831.512	4.8 a/o -6.0	34:3 PI a/o 40:1 PG	
835.585	835.584	1.2	34:1 PI	
836.552	836.545	8.4	40:5 PS	
836.660	836.657 a/o 836.654	3.6 a/o 7.2		40:5 PC a/o 40:6 PS
846.701	846.696, 846.703 a/o 846.705	5.9, -2.4 a/o -4.7	42:6 PSp, 40:0 PS a/o 44:6 PE	
846.629	846.625, 846.622 a/o 846.637	4.7, 8.3 a/o -9.4		40:0 PC, 40:1 PS a/o 42:6 PCp
847.577	847.580, 847.571 a/o 847.571	-3.5, 7.1 a/o 7.1	42:0 Pge, 36:1 PIp a/o 36:2 PIe	

Measured mass	Theoretical mass	Error (ppm)	Ionization mode	
			Negative	Positive
848.601	848.595 a/o 848.608	7.1 a/o -8.2	42:5 PS a/o 44:5 PE	
848.640	848.633, 848.638 a/o 848.646	8.3 2.4 a/o -7.1		42:6 Pce, 40:0 PS a/o 44:6 PE
850.595	850.603 a/o 850.597	-9.4 a/o -2.4	44:4 PE a/o 42:5 PSe	
850.677	850.672, 850.668 a/o 850.668	5.9, 10 a/o 10.0		44:5 PE, 42:4 PCp a/o 42:5 PCe
856.650	856.643 a/o 856.659	8.2 a/o -10.0		42:2 PSp a/o 44:2 PE
857.509	857.505 a/o 857.512	5.8 a/o -4.7	36:4 PI a/o 42:2 PG	
858.703	858.701, 858.701 a/o 858.697	2.3, 2.3 a/o 7.0		42:0 PCp, 42:1 PCe a/o 44:1 PE
861.653	861.650 a/o 861.659	3.5 a/o -7.0	36:2 PI a/o 42:0 PG	
864.555	864.557	-3.5	42:5 PS	
864.541	864.545 a/o 864.548	-4.6 a/o -8.1		42:5 PC a/o 42:6 PS
866.700	866.692	9.2	42:4 PS	
866.669	866.663 a/o 866.671	6.9 a/o -2.3		42:4 PC a/o 42:5 PS
868.611	868.607	4.6	42:3 PS	
868.603	868.599 a/o 868.606	4.6 a/o -3.5		42:3 PC a/o 42:4 PS
877.613	877.618 a/o 877.618	-5.7 a/o -5.7	38:0 PIp a/o 38:1 PIe	
880.682	880.679	3.4		43:4 PC
881.482	881.477	6.8	38:6 PI	
890.638	890.632	7.9	44:6 PS	
890.670	890.663	4.2		44:6 PC
892.602	892.607	-5.6	44:5 PS	
892.610	892.606 a/o 892.619	4.5 a/o -10.0		44:6 PS a/o 44:5 PC
894.702	894.696	6.7	44:3 PC	
894.697	894.695 a/o 894.702	2.2 a/o -5.6		44:4 PC a/o 44:5 PS
898.503	898.509	-7.8	44:2 PS	
898.629	898.626 a/o 898.633	3.3 a/o -4.5		44:2 PC a/o 44:3 PS

Measured mass	Theoretical mass	Error (ppm)	Ionization mode	
			Negative	Positive
899.497	899.502 a/o 899.502	-5.6 a/o -5.6	40:3 PIp a/o 40:4 PIe	
901.514	901.518 a/o 901.518	-4.4 a/o -4.4	40:2 PIp a/o 40:3 PIe	
921.483	921.486	-3.3	42:6 PIp	
923.607	923.602 a/o 923.602	5.4 a/o 5.4	42:5 PIp a/o 42:6 PIe	
929.657	929.649	8.6	42:2 PIp	
945.650	945.644	6.3	42:2 PI	
953.562	953.553 a/o 953.553	9.4 a/o 9.4	38:2 PIPp a/o 38:3 PIPe	
955.571	955.568 a/o 955.568	3.1 a/o 3.1	38:1 PIPp a/o 38:2 PIPe	
957.589	957.584 a/o 957.584	5.2 a/o 5.2	38:0 PIPp a/o 38:1 PIPe	
963.508	963.501	7.3	38:5 PIP	
969.638	969.633 a/o 969.644	5.2 a/o -6.2	38:2 PIP a/o 44:4 PI	
973.584	973.579 a/o 973.575	5.1 a/o 9.2	38:0 PIP a/o 44:2 PI	
979.570	979.568 a/o 979.568	2.0 a/o 2.0	40:3 PIPp a/o 40:4 PIPe	

Table A-2 Library of identified phospholipid species extracted from cells by microchip. Phospholipids are presented with a class abbreviation preceded by *xx:y*, where *xx* is the total fatty acid carbon number and *y* is the number of double bonds. The following abbreviations are used: PA, phosphatidic acid; PC, phosphatidylcholine; PE, phosphatidylethanolamine; PG, phosphatidylglycerol; PI, phosphatidylinositol; PS, phosphatidylserine; LPA, lysophosphatidic acid; LPC, lysophosphatidylcholine; LPE, lysophosphatidylethanolamine; LPG, lysophosphatidylglycerol; LPI, lysophosphatidylinositol; LPS, lysophosphatidylserine; PIP, phosphatidylinositol phosphate. PC, PE, PI and PIP with a lower case *e* and/or *p* refer to plasmanyl and plasmenyl (alkyl ether and plasmalogens) subspecies, respectively.